Analysis of *Yersinia*-mediated cell death pathways in human and murine macrophages

Dissertation

Zur Erlangung des Doktorgrades an der Fakultät für Mathematik, Informatik und Naturwissenschaften der Universität Hamburg

Fachbereich Biologie

vorgelegt von

Marie Kriwet

Hamburg, 2024

Datum der Disputation: 12.04.2024

Dissertationsgutachter: Prof. Dr. med. Klaus Ruckdeschel

Prof. Dr. rer. nat. Wolfgang Streit

Table of contents

Table of contents I

List of figures V

List of tables VI

Abbreviations VII

Summary 1

Zusammenfassung 3

1 Introduction 6

1.1 The genus *Yersinia* 6

1.2 *Yersinia enterocolitica* 7

1.2.1 Classification 7

1.2.2 Yersiniosis and Pathogenesis 7

1.2.3 Chromosomally-encoded virulence factors 8

1.2.4 Plasmid-encoded virulence factors 9

1.2.4.1 YadA 10

1.2.4.2 Type III secretion system 10

1.2.4.3 Effector proteins 11

1.3 Innate immunity and macrophages 14

1.4 Programmed cell death 15

1.4.1 Apoptosis 15

1.4.2 Necroptosis 17

1.4.3 Pyroptosis 19

1.4.4 Gasdermins 21

1.4.5 Crosstalk between programmed cell death pathways 23

1.5 *Yersinia* induced cell death 25

1.6 Aim of this study 28

2 Material and Methods 29

2.1 Materials 29
2.1.1 Devices 29
2.1.2 Disposables 30
2.1.3 Enzymes, Kits and reagents 30
2.1.4 Plasmids and Oligonucleotides 32
2.1.5 Antibiotics 33
2.1.6 Buffers and solutions 34
2.1.7 Antibodies 35
2.1.8 Growth media and additives 36
2.1.9 Inhibitors and stimulators 37
2.1.10 *E. coli* strains 38
2.1.11 *Yersinia* strains 38
2.1.12 Eukaryotic cells 38
2.1.13 Software 39
2.2 Methods 40
2.2.1 Molecular biology methods 40
2.2.1.1 Plasmid preparation and sequencing 40
2.2.1.2 Cloning and transformation 40
2.2.2 Microbiological methods 41
2.2.2.1 Cultivation of Yersinia enterocolitica strains 41
2.2.2.2 Yersinia infection 41
2.2.3 Cell culture methods 41
2.2.3.1 Isolation and cultivation of primary human macrophages 41
2.2.3.2 Cultivation and differentiation of THP-1 cells 42
2.2.3.3 Generation of THP-1 knockout cell lines using CRISPR/CAS9 and lentiviral transduction 43
2.2.3.4 Cultivation of iWT 44
2.2.3.5 Generation of knockout cell lines using the Alt-R® CRISPR-Cas9 system 45

2.2.3.6 Generation of iWT based knockout cell lines using CRISPR/CAS9 lentiviral transduction 46
2.2.3.7 Infection and stimulation experiments 46
2.2.3.8 Measurement of cell death rates using SYTOX® Green 46
2.2.3.9 Cryoconservation and re-cultivation of eukaryotic cell lines 47
2.2.4 Proteinbiochemical methods 47
2.2.4.1 Production of cell lysates 47
2.2.4.2 SDS-polyacrylamide gel electrophoresis (SDS-PAGE) 48
2.2.4.3 Western Blotting and immunodetection 48
2.2.4.4 Enzyme-linked immunosorbent assay (ELISA) 49
3 Results 50
3.1 Yersinia-induced cell death in primary human macrophages 50
3.1.1 *Yersinia*-infected human macrophages die in a YopP-dependent manner 50
3.1.2 YopP inhibits TAK1 phosphorylation 51
3.1.3 YopP triggers RIP1 phosphorylation 52
3.1.4 *Yersinia* infection leads to activation of caspases-3 and -8 53
3.1.5 GSDME but not GSDMD is activated after infection 54
3.1.6 YopP inhibits release of cytokines 56
3.2 THP-1 cells as human macrophage model for *Yersinia* infection 57
3.2.1 *Yersinia* induced cell death in THP-1 macrophages 57
3.2.2 Generation of GSDME-deficient THP-1 cells 58
3.2.3 Absence of GSDME leads to reduction of *Yersinia*-induced cell death 58
3.3 Examining *Y. enterocolitica* mediated cell death in different murine knockout cell lines 59
3.3.1 Investigation of *Yersinia* induced cell death rates in murine knockout macrophages 60
3.3.2 Influence of BID deficiency on activation of different caspases 61
3.3.3 Activation of GSDMD in BID-deficient macrophages 65
4 Discussion 67
4.1 Cell death induction by *Y. enterocolitica* infection in primary human macrophages 67

4.2 *Y. enterocolitica*-mediated cell death in THP-1 macrophages 74

4.3 The role of BID in *Y. enterocolitica*-mediated cell death of murine macrophages 76

5 Literature 82

6 Danksagung 97

7 Eidesstattliche Versicherung 99

List of figures

Figure 1: Schematic overview of intrinsic and extrinsic apoptotic signalling pathways. 17
Figure 2: Schematic overview of necroptotic cell death pathways. 19
Figure 3: Schematic overview of pyroptotic cell death pathways. 21
Figure 4: Relative cell death rates of primary human macrophages upon *Yersinia* infection after (A) 5 h and (B) 23-24 h. 51
Figure 5: TAK1 and its phosphorylation in infected primary human macrophages. 52
Figure 6: RIP1 and its phosphorylation in infected primary human macrophages with Actin control. 53
Figure 7: Processing of caspase-3 and -8 in infected primary human macrophages. 54
Figure 8: Processing of GSDMD and GSDME upon *Yersinia* infection in human macrophages. 55
Figure 9: Concentration of inflammatory cytokines in cell culture supernatants of untreated and *Y. enterocolitca* infected primary human macrophages. 57
Figure 10: Investigating TAK1 phosphorylation and processing of caspase-3 and GSDME in THP-1 macrophages. 58
Figure 11: Validation of the Gsdme knock-out in THP-1 cells using immunodetection. 58
Figure 12: Relative cell death rates of wildtype THP-1 cells and GSDME-deficient THP-1 cells upon *Yersinia* infection after (A) 5 h and (B) 18 - 20 h. 59
Figure 13: Validation of murine knockout cell lines. 60
Figure 14: Relative cell death rates of different murine knockout cell lines upon *Y. enterocolitica* infection. 61
Figure 15: Caspase-8 processing in iWT and i*Bid*$^{-/-}$ cells. 62
Figure 16: Caspase-9 processing in iWT, i*Bid*$^{-/-}$ and i*Bid*$^{-/-}$ *Gsdmd*$^{-/-}$ macrophages. 63
Figure 17: Caspase-3 processing in two different BID deficient cell lines. 64
Figure 18: Cleavage of GSDMD in two different BID deficient cell lines. 66

List of tables

Table 1: Used devices 29
Table 2: Used disposables 30
Table 3: Used enzymes, kits and reagents 30
Table 4: Used plasmids 32
Table 5: Used DNA and RNA oligonucleotides 32
Table 6: Used antibiotics 33
Table 7: Buffer compositions of general buffers and solutions 34
Table 8: Buffer compositions of buffers used for SDS-PAGE and western blotting 35
Table 9: Used primary antibodies 35
Table 10: Used secondary antibodies 36
Table 11: Used cell culture media 36
Table 12: Used cell culture additives 37
Table 13: Used inhibitors and stimulators 37
Table 14: Used *E. coli* strains 38
Table 15: Used *Yersinia enterocolitica* strains 38
Table 16: Used eucaryotic cell lines and cells 38
Table 17: Overview – number of seeded human macrophages in different multi plates 42
Table 18: Overview – number of seeded THP-1 cells in different multi plates 43
Table 19: Overview – number of seeded murine bone marrow derived macrophages in different multi plates 45

Abbreviations

° C	degree Celsius
µg	microgram
µl	microliter
µm	micrometer
µM	micromolar
Ail	attachment invasion locus
AIM2	absent in melanoma 2
Amp	ampicilline
APAF-1	apoptotic protease activating factor-1
APS	ammonium persulfate
ASC	apoptosis-associated speck-like protein containing a CARD
ATP	adenosine triphosphate
Bcl-2	B-cell lymphoma 2
BID	BH-3-interacting domain
Blast	Blasticidine
BSA	bovine serum albumin
CARD	caspase recruitment domain
Cas	CRISPR-associated protein
caspase	cysteinyl-aspartate specific protease
cFLIP	cellular FLICE-inhibitory protein
Chlor	chloramphenicol
cIAP	cellular inhibitor of apoptosis protein
CRISPR	clustered regularly interspaced short palindromic repeats
crRNA	CRISPR RNA
CYLD	cylindromatosis protein
DAMP	damage associated molecular pattern
ddH_2O	double distilled water
DED	death effector domain
DISC	death-inducing signalling complex
DMEM	Dulbecco's modified eagle's medium
DMSO	dimethyl sulfoxide
DNA	deoxyribonucleic acid
DTT	dithiothreitol
EDTA	ethylenediamine tetra-acetic acid
EFSA	European Food Safety Authority
EGTA	ethylene glycol-bis(β-aminoethyl ether)-N,N,N',N'-tetraacetic acid
et al.	latin: „et alteri" – and others

FADD	Fas-associated protein with death domain
FCS	fetal calf serum
GAP	GTPase activating protein
GDP	guanosine diphosphate
Genta	Gentamycin
GFP	green fluorescent protein
GSDM	gasdermin
GTP	guanosine triphosphate
h	hour
HEPES	4-(2-hydroxyethyl)-1-piperazineethanesulfonic acid
HMGB1	high mobility group protein1
HRP	horseradish peroxidase
HSP	heat shock protein
Ig	immunoglobulin
IKK	IκB kinase
IL	interleukin
Inv	invasin
IκB	inhibitor of κB
Kana	kanamycin
kDa	kilo Dalton
L	liter
LB	Luria-Bertani
LPS	lipopolysaccharide
M	molar
mA	milliampere
MAP	mitogen activated protein
MAPK	mitogen activated protein kinase
M-cells	microfold cells
mg	milligram
ml	milliliter
MLKL	mixed lineage kinase domain like pseudokinase
mM	millimolar
MOI	multiplicity of infection
MOMP	mitochondrial outer membrane permeabilization
NEAA	non-essential amio acids
Nec1s	Necrostation-1s
NFκB	nuclear factor kappa B
NLRC4	NLR family CARD domain-containing protein 4
NLRP3	nucleotide-binding domain, leucine-rich-containing family, pyrin domain-containing-3
NOD	nucleotide oligomerization domain

OD	optical density
PAGE	polyacrylamide gel electrophoresis
PAMP	pathogen associated molecular pattern
PBS	phosphate-buffered saline
PBMC	peripheral blood mononuclear cell
PCD	programmed cell death
PEI	polyethylenimin
PGE2	prostaglandin E2
pH	power of /potential for hydrogen
PVDF	polyvinylidendifluoride membrane
pYV	plasmid of *Yersinia* virulence
RFP	red fluorescent protein
RHIM	RIP homotypic interaction motif
RIP	receptor-interacting serine/threonine-protein kinase
RNA	ribonucleic acid
rpm	revolutions per minute
RSK	ribosomal S6 kinase
RT	room temperature
s	second
SDS	sodium dodecylsulfate
SEM	standard error of the mean
Ser	serine
SMAC	second mitochondria-derived activator of caspases
TAB	TAK1-binding protein
TAK1	TGF-β-activated kinase 1
TBS	Tris buffered saline
TBS-T	TBS with Tween-20
TCA	trichloroacetic acid
TEMED	N,N,N',N'-tetramethyl ethylenediamine
Thr	theronine
TIR	Toll/IL-1 receptor
TLR	toll-like receptors
TNF-α	tumor necrosis factor-α
tracrRNA	transactivating crRNA
TRADD	TNFR1-associated death domain
TRAF	TNFR-associated factors
TRIF	TIR-domain-containing adapter-inducing interferon-β
Tris	Tris-(hydroxymethyl)aminomethane
TTSS	type three secretion system
v/v	volume per volume

w/v	weight per volume
YadA	*Yersinia* adhesin A
Yop	*Yersinia* outer protein
Ysc	*Yersinia* secretion
Yst	*Yersinia* stable toxin
α	anti

Summary

Infection with the enteropathogenic bacterium *Yersinia enterocolitica* causes macrophage cell death and inflammation. *Yersinia* translocates different effector proteins into the host cell via a type III secretion system, among them YopP. YopP has been found to be responsible for *Yersinia*-mediated cell death, which it causes by inhibition of different important regulatory molecules, like IKKβ, MAPKK and TAK1 through acetylation. This leads to a disruption of pro-survival signalling via the MAPK and NF-κB pathways. In murine macrophages, YopP-mediated blockage of TAK1 phosphorylation combined with TLR4 activation by LPS of the bacterial outer membrane then triggers formation of the death-inducing complex. The key components that form this complex are RIP1, activated through auto-phosphorylation at Ser-166, FADD and caspase-8. Cleaved and thus activated caspase-8 can have different downstream targets. Traditionally, *Yersinia* infection of macrophages was connected to apoptosis, which is mediated by caspase-8. Caspase-9 activates the executioner caspase-3, which subsequently triggers apoptotic cell death. However, more recent studies reported that caspase-8 also cleaves the pore-forming protein GSDMD into its active fragment during *Yersinia* infection. The active N-terminus of GSDMD forms pores in the cell membrane and causes pyroptotic cell death and interleukin release. Loss of GSDMD has been connected to a delay in *Yersinia*-mediated cell death and decreased levels of released IL-1β. The closely related protein GSDME, however, does not play a role in *Yersinia*-mediated cell death in murine macrophages, even though it is cleaved into its processed fragment during infection. As most research on this was so far conducted in murine macrophages, one goal of this study was to investigate *Yersinia*-mediated cell death in human macrophages.

First, cell death rates of primary human macrophages were assessed, and results showed that the cells died in a YopP-dependent manner about 23 to 24 h post-infection. Next, important regulatory molecules of cell death were examined. Phosphorylation of TAK1 was inhibited in human macrophages by YopP, comparable to what has been described for murine macrophages. This implies that *Yersinia* infection of human macrophages also leads to a disruption of MAPK and NF-κB signalling. In accordance with that, TNF-α release was significantly reduced in the presence of YopP, compared to release upon infection with a YopP-deficient strain. Like in their murine counterparts, phosphorylation of RIP1 at Ser-166 was induced by YopP in human macrophages infected with *Y. enterocolitica.* However, inhibition of RIP1 kinase activity through the inhibitor Necrostatin-1s did not affect cell death rates 23 to 24 h post-infection, suggesting that the RIP1 kinase activity is dispensable for *Yersinia*-mediated death of human macrophages. Further studies are needed to determine the exact role of RIP1 kinase activity in *Yersinia* infection of human macrophages. Caspase-8 was found to be cleaved into its active fragment in human macrophages, as was caspase-3. Interestingly, unlike what has been reported for murine macrophages,

no activation of GSDMD could be detected in *Yersinia*-infected human macrophages. However, GSDME was processed into its cell death conferring fragment. This suggests that the features of pyroptosis during *Yersinia* infection are regulated differently in murine and human macrophages. To further investigate this, GSDME-deficient THP-1 macrophages were generated. 18 to 20 h post-infection, GSDME-deficient macrophages exhibited significantly lower cell death rates compared to wild type cells. This gives further indication, that GSDME plays a role in *Yersinia*-mediated cell death in human macrophages which is contrary in murine macrophages.

The second part of this study focussed on investigating the role of the pro-apoptotic molecule BID in murine macrophages during *Yersinia* infection. BID is activated during intrinsic apoptosis and causes MOMP via BAK and BAX. MOMP leads to the release of SMAC and cytochrome c into the cytosol which then triggers activation of caspase-9 and subsequently of caspase-3. Additionally, BID can be activated by caspases-8 in during extrinsic apoptosis and by caspase-1. Deficiency of BID alone did not alter cell death rates of murine macrophages during *Yersinia* infection. However, the results indicated that absence of BID and GSDMD together might protect macrophages from cell death even more than deletion of GSDMD alone. Caspase-8 cleavage was not affected in BID-deficient macrophages, as caspase-8 operates upstream of BID. Caspase-9, on the other hand, was preferentially cleaved into its p37 fragment generated by caspase-3 when cells did not express BID. In wild type macrophages, both the p37 fragment and the fully active p35 fragment generated by auto-cleavage could be detected. This could be due to impaired release of cytochrome c from the mitochondria in BID-deficient cells, which is necessary for apoptosome formation and caspase-9 auto-activation. Active caspase-3 was detectable in both macrophage lines, but the absence of BID appeared to result in delayed and decreased activation of caspase-3. This might be connected to BID-driven SMAC release during MOMP. Finally, activation of GSDMD was investigated. Interestingly, the active p30 fragment of GSDMD was only detected in BID-deficient cells, whereas in wild type macrophages, the inactive fragments p43 and p21 were apparent. This may indicate that BID-deficiency leads to increased GSDMD activation, which could result from reduced inactivation of GSDMD by caspase-3, as generation of the active caspase-3 fragment seemed decreases in BID-deficient cells. These data suggest that BID may critically determine whether the cell rather dies with apoptosis- than with pyroptosis-like characteristics.

Zusammenfassung

Eine Infektion mit dem enteropathogenen Bakterium *Yersinia enterocolitica* löst bei Makrophagen Zelltod und Entzündung aus. Das Bakterium transloziert mittels eines Typ III Sekretionssystems verschiedene Effektorproteine in die Wirtszelle, unter anderem YopP. YopP ist eine Acetyltransferase, die eine Blockierung verschiedener regulatorischer Moleküle verursacht, unter anderem von IKKβ, MAPKK und TAK1. Dies führt zu einer Unterbrechung der, zelluläres Überleben vermittelnden, MAPK und NF-κB Signalwege, und folglich zu einem YopP-abhängigen Zelltod. In Mausmakrophagen führt die YopP-abhängige Inhibierung der TAK1-Phosphorylierung zusammen mit der Aktivierung des Rezeptors TLR4 durch bakterielles LPS zur Bildung des sogenannten *death-inducing complex*. Die Schlüsselkomponenten dieses Komplexes sind die Kinase RIP1, welche durch Phosphorylierung an Ser-166 aktiviert wird, und Caspase-8 und FADD. Prozessierte und somit aktive Caspase-8 kann unterschiedliche Substrate spalten. Ursprünglich wurde eine Yersinien-Infektion mit Apoptose in Verbindung gebracht, wobei Caspase-8 die ausführende Caspase-3 aktiviert, welche wiederum durch Spaltung verschiedener Moleküle Zelltod auslöst. Allerdings zeigen neuere Studien, dass während des Yersinien-induzierten Zelltods das porenbildende Protein GSDMD durch Caspase-8 gespalten wird. Der aktive N-Terminus von GSDMD kann Poren in der Zellmembran bilden und somit pyroptotischen Zelltod und die Ausschüttung von Interleukinen auslösen. GSDMD-negative Mausmakrophagen weisen verzögerten Zelltod und eine verringerte IL-1β-Auschüttung auf. Anders als GSDMD scheint das nahe verwandte Molekül GSDME keine Rolle im Yersinien-induzierten Zelltod von murinen Makrophagen zu spielen. Zwar wird es während der Infektion prozessiert, allerdings hat der Verlust von GSDME keinen Einfluss auf Zelltod oder Interleukin-Freisetzung. Da bisher die meisten Studien zu Zelltod nach *Y. enterocolitica* Infektion in Mausmakrophagen durchgeführt wurden, war ein Ziel dieser Arbeit den Yersinien-induzierten Zelltod von humanen Makrophagen zu analysieren.

Die Infektion von primären humanen Makrophagen mit *Y. enterocolitica* führte nach 23 bis 24 Stunden zum Zelltod. Dieser war abhängig von YopP. Zudem wurden diverse, für die Zelltod-Regulation wichtige, Moleküle näher untersucht. Wie auch in Mausmakrophagen wurde die Phosphorylierung von TAK1 in humanen Makrophagen durch YopP verhindert. Folglich ist davon auszugehen, dass auch hier die MAPK und NF-κB Signalwege durch eine Yersinien-Infektion unterbrochen werden. Passend dazu konnte im Rahmen dieser Arbeit gezeigt werden, dass die Freisetzung des Zytokins TNF-α aus humanen Makrophagen signifikant durch YopP reduziert wurde. Zudem führte eine Infektion zu einer YopP-abhängigen Ser-166 Phosphorylierung von RIP1, ganz so wie auch in Mausmakrophagen. Allerdings hatte die Blockierung der Kinaseaktivität von RIP1 durch den Inhibitor Necrostatin-1s 23 Stunden nach Infektion keinen Einfluss auf die Zelltodrate von humanen Makrophagen. Dies weist darauf hin, dass die

Kinaseaktivität von RIP1 für die Auslösung von Zelltod bei humanen Makrophagen offenbar entbehrlich ist. An dieser Stelle ist weitere Forschung notwendig, um zu klären, welche Rolle RIP1 während des Yersinien-induzierten Zelltods von humanen Makrophagen genau spielt. Desweitern wurde im Rahmen dieser Arbeit festgestellt, dass bei einer Yersinien-Infektion sowohl Caspase-8, als auch Caspase-3 in ihre jeweils aktiven Fragmente gespalten wurden. Interessanterweise konnte in humanen Makrophagen keine Spaltung von GSDMD in das aktive, porenbildende Fragment nachgewiesen werden. Dies steht im Gegensatz zu dem, was bereits in verschiedenen Studien in Mausmakrophagen gezeigt werden konnte. Andererseits wurde eine aktivierende Spaltung von GSDME nach Yersinien-Infektion von humanen Makrophagen detektiert. Es ist folglich denkbar, dass die Yersinien-induzierten Pyroptose-Merkmale bei Maus- und humanen Makrophagen unterschiedlich reguliert sind. Um diesem Ansatz weiter nachzugehen, wurden GSDME-defiziente THP-1 Makrophagen generiert. Infektion mit Yersinien für 18 bis 20 Stunden führte bei THP-1 Makrophagen ohne GSDME zu signifikant niedrigeren Zelltodraten im Vergleich zu Wildtypzellen. Dies ist ein weiterer Hinweis darauf, dass GSDME, aber nicht GSDMD, eine Rolle im Yersinien-induzierten Zelltod von humanen Makrophagen spielen könnte, wobei dies in Mausmakrophagen gegensätzlich zu sein scheint.

Im zweiten Teil dieser Arbeit lag der Fokus auf dem pro-apoptotischen Molekül BID bei Yersinien-infizierten Mausmakrophagen. Im Zuge der intrinsischen Apoptose wird BID aktiviert und vermittelt über BAX und BAK die Permeabiliserung der mitochondrialen Membran. Dies führt zu einer Freisetzung verschiedener Moleküle ins Zytosol, unter ihnen Cytochrom C und SMAC. Während Cytochrom C eine wichtige Rolle bei der Aktivierung von Caspase-9 spielt, begünstigt SMAC die Aktivierung von Caspase-3. BID kann zudem von den Caspase-8 im Zuge der extrinsischen Apoptose und von Caspase-1 aktiviert werden. Im Rahmen dieser Arbeit wurde gezeigt, dass eine BID-Defizienz in murinen Makrophagen keinen Einfluss auf die Zelltodrate von Yersinien-infizierten Zellen hatte. Allerdings waren Makrophagen, denen sowohl BID, als auch GSDMD fehlten, besser vor Yersinien-induziertem Zelltod geschützt als nur GSDMD-defiziente Zellen. Die Spaltung von Caspase-8 wurde nicht durch den BID-Verlust beeinflusst, da diese Caspase oberhalb von BID agiert. Im Gegensatz dazu wurden Unterschiede bei der Spaltung von Caspase-9 festgestellt. Bei Yersinien-infizierten BID-negativen Makrophagen wurde vorwiegend das p37 Fragment detektiert, welches durch Caspase-3-abhängige Spaltung entsteht. Bei Wildtyp-Makrophagen konnte sowohl das p37 Fragment also auch das vollständig aktive p35 Fragment von Caspase-9 detektiert werden. Das p35 Fragment entsteht hierbei durch auto-katalytische Spaltung. Eine denkbare Ursache für diesen Unterschied bei der Caspase-9 Aktivierung könnte sein, dass bei BID-defizienten Zellen kein Cytochrom C aus dem Mitochondrium freigesetzt werden kann, welches eine wichtige Rolle bei der Bildung des Apoptosoms und der anschließenden Caspase-9 Spaltung spielt. Das aktive Fragment von Caspase-3 wurde sowohl in Wildtyp- also auch in BID-defizienten

Makrophagen detektiert. Allerdings scheint der Verlust von BID zu einer verzögerten oder verringerten Aktivierung zu führen. Anschließend wurde die Aktivierung von GSDMD nach Yersinien-Infektion untersucht. Das aktive p30 Fragment von GSDMD konnte, interessanterweise, präferentiell in BID-defizienten Makrophagen nachgewiesen werden, während bei Wildtyp-Makrophagen lediglich die inaktiven Fragmente p43 und p21 detektiert wurden. Dieses Ergebnis könnte ein Hinweis darauf sein, dass der Verlust von BID zu einer verstärkten Aktivierung von GSDMD führt, was mit einer verringerten Aktivierung von Caspase-3 über den mitochondrialen Weg in Zusammenhang stehen könnte. Somit scheint BID ein wichtiges Kontrollelement dafür zu sein, dass die sterbenden Zellen präferentiell eher apoptotische als pyroptotische Merkmale aufweisen.

1 Introduction

1.1 The genus *Yersinia*

Bacteria belonging to the genus *Yersinia* are part of the family Yersiniaceae and the order Enterobacterales. They are Gram-negative and appear as either coccoid or rod-shaped cells that are 1 – 3 µm long and 0.5 – 0.8 µm wide. All species except for *Yersinia pestis* are peritrichously flagellated and motile in a temperature range between 22 and 30 °C but not at 37 °C. Furthermore, they are known to be catalase positive, oxidase negative and able to grow under both aerobic and anaerobic conditions between 0 and 45 °C with optimal growth between 25 and 28 °C. *Yersinia* do not form endospores (Fàbrega and Vila, 2012).

While overall there are 20 species belonging to this genus, only three of them are relevant human pathogens. These are *Yersinia pestis*, *Yersinia pseudotuberculosis* and *Yersinia enterocolitica* (McNally et al., 2016, Le Guern et al., 2020). Research shows, that *Y. enterocolitica* split off from a common *Yersinia* ancestor somewhere between 41 and 186 million years ago. The remaining two species are closer related, with *Y. pestis* branching off from Y. p*seudotuberculosis* only 1.500 to 20.000 years ago (Achtman et al., 1999). *Y. pestis* was first isolated in Hong Kong. In June 1894, the two scientists Alexandre Yersin and Sibasaburo Kitasato independently from each other discovered *Y. pestis* as the cause of the plague pandemic at that time (Perry and Fetherston, 1997).

Even though all three *Yersinia* species pathogenic to humans share certain traits, they differ in means of infection and resulting diseases. *Y. pestis* is a zoonotic disease, able to cause different forms of infections, with the main ones being bubonic and pneumonic plague. Three major plague pandemics have been recorded in history, the last one leading to the isolation and identification of the bacterium in 1894 (Perry and Fetherston, 1997). The most common route of infection is via infected rodents, the bacterium's main reservoir, and consequently infected rat fleas (*Xenopsylla cheopis)* that in turn bite and infect humans. Furthermore, spreading via aerosols from human to human is possible in the case of the pneumonic plague (Pechous et al., 2016). Untreated infections have a fatality rate of 30 – 60 % for bubonic plague and 100 % for pneumonic plague. Today, however, treatment with antibiotics is possible and available. Cases of plague are still reported yearly with the highest numbers of infection occuring in the Democratic Republic of Congo, Madagascar and Peru (Bertherat, 2016, WHO, 2022)

Meanwhile, *Y. pseudotuberculosis* and *Y. enterocolitica* infections are mostly caused by ingestion of contaminated food or water (Jalava et al., 2006, Fredriksson-Ahomaa et al., 2007). Infection results in a gastrointestinal disease called yersiniosis, with typical symptoms being fever, abdominal pain and diarrhoea (Tertti et al., 1989, Robert-Koch-Institut, 2019). In the US and the EU, only 0.5 – 1 % of cases

of yersiniosis are caused by *Y. pseudotuberculosis,* with *Y. enterocolitica* being responsible for the majority of infections (Long et al., 2010, ECDC, 2019). Yersiniosis is usually self-limiting.

Even though modes of transmission and resulting diseases differ widely between the three human pathogenic *Yersinia* species, all of them share certain virulence traits. Not only do they all exhibit a tropism for lymphatic tissue, they also all have the ability to evade and silence immune responses of host cells (Cornelis, 1998). In all three species, virulence factors are encoded on both plasmids and on the chromosome. They carry a 70 kb virulence plasmid called pYV (plasmid of *Yersinia* virulence), that cannot be found in non-pathogenic *Yersinia* species. On this plasmid, different proteins that enable infection of host cells are encoded, including so-called Ysc proteins that form a type III secretion system (TTSS). The TTSS pierces the membrane of host cells and enables the transfer of the *Yersinia* outer proteins, short Yops, from the bacteria to the host's cytosol (Cornelis, 2002). These Yops are also encoded on the virulence plasmid and, once translocated to the host cell, they are able to secure extracellular survival in the host organism by inhibiting and silencing the innate immune response (Pha and Navarro, 2016, Viboud and Bliska, 2005).

1.2 *Yersinia enterocolitica*

1.2.1 Classification

Y. enterocolitica was first discovered in the US in 1939, where it was isolated from abscesses and intestinal contents of 5 patients. It was initially called *Bacterium enterocoliticum* but was later renamed to *Yersinia enterocolitica* (Frederiksen, 1964, Schleifstein and Coleman, 1939). As the diverse strains of *Y. enterocolitica* exhibit high heterogeneity, the species is further divided into different biovars and serotypes. Strains are traditionally categorized into 6 biovars (1A, 1B, 2 – 5) based on their biochemical reactions, and additionally divided into 60 serotypes in total. Division into those serotypes is based on variations in O-antigens presented on the bacterial cell wall (Aleksić and Bockemühl, 1984, Wauters et al., 1987). Biovar 1A is the only one that does not possess a virulence plasmid, which renders this biovar supposedly apathogenic. However, studies suggest that certain strains belonging to this biovar can still cause gastrointestinal diseases (Tennant et al., 2003, Bottone, 1999). Of the strains that are pathogenic to humans, serotypes O:3, O:8 and O:9 are most commonly found with 4/O:3 specifically being responsible for the majority of cases of yersiniosis reported in the EU (Pavlidis et al., 2019, Fàbrega and Vila, 2012, Robert-Koch-Institut, 2019).

1.2.2 Yersiniosis and Pathogenesis

Naturally, *Y. enterocolitica* can be found in the intestinal tract of different aquatic and terrestrial animals, with pigs being the bacteria's main reservoir (Fredriksson-Ahomaa et al., 2007). Most commonly,

humans get infected when ingesting contaminated water or food, often pork (Le Guern et al., 2016, Fàbrega and Vila, 2012, Shayegani et al., 1981). This leads to yersiniosis, a disease whose clinical manifestation can differ depending on various factors, including the serotype of infecting strain and the age of the infected person. Mainly though, yersiniosis presents as gastroenteritis. According to the European Food Safety Authority, *Y. enterocolitica* infection is the third most common food-borne disease after infection with *Campylobacter* spp. and *Salmonella* spp. (EFSA et al., 2019).

Once *Y. enterocolitica* is ingested, bacteria travel to the small intestine and the terminal ileum (Hanski et al., 1989). There, they adhere to the follicle associated epithelium and then cross the intestinal barrier by invading microfold (M) cells (Autenrieth and Firsching, 1996, Grützkau et al., 1990). The bacterial proteins YadA, invasin and ail play an important role in these first steps of infection by enabling attachment to the host tissues, triggering intracellular uptake and mediating serum resistance (Pepe and Miller, 1993, Leo and Skurnik, 2011). From M cells on, bacteria invade the underlying Peyer's patches, where they can multiply, cause abscesses and trigger tissue destruction (Carter, 1975, Autenrieth and Firsching, 1996, Grassl et al., 2003). *Y. enterocolitica* can then disseminate further either via the blood stream or the lymphatic system, consequently colonizing mesenteric lymph nodes and inner organs like spleen or liver (Carter, 1975, Trülzsch et al., 2007, Handley et al., 2005). Due to the formation of micro colonies, bacteria are protected against phagocytosis by neutrophils or macrophages. Furthermore, effector proteins can modulate and silence responses of immune cells to secure bacterial survival in the host (Sansonetti, 2004, Pujol and Bliska, 2005, Viboud and Bliska, 2005).

1.2.3 Chromosomally-encoded virulence factors

In order to ensure pathogenicity and survival in host organisms, *Y. enterocolitica* relies on both chromosomally- and plasmid encoded virulence factors, with different chromosomal factors playing important roles in early stages of *Yersinia* infection (Atkinson and Williams, 2016, Straley and Perry, 1995). Some of them are described in the following section.

The aforementioned invasin, for example, is essential for invasion of M cells and subsequently of Peyer's patches. It binds to β-integrins on the surface of host cells and activates several signalling cascades that result in the uptake of the bacterium into cells via reorganisation of the host cell actin cytoskeleton (Grassl et al., 2003, Young et al., 1992, Leong et al., 1990, Clark et al., 1998). Interestingly, expression of invasin is higher between 18 and 25 °C compared to expression at 37 °C, though expression at 37 °C is heightened in an acidic environment (Simonet and Falkow, 1992, Pepe et al., 1994). Invasin plays an important role in the initial invasion of the intestinal mucosa (Pepe and Miller, 1993). Additionally, invasin is able to trigger the production of cytokines in epithelial cells and is involved in inducing autophagy in macrophages (Grassl et al., 2003, Deuretzbacher et al., 2009).

Another virulence factor involved in cell invasion is ail (attachment invasion locus). This protein is expressed in a temperature range between 30 and 37 °C (Miller et al., 1990). Ail does not only play a role in penetration of host cells, it is also responsible for conferring resistance to human serum and thus enabling bacterial survival (Bliska and Falkow, 1992, Pierson and Falkow, 1993). It does that by binding and deactivating different factors of the complement system (Kirjavainen et al., 2008, Miller and Falkow, 1988).

Yst is another chromosomally-encoded virulence factor. It is a heat-stable enterotoxin that was found to be similar to heat-stable *E. coli* enterotoxins (Revell and Miller, 2001). Yst is able to activate the internal guanylate cyclase, which leads to increased levels of cGMP (cyclic guanosine monophosphate) resulting in diarrhoea (Pai and Mors, 1978, Delor and Cornelis, 1992). However, its exact clinical involvement in Yersiniosis remains unclear as Yst is not produced in all infectious *Y. enterocolitica* strains and the corresponding gene can be silenced by other virulence molecules or other factors like temperature (Mikulskis et al., 1994).

Lipopolysaccharide (LPS) is a major component of the outer membrane of Gram-negative bacteria and another important virulence factor in *Y. enterocolitica* (Fenton and Golenbock, 1998, Białas et al., 2012). LPS is comprised of three distinct parts. Lipid A anchors LPS in the outer bacterial membrane and serves as an endotoxin, while the core region consists of different oligosaccharides. The third part, the O-antigen, is a polysaccharide and responsible for dividing *Y. enterocolitica* strains into their respective serotypes (Białas et al., 2012, Skurnik and Toivanen, 1993). The O-antigen is especially important for bacterial virulence and its absence leads to down regulation of invasin expression and blocks ail expression (Bengoechea et al., 2004, Skurnik et al., 1999).

Finally, the highly pathogenic *Y. enterocolica* biotype 1B possesses a siderophore-dependent iron absorption system. This enables the protein yersiniabactin to complex iron ions which in turn allows the bacterium to utilize iron and even grow under conditions where iron is limited in host tissues (Sabina et al., 2011, Carniel, 1999). The genes encoding for this absorption system are part of the so called high-pathogenicity island (HPI), a cluster of genes specific for highly pathogenic strains (Carniel et al., 1996).

1.2.4 pPlasmid-encoded virulence factors

In addition to chromosomally encoded virulence factors, a number of proteins important for *Yersinia* virulence are encoded on the 70 kb virulence plasmid pYV which can be found in all human pathogenic species (Atkinson and Williams, 2016, Cornelis, 2002). Expression of pYV is highest at 37 °C and under low concentrations of calcium (Cornelis et al., 1998). The plasmid harbours genes encoding for a variety

of virulence factors, including YadA (*Yersinia* adhesin A), components of the TTSS and several effector proteins.

1.2.4.1 YadA

YadA plays an important role in establishing contact between bacteria and host cells (Atkinson and Williams, 2016). Its expression is calcium independent and heightened at 37 °C (Skurnik and Toivanen, 1993). YadA is located on the bacterial outer membrane and can cover almost the entire bacterial surface (Pepe et al., 1995, El Tahir and Skurnik, 2001). There, it is able to bind to a variety of extracellular matrix proteins of the host cell, including collagen, fibronectin and indirectly integrin (Tertti et al., 1992, Flügel et al., 1994, Schulze-Koops et al., 1993). This adhesion is important for the injection of effector proteins via the TTSS (Mühlenkamp et al., 2015). Additionally, YadA plays a role in bacteria-bacteria autoagglutination and is consequently involved in the formation of micro-colonies and abscesses (Hoiczyk et al., 2000). Finally, YadA mediates serum resistance as it can bind and thus inactivate factor H of the complement system. Consequently, it is also important for bacterial survival in host organisms (Biedzka-Sarek et al., 2005, China et al., 1993).

1.2.4.2 Type III secretion system

The TTSS is a needle-like structure that is used to transport proteins from the bacterium into the cytosol of host cells (Cornelis, 2002). Function and structure of the TTSS are highly conserved and comparable between different species of pathogenic bacteria, including *Yersinia*, *Salmonella, E. coli* and *Shigella* (Rocha et al., 2018, Troisfontaines and Cornelis, 2005, Hoiczyk and Blobel, 2001). Evolutionary, the structure of the TTSS is related to that of the bacterial flagellum (Abby and Rocha, 2012).

In *Yersinia enterocolitica* the TTSS is comprised of 25 different molecules, mostly so called Ysc proteins (*Yersinia* secretion system), and can be divided into three segments: basal body, needle and pore complex (Dewoody et al., 2013). First, YscC oligomerizes and forms a ring in the outer bacterial membrane. Next, YscD forms a ring in the inner membrane, connecting to the ring in the outer membrane. It then recruits YscJ to complete the inner ring. These two rings comprise the foundation of the basal body (Dewoody et al., 2013, Diepold et al., 2010, Cornelis, 2006). Then, two different complexes form on the cytosolic side of the basal body: an ATPase complex and the export apparatus. While the proteins YscK, YscL and YscN form the ATPase complex, the export apparatus is built up out of YscR, YscS, YscT, YscU and YscV, which are all integral membrane proteins (Dewoody et al., 2013). Meanwhile, YscQ forms a cytosolic ring which associates with the ATPase complex and forms the sorting platform together with YscL and YscK (Lara-Tejero et al., 2011). Once the basal body is assembled, YscF polymerizes and forms a hollow needle structure that extends into the intracellular space while YscP is responsible for regulating the length of that needle (Hoiczyk and Blobel, 2001, Journet et al., 2003). To connect the needle

with the host cell, LcrV (low calcium response protein V or V-antigen) is recruited to its tip and YopB and YopD form the translocation pore that is inserted into the host cell membrane (Neyt and Cornelis, 1999, Mueller et al., 2005). Once the TTSS is fully formed, it is used to inject different effector proteins into host cells, the so-called Yops, which are described in the following chapter.

1.2.4.3 Effector proteins

A variety of Yops is translocated into *Yersinia* infected host cells via the TTSS where they influence a range of different signalling pathways to ensure bacterial survival (Pha and Navarro, 2016).

YopH is a protein tyrosine phosphatase that is involved in inhibiting phagocytosis (Guan and Dixon, 1990, Zhang et al., 1992). It contains an N-terminal domain with a TTSS secretion signal and a substrate targeting domain, and a C-terminal domain with a catalytic centre, a loop-like structure for localisation to focal complexes and a second substrate targeting domain (Ivanov et al., 2005, Viboud and Bliska, 2005). YopH promotes bacterial survival in a variety of ways, including inhibition of phagocytosis by dephosphorylating phosphotyrosine proteins in macrophages (Fällman et al., 1997, Andersson et al., 1996). Additionally, it can antagonize the production of reactive oxygen species in neutrophiles and macrophages (Bliska and Black, 1995). In macrophages, YopH is furthermore able to block production of the proinflammatory cytokine chemoattractant protein 1 (Sauvonnet et al., 2002). Finally, YopH is able to inhibit activation of B and T cells and subsequent production of IL-2 (Alonso et al., 2004, Yao et al., 1999, Sauvonnet et al., 2002).

YopE , YopT and YopO all target different Rho GTPases (Viboud and Bliska, 2005). Rho GTPases are a family of proteins that can bind GTP (guanosine triphosphate) to regulate a variety of cell functions like gene expression or cytoskeleton organization. When these GTPases are bound to GTP, they are in their active state, but if GTP is hydrolysed to GDP (guanosine diphosphate), they become inactive and do not interact with downstream molecules in the respective signalling pathways (Viboud and Bliska, 2005, Barbieri et al., 2002).

As a GTPase activating protein (GAP), **YopE** is able to promote hydrolysis of GTP by introducing a sequence containing arginine into the catalytic site of GTPases. This leads to a change if GTPase confirmation, deactivation and disruption of downstream signalling (Aepfelbacher, 2004). YopE is able to target different GTPases including Rac1, Rho and Cdc42 (Andor et al., 2001). As these are known regulators of the actin cytoskeleton, the YopE activity consequently leads to disruption thereof and to heightened resistance of the bacteria against phagocytosis (Aepfelbacher and Heesemann, 2001, Bliska and Black, 1995, Rosqvist et al., 1990). Additionally, YopE can negatively influence cytokine production by blocking IL-1β maturation by caspase-1 (Schotte et al., 2004).

YopT is a cysteine protease with a Rho GTPases targeting C-terminus that is overall similar to the previously described YopE (Viboud and Bliska, 2005). It plays an important role in the disruption of the host cells' actin structure, inhibition of phagocytosis and induction of cytotoxicitiy (Iriarte and Cornelis, 1998, Fueller and Schmidt, 2008). YopT deactivates Rho GTPases by cleavage of their C-terminal lipid modification, which impairs their anchorage to the cell membrane (Shao et al., 2003, Chung et al., 2016). It has been shown that YopT is able to inactivate RhoA, Rac1 and Cdc42 but it displays a preference for RhoA (Fueller and Schmidt, 2008, Zumbihl et al., 1999, Aepfelbacher, 2004). However, the exact role of YopT remains elusive, as studies have shown that infection of cells with YopT-deficient *Y. enterocolitica* did not alter virulence in comparison to wildtype infection. It is furthermore suggested that YopT may be redundant when YopE is present (Trülzsch et al., 2004, Viboud and Bliska, 2005).

YopO is comprised of three parts: a C-terminal GTPase interaction domain, an N-terminal serine/threonine kinase and a domain for membrane localization (Galyov et al., 1993, Prehna et al., 2006, Grabowski et al., 2017). The protein is inactive upon injection into the host cell but activates its kinase domain after binding to the cell membrane. This is mediated by interaction with actin followed by autophosphorylation of YopO and phosphorylation of its substrate (Juris et al., 2000, Lee et al., 2015, Håkansson et al., 1993). It was shown that YopO can phosphorylate different substrates *in vitro*, including actin and regulators of actin polymerisation, which implies that YopO plays a role in the disruption of the cytoskeleton of host cells (Juris et al., 2002). However, studies in yeast demonstrated that YopO is still involved in bacterial virulence, even if the kinase-activity is silenced (Nejedlik et al., 2004). Comparable to YopE and YopT, the GTPase interaction domain of YopO can interact with Rac1 and RhoA, which blocks their activation. Consequently, YopO also plays a role in disrupting Rac mediated phagocytosis (Dukuzumuremyi et al., 2000, Groves et al., 2010).

YopM is an effector protein without enzymatic function. It is a protein with a leucin rich repeat motif that can be found in the cytosol and the nucleus of infected cells (Viboud and Bliska, 2005, Benabdillah et al., 2004). It plays an important role in virulence as no systemic *Yersinia* infections occur when YopM is absent (Trülzsch et al., 2004). Studies showed that YopM monomers have a horseshoe-like structure and that four monomers adhere, resulting in a structure similar to hollow cylinder (Evdokimov et al., 2001). As an adaptor protein, YopM can form a complex with RSK1 (ribosomal S6 protein kinase) and PKN2 (protein kinase N2). This interaction leads directly to activation of RSK1 and consequently to RSK1-mediated activation of PKN2. This is accomplished by inhibiting dephosphorylation of the kinases' phosphorylation and activation sites (McDonald et al., 2003, Hentschke et al., 2010). Additionally, interaction of YopM with RSK1 leads to increased levels of IL-10 on mRNA and protein level (Berneking et al., 2016, McPhee et al., 2010). In the nucleus, YopM can form a complex with DEAD-box helicase 3 (DDX3), a molecule that regulates its export from the nucleus. This interaction in turn influences levels

of RSK1 phosphorylation in the nucleus and consequently regulates cytokine production (Berneking et al., 2016). Furthermore, YopM influences inflammasome formation. Firstly, it can directly bind to caspase-1 and hence block its activity and downstream inflammasome assembly. Alternatively, YopM, in complex with RSK1 and PKN2, is able to inhibit pyrin by phosphorylation, a molecule that can trigger caspase-1-mediated inflammasome formation upon Rho-GTPase inhibition (Malik and Bliska, 2020, LaRock and Cookson, 2012).

YopQ, also referred to as YopK in *Y. pestis* and *Y. pseudotuberculosis,* has no enzymatic function either but has been shown to play an important role in regulating and limiting translocation of other Yops through the TTSS (Holmström et al., 1995, Dewoody et al., 2011). Absence of YopQ is associated with higher levels of Yops injected into infected cells, whereas overexpression of YopQ leads to decreased Yop levels and cytotoxicity. Studies demonstrated that YopQ regulates the TTSS translocation from within the host cell and that heightened levels of YopQ apparently correlate with smaller translocation pore sizes (Holmström et al., 1997, Dewoody et al., 2011). Additionally, YopQ is involved in promoting bacterial survival in host cells by preventing cellular detection of the TTSS and subsequent inflammasome pathway activation. YopQ has been shown to block activation of caspase-1 and to negatively regulate IL-1β release (Brodsky et al., 2010).

The final effector protein **YopP**, or YopJ in *Y. pestis* and *Y. pseudotuberculosis,* plays an important role in mediating cell death, and more specifically in inducing apoptosis in *Yersinia* infected macrophages (Monack et al., 1997, Ruckdeschel et al., 2004). Early studies showed that firstly, *Yersinia* infection triggers apoptosis through disruption of signalling cascades usually connected to ensuring cell survival, like the NF-κB (nuclear factor-κB) and MAPK (mitogen-activated protein kinase) pathways, and secondly, that production of TNF-α (tumor necrosis factor-α) is inhibited upon infection. Both these functions were attributed to the presence of YopP (Monack et al., 1997, Palmer et al., 1998, Ruckdeschel et al., 1998). Later studies found that YopP acts as a serine/threonine acetyl-transferase to trigger the described effects (Mukherjee et al., 2006). The protein is able to acetylate serine and threonine residues in the activation loop of its substrates. This acetylation blocks phosphorylation at these sites, that would be necessary for activation. Among the substrates that can be acetylated and thus blocked by YopP are MAPKK-6, IKKα and IKKβ. By inhibiting the activities of these molecules YopP can disrupt NF-κB and MAPK signalling and consequently trigger apoptosis in macrophages (Mukherjee et al., 2006, Haase et al., 2005, Paquette et al., 2012, Mittal et al., 2006). Another target of YopP and an important regulator in these pathways is TAK1 (TGF-β-activated kinase-1). TAK1 activity depends on the association with TAB1 (TAK1 binding protein 1) and auto-phosphorylation at Threonine-184 and Threonine-187, which can be blocked by YopP acetylation (Paquette et al., 2012, Haase et al., 2005, Sakurai et al., 2000). This similarly leads to a disruption of NF-κB and MAPK signalling. Additionally, inhibition of the

described pathways leads to a YopP mediated decrease in production of proinflammatory cytokines, including TNF-α, IL-6 and IL-8, which in turn downregulates the host's immune response (Ruckdeschel et al., 2008). Furthermore, it was described that YopP is able to block caspase-1 activation in macrophages, hence inhibiting inflammasome formation downstream (Schoberle et al., 2016). Other studies found additional functions for YopP, including inhibition of immunomodulatory lipid prostaglandin E2 (PGE2) via MAPK signalling pathways and involvement in intestinal barrier dysfunction via blockage of TAK1 and modulation of NOD2 (nucleotide oligomerization domain 2) signalling (Sheppe et al., 2021, Meinzer et al., 2012).

1.3 Innate immunity and macrophages

The mammalian immune system can be divided into adaptive and innate immunity. Adaptive immunity mainly plays a role in elimination of pathogens in later stages of infection, and it is comprised largely of antibodies and T and B cells that express antigen-specific receptors. It is also responsible for forming the immunological memory which allows the system to react faster upon repeated encounter with the same pathogen (Kawai and Akira, 2006, Rink et al., 2012, Medzhitov and Janeway, 2000). The innate immune system, on the other hand, is highly evolutionary conserved and often referred to as the first line of immunological defense (Rink et al., 2012). There is a variety of cells involved in forming the innate immune system, including granulocytes, dendritic cells and macrophages. The latter develop from monocytes that circulate in the blood stream and eventually migrate into different tissues where they differentiate to macrophages. They play an important role in immunological defense as they can engulf pathogens into intracellular phagosomes which then fuse with lysosomes, where the pathogens are degraded. Additionally, macrophages can induce immune responses in other cells by releasing inflammatory cytokines (Bröker et al., 2019). In order to recognise pathogens, macrophages and other immune cells express pattern recognition receptors (PRRs) on their surface. These PRRs can bind and recognise different pathogen-associated molecular patterns (PAMPs), sometimes also referred to as MAMPs (microorganism-associated molecular patterns). These can be bacterial membrane compounds or microbial nucleic acids (Medzhitov and Janeway, 2000, Kaisho and Akira, 2006). An important class of PRRs are the so-called toll-like receptors (TLR). Each receptor is comprised of a domain called leucin-rich repeat that is responsible for recognizing pathogens, and an intracellular region, the TIR (Toll/IL-1 receptor) domain. The TIR domain plays a key role in signal transduction and activation of different pathways like of MAPKs and NF-κB. This subsequently leads to release of inflammatory cytokines. The different TLRs mediate recognition of different kinds of PAMPs, including nucleic acids, lipids or proteins. TLR4, for example, is responsible for recognizing lipid A of LPS, an important part of the outer membrane of Gram-negative bacteria, including *Y. enterocolitica* (Kawai and Akira, 2006). Another sub-

group of PRRs is comprised of NOD1 and NOD2. These receptors have a Nod domain and a CARD domain (caspase activation and recruitment domain). Like TLRs, they are able to activate MAPK and NF-κB signalling pathways after PAMP recognition (Inohara and Nuñez, 2003, Kaisho and Akira, 2006).

1.4 Programmed cell death

Eukaryotic cells can die in a number of ways, including accidental and spontaneous forms (necrosis) and in highly regulated and induced manners. The latter are referred to as modes of programmed cell death (PCD). PCD plays an important role in many cellular functions, including host defense against pathogens, embryonic development and the removal of damaged, altered or superfluous cells. There is a variety of distinct forms of PCD, with the most well-studied being apoptosis, necroptosis and pyroptosis. However, numerous studies have shown that there can be a lot of crosstalk between the separate pathways and that differentiation of function and involvement can be difficult (Snyder and Oberst, 2021, Wang and Kanneganti, 2021).

1.4.1 Apoptosis

Of the three forms of PCD mentioned above, apoptosis was discovered first and has since then been extensively studied (Kerr et al., 1972). There are several morphological characteristics exhibited by cells undergoing apoptosis, including pyknosis (shrinkage of the nucleus), DNA degradation, membrane blebbing and the formation of so-called apoptotic bodies. Traditionally, apoptosis was thought to be immunologically silent, as this pathway prevents the release of inflammatory signalling molecules and cytosolic content by packing the cellular contents into vesicles, that are then removed by phagocytes. Thus, no immune responses by neighbouring cells are triggered. Today however, it has become evident that PCD is too complex to allow a clear separation between inflammatory and non-inflammatory pathways (Kerr et al., 1972, Taylor et al., 2008, Snyder and Oberst, 2021).

Apoptosis can be triggered via two different routes. **Intrinsic apoptosis** describes the mitochondria-dependent pathway that can be caused by a variety of cell-intrinsic stressors like reactive oxygen species, DNA damage or compromising the endoplasmatic reticulum (Snyder and Oberst, 2021). All these factors then influence the composition of a specific protein family termed Bcl-2 (B-cell lymphoma 2). Proteins of this family can be divided into three different groups: the pro-survival proteins (e.g. MCL-1, BCL-2, BCL-XL), the pro-apoptotic proteins (e.g. BIM, BID), and the effector proteins (BAX, BAK) (Kalkavan and Green, 2018, Czabotar et al., 2014). If the balance of this protein family is shifted in favour of pro-apoptotic proteins by intrinsic stimuli, the effector proteins are activated and cause mitochondrial outer membrane permeabilization (MOMP) (Green and Kroemer, 2004). Through MOMP, different pro-apoptotic molecules are released into the cytosol, including cytochrome C and SMAC (second mitochondria-derived activator of caspases) (Tait and Green, 2010). SMAC is responsible for

inhibiting the pro-survival molecules XIAP (X-linked inhibitor of apoptosis) and cIAP (cellular inhibitor of apoptosis protein), whose function is to suppress the activities of caspases-9, -7 and -3 (Jost et al., 2009). Cytochrome c on the other hand interacts with the APAF-1 (apoptotic protease activating factor-1), which subsequently changes conformation and binds and activates caspase-9 via its caspase recruitment domain (CARD) by forming a heptameric complex (Li et al., 1997, Cain et al., 2002, Shiozaki et al., 2002, Acehan et al., 2002). Caspase-9, in turn, is responsible for activation of caspases-3 and -7, so called executioner caspases. They then cleave a variety of cellular substrates and thus trigger cell death and the display of apoptotic characteristics described above (Snyder and Oberst, 2021).

As evident from the description of this pathway, caspases play an important role in PCD (Kesavardhana et al., 2020). They are a highly conserved family of cysteine proteases that can cleave their substrates after aspatic acid residues (Man and Kanneganti, 2016, Lamkanfi et al., 2002). They are comprised of a C-terminal caspase-domain that is responsible for proteolytic cleavage and, in some cases, a non-enzymatic N-terminal domain that can function as a CARD domain or a death effector domain (DED) (Kesavardhana et al., 2020). All caspases first exist as inactive zymogens (pro-caspases), that need to be activated through di- or oligomerization in order to carry out their enzymatic functions. Members of the family of caspases can be divided into three groups. Caspases-2, -8, -9 and -10 are called initiator caspases, they are activated by different pathways and relay the signal by activating the so-called effector caspases (caspases-3, -6, -7). Like described above, their function is the cleavage of cellular substrates which results in cell death. Finally, several caspases are grouped together and referred to as inflammatory caspases (caspases-1, -4, -5, -11, -12). These have several functions in other, non-apoptotic pathways (Man and Kanneganti, 2016, Kesavardhana and Kanneganti, 2017).

The **extrinsic pathway** is also referred to as death receptor-mediated apoptosis (Ketelut-Carneiro and Fitzgerald, 2022). It is triggered by extracellular signals binding to specific death receptors (DR) on the plasma membrane of immune cells (Walczak, 2013). Each so-called death ligand is recognized by its respective DR, with, for example, TNF binding to TNFR1/2, TRAIL (TNF-related apoptosis-inducing ligand) binding to DR4 and DR5, and Fas/CD95 binding to FasL (Walczak, 2011, Wajant, 2014, de Miguel et al., 2016, Pan et al., 1997). These interactions on the cell surface trigger apoptosis. First, adaptor proteins, like FADD (Fas-associated death domain) or TRADD (TNFR1-associated death domain), are recruited to the DR, with the underlying ligand-receptor combination being responsible for the exact composition of the recruited adaptors (Chinnaiyan et al., 1995, Hsu et al., 1995). Next, these adaptor proteins trigger assembly of the death-initiating signalling complex (DISC), which recruits pro-caspase-8 via its DED (Ramirez and Salvesen, 2018, Tummers and Green, 2017). Another important part of this complex is RIP1 (receptor-interacting serine/threonine-protein kinase 1), a key regulator in multiple cell death pathways (Micheau and Tschopp, 2003). Posttranslational modifications of RIP1, depending

on ubiquitination and phosphorylation, are responsible for downstream signalling and ultimately the cell fate, with auto-phosphorylation of RIP1 at Ser-166 being essential for inducing cell death (Laurien et al., 2020). Once complex formation is complete, it enables autocatalytic activation of caspase-8. Thereafter, caspase-8 is able to cleave and hence activate effector caspases-3 and -7, which then go on to induce apoptosis. Alternatively, caspase-8 can cleave BID (BH-3-interacting domain) into its active form tBID. As a pro-apoptotic member of the Bcl-2 family, tBID then triggers MOMP via BAK and BAX. This again amplifies the apoptotic process (Jost et al., 2009, Kaufmann et al., 2012).

Even though the initial triggers differ, the ability of extrinsically induced caspase-8 to activate pathways of intrinsic apoptosis via BID cleavage and MOMP, shows, that both modes of apoptosis are interconnected. In general cells that undergo apoptosis only through activation of caspase-8 and caspase-3 are classified as type I cells, whereas cells that additionally rely on caspase-8-mediated MOMP to undergo apoptosis are referred to as type II (Kesavardhana et al., 2020). In Figure 1 the molecular mechanisms of apoptosis are depicted.

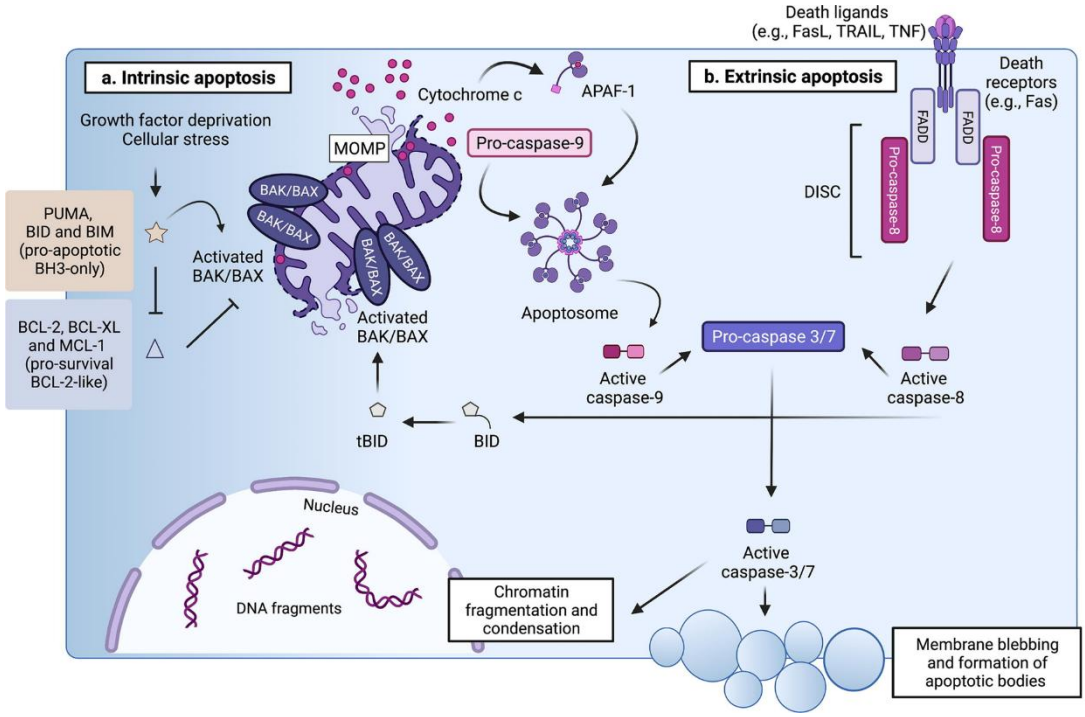

Figure 1: Schematic overview of intrinsic and extrinsic apoptotic signalling pathways. Details are described in the text above (1.4.1). Figure adapted from (Ketelut-Carneiro and Fitzgerald, 2022).

1.4.2 Necroptosis

Several years after the first description of apoptosis, another form of programmed cell death was discovered. It was termed necroptosis (Degterev et al., 2005). This variant of PCD differs from apoptosis in multiple ways. It is a form of lytic cell death that is independent of caspases. First morphological characteristics of cells dying by necroptosis are organelle swelling and influx of water, followed by

rupture of the plasma membrane. This leads to the release of DAMPs (damage-associated molecular patterns) that can subsequently trigger an immunological response in other cells, leading to inflammation (Vandenabeele et al., 2010, Kaczmarek et al., 2013).

Mechanistically, necroptosis relies on the kinase activity of the key molecules RIP1 and RIP3 (Holler et al., 2000). RIP1 interacts with RIP3 via their respective RHIM (RIP homotypic interaction motif) domains and both kinases form a complex that is referred to as the necrosome (Li et al., 2012). As part of this complex, RIP3 is able to first self-activate via autophosphorylation, and secondly to phosphorylate the effector protein MLKL (mixed lineage kinase domain-like) at Thr-357 and Ser-358, which leads to its activation. MLKL can then undergo multimerization and form pores in the plasma membrane, which leads to influx of water and consequent cell death by lysis (Sun et al., 2012, Huang et al., 2017).

Studies showed that under physiological conditions necroptosis can be inhibited by the presence of caspase-8 and cFLIP (cellular FLICE-inhibitory protein) (Kaiser et al., 2011, Oberst et al., 2011). Necroptosis initiation then depends on the mode of cell activation and its connection to the induction of apoptosis. TNF signalling in the form of TNF binding to its respective receptor TNFR1, triggers formation of the so-called complex I. This complex is comprised of TRADD, FADD, TRAF (TNFR-associated factors), cIAP1 and cIAP2 and finally the key signalling molecule RIP1. TRAF and cIAPs mediate ubiquitination of RIP1 which leads to the activation of NF-κB signalling and the promotion of cell survival. However, if this ubiquitination is either blocked or removed by CYLD (cylindromatosis protein), RIP1 disassociates from complex I and forms complex II by recruiting TRADD, FADD and pro-caspase-8. This leads to activation of caspase-8 which consequently triggers apoptosis. In case of absence or inhibition of caspase-8 though, RIP1 instead recruits RIP3 to form the necroptosome and triggers necroptosis as described above (Meng et al., 2021, Ketelut-Carneiro and Fitzgerald, 2022, Vandenabeele et al., 2010). Alternatively, RIP3 can also be activated directly through a signalling molecule binding to TLR3 and TLR4 and recruitment of TRIF (TIR-domain-containing adapter-inducing interferon-β), as TRIF possesses a RHIM domain (Kaiser and Offermann, 2005). Additionally, it has been shown that necroptosis can be induced upon virus infection by ZBP1, a cytoplasmic DNA sensor that contains a RHIM domain and is therefore able to promote formation of the necroptosome (Rebsamen et al., 2009). These different methods of activation suggest that necroptosis might serve as a backup mechanism in case cell death via apoptosis is blocked through pathogenic infection (Pearson and Murphy, 2017). Below, a schematic overview of the molecular mechanisms of necroptosis can be found (Figure 2)

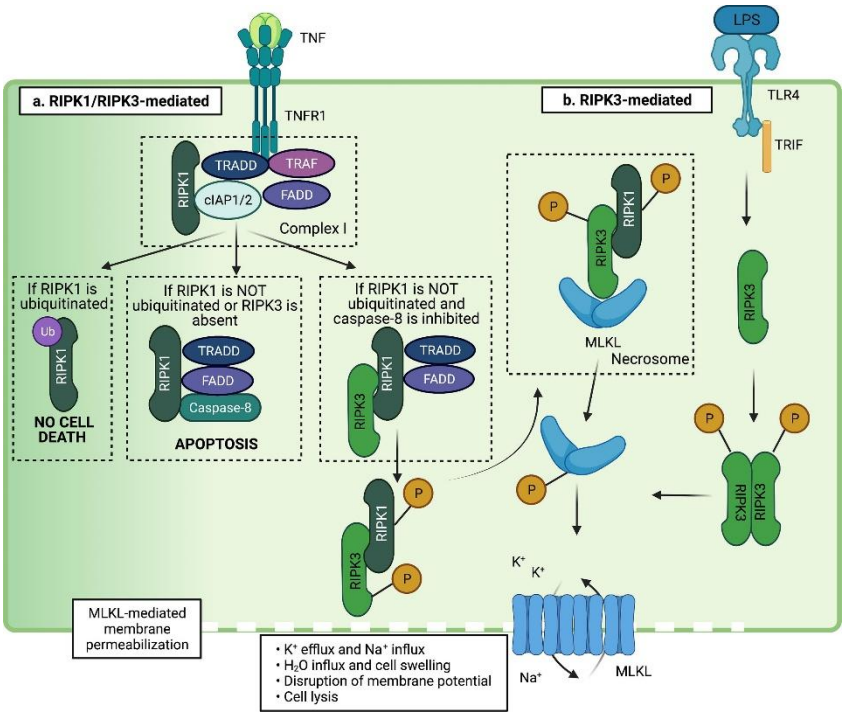

Figure 2: Schematic overview of necroptotic cell death pathways. Details are described in the text above (1.4.2). Figure adapted from (Ketelut-Carneiro and Fitzgerald, 2022).

1.4.3 Pyroptosis

Pyroptosis was first observed in 1992 and originally described as a form of lytic cell death, that is caspase-1-dependent and independent of signalling via DR or TLR (Brennan and Cookson, 2000, Fink and Cookson, 2006, Kovacs and Miao, 2017). The term is derived from the Greek words *pyros* for fire and *ptosis* for falling (Kesavardhana et al., 2020). Pyroptosis can be set off by a variety of different triggers, including PAMPs or products of cellular stress (Lamkanfi and Dixit, 2014). It plays an important role in host defense against pathogens. More specifically, pyroptosis has a protective effect against intracellular infection as pathogens get trapped inside dying host cells that are consequently eliminated through efferocytosis (Jorgensen et al., 2017). Additionally, pyroptotic cell death is pro-inflammatory. In turn, different pathogens have developed ways to hinder activation of this cell death pathway (Bergsbaken et al., 2009). Like necroptosis, pyroptosis results in pore formation, and cell death via this pathway is characterised by influx of fluids into the cell, membrane rupture and release of DAMPS and inflammatory cytokines that subsequently trigger an immunological reaction and recruit other cells of the immune system to the site of inflammation (Kesavardhana et al., 2020, Snyder and Oberst, 2021). There are two distinct pathways that induce pyroptosis, the canonical and the non-canonical pathway. Comparable to apoptosis, caspases play a key role in both pathways, though they are distinct from those involved in apoptotic signalling (Jorgensen and Miao, 2015).

The **canonical inflammasome activation** is dependent of caspase-1 and is set in motion through PAMPs connected to infection (Lamkanfi and Dixit, 2014). These signals lead to the formation of inflammasomes, multiprotein complexes comprised of a number of varying proteins, like AIM2 (absent in melanoma 2) and members of the NLR (nucleotide-binding domain like receptor) family like NLRP3 or NLRP4. These latter factors are most likely activated in an indirect manner. NLRC4 is activated by sensor molecules called NAIPs (NLR family apoptosis inhibitory protein) that are able to recognise bacterial components like flagellin or parts of the secretion system that are present in the cytosol. NLRP3 can be indirectly triggered by a variety of DAMPs and PAMPs (Zhao and Shao, 2015, Vance, 2015, Cullen et al., 2015). AIM2, on the other hand, contains a HIN2000 domain that can directly sense double-stranded DNA which leads to integration of this factor into the inflammasome. After the assembly, the pyrin domains of AIM2 and NLRP3 are responsible for recruiting the adaptor ASC (apoptosis-associated speck like protein containing a CARD), which in turn recruits pro-caspase-1 via their respective CARD domains (Srinivasula et al., 2002, Hornung et al., 2009). Caspase-1 recruited to inflammasomes is activated via autocatalytic cleavage and then able to activate the effector protein of pyroptosis: gasdermin D (GSDMD) (Snyder and Oberst, 2021). Studies showed that inflammasomes can differ regarding their exact composition, which reflects variations in their activating triggers and their downstream targets (Ketelut-Carneiro and Fitzgerald, 2022).

The **non-canonical pathway** that results in pyroptosis relies on the murine caspase-11 or its human orthologs caspases-4 and -5. These caspases are able to recognise intracellular LPS, an important component of the outer membrane of Gram-negative bacteria (Kayagaki et al., 2015, Hagar et al., 2013). This leads to caspase-11 or caspases-4 and -5 dimerization and activation. Once activated, caspase-11 or caspases-4 and -5 are able to activate GSDMD, similar to caspase-1 (Kayagaki et al., 2015).

GSDMD is consequently the executing protein of pyroptosis and the point where the canonical and the non-canonical pathways merge. It is comprised of an active N-terminal domain (p30) and a C-terminal domain with an autoinhibitory function (p20) (Kayagaki et al., 2015). The caspases activated upstream can cleave the linker region between these domains which results in release of the N-terminal domain that then oligomerises and forms pores in the cell membrane (Shi et al., 2015, Liu et al., 2016). Through these pores, cytokines like IL-18 and IL-1β are released to cause inflammatory stimulation in neighbouring cells. However, only caspase-1 can promote maturation of these interleukins into their active form. If pyroptosis is executed noncanonically, the efflux of potassium ions (K^+) after GSDMD pore formation promotes formation of NLRP3 inflammasomes, thus resulting in caspase-1 activation and interleukin maturation (Sims and Smith, 2010, Rühl and Broz, 2015). Studies have shown that GSDMD pores are also responsible for the release of these cytokines from living cells, for example prior to pyroptosis (Kesavardhana et al., 2020). In contrast to its function in macrophages, GSDMD seems to have an anti-

inflammatory effect in neutrophils. There, it is cleaved in a caspase-independent manner by ELANE (elastase, neutrophil expressed) but not in the same position as cleavage by caspases occurs (Kambara et al., 2018). Another molecule of the gasdermin family, that is involved in pyroptosis is gasdermin E (GSDME), which was originally referred to as DFNA5 (deafness, autosomal dominant 5). Like GSDMD, GSDME has an N-terminal domain that forms pores in the cell membrane, but this protein is activated by caspase-3, an effector caspase of apoptosis (Wang et al., 2017). This activation can switch cell death by apoptosis to pyroptosis or it can mediate secondary necrosis. Additionally, caspase-3 can deactivate GSDMD through cleavage in its N-terminal domain which again reflects the extensive crosstalk between the separate ways of programmed cell death (Rogers et al., 2017).

A schematic overview of pyroptotic cell death is shown below (Figure 3).

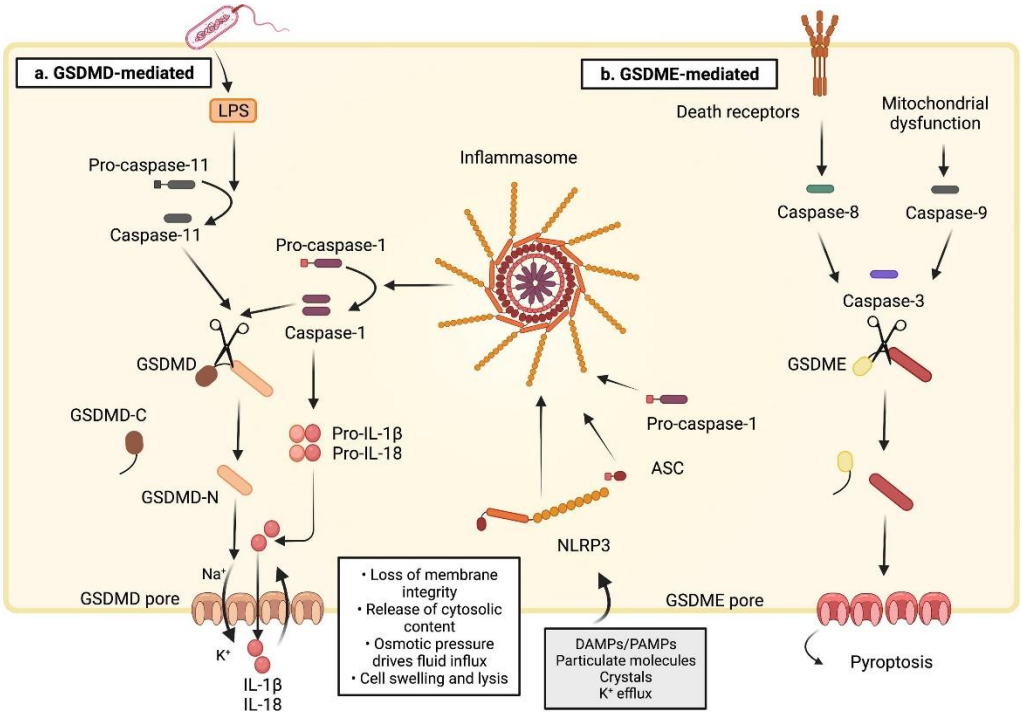

Figure 3: Schematic overview of pyroptotic cell death pathways. Details are described in the text above (1.4.3). Figure adapted from (Ketelut-Carneiro and Fitzgerald, 2022).

1.4.4 Gasdermins

GSDMD, the executive protein of pyroptosis, and GSDME are members of the gasdermin family. Their name is derived from the expression pattern observed for gasdermin A (GSDMA), which is in the gastrointestinal tract and the dermis (Broz et al., 2020, Feng et al., 2018). There are six members of the gasdermin family, that can be found in humans: GSDMA, GSDMB, GSDMC, GSDMD, GSDME and PJVK (pejvakin). In contrast, there are 10 gasdermins expressed in mice. While GSDMB cannot be found, mice express three homologs of GSDMA and four homologs of GSDMC in addition to one each of GSDMD, GSDME and PJVK (Feng et al., 2018). All gasdermins except PJVK are comprised of an

autoinhibitory C-terminal domain and an N-terminal domain that has the ability to form pores in cell membranes (Lieberman et al., 2019). The linker region where both domains are cleaved, however, differs from one protein to the next which implies that they are also activated by different molecules (Shi et al., 2015, Kesavardhana et al., 2020). Expression of gasdermins is mostly detected in immune cells, the skin and the gastrointestinal tract which implies an immunological function (Feng et al., 2018).

Of all gasdermin family members, GSDMD remains the best studied one. It was first identified as playing a key role in pyroptosis, as studies showed that pyroptosis downstream of canonical inflammasome activation and release of IL-1β are diminished in GSDMD-deficient cells (Shi et al., 2015). Full-length GSDMD is comprised of 480 amino acids. Its linker region that connects the functional N-terminal domain to the inhibitory C-terminal domain, can be cleaved by caspase-1 and caspases-4/-5 and -11 in the process of pyroptotic cell death (Kayagaki et al., 2015). This cleavage leads to the release of the 30 kDa big pore-forming part of the protein. Recently it has been shown that caspase-8 also has the ability to activate GSDMD through cleavage. Though traditionally associated with apoptosis, studies demonstrated that active caspase-8 cleaves GSDMD upon infection of cells with *Yersinia*. This leads to the generation of the pore-forming fragment and pyroptosis (Sarhan et al., 2018, Demarco et al., 2020). Additionally, caspases-3 and -7-mediated cleavage of GSDMD at aspartate 88 results in the generation of an inactive 43 kDa fragment, that is unable to form pores. Thus, these apoptotic caspases seem to have an inhibitory effect on pyroptosis (Taabazuing et al., 2017).

Another member of the gasdermin family involved in PCD is GSDME. Its original name DFNA5 stems from the connections found between mutations in the *Gsdme* gene and heritable deafness. Expression of GSDME can be localised to kidney, heart and brain (Laer et al., 1998). GSDME is structurally similar to GSDMD, with the difference that caspase-3 could be identified as its activator. Once these caspases release the N-terminal domain, pore formation occurs, which leads to lytic cell death. As caspase-3 is also an executioner caspase of apoptosis, this mechanism might be a strategy to trigger inflammatory cell death when required to fight pathogens. Alternatively, it plays a role in secondary necrosis after cells undergo apoptosis (Rogers et al., 2017, Wang et al., 2017, Feng et al., 2018).

The details of pore formation by gasdermins have been the focus of various studies. It could be shown that in full-length GSDMD, the C-terminus is inserted into the N-terminal domain which leads to stabilisation of the protein and autoinhibition until cleavage in the linker region (Kuang et al., 2017, Liu et al., 2019). Upon its release, the N-terminus forms a pore through oligomerisation of presumably 16 monomers for most gasdermins, though a formation with 24 monomers has been proposed for GSDMD (Ding et al., 2016, Aglietti et al., 2016). The exact mechanisms of pore formation and insertion into the plasma membrane remain unresolved, however it has been shown that the pore forming domain can interact with and bind to membrane lipids like cardiolipin and phosphoinositides (Ding et al., 2016).

Different studies have focused on the size of the formed pores and reported inner diameters of either 10 – 14 nm or 21 nm (Ding et al., 2016, Sborgi et al., 2016). This size enables the passage of water, different ions and interleukins like IL-1β and IL-18 (Kesavardhana et al., 2020). As mentioned above, GSDMD pores are involved in interleukin release from living cells and pore formation does not always result in cell death. If there is only a small number of pores in the cell membrane, influx of calcium leads to the activation of the ESCRT (endosomal sorting complexes required for transport) machinery which initiates membrane repair and pore removal (Rühl et al., 2018). However, a higher amount of GSDMD pores leads to membrane rupture, cell death and release of cytosolic content (Kovacs and Miao, 2017).

1.4.5 Crosstalk between programmed cell death pathways

As already mentioned above, pathways of programmed cell death are interconnected in various ways. A key player in this PCD network is **RIP1**, which is not only important for determining the mode of cell death but also for promoting cell survival (Schwarzer et al., 2020). It can be ubiquitinated by various molecules which inhibits the assembly of the death-inducing complex II and therefore leads to survival of the cell (Peltzer et al., 2016, Feltham and Silke, 2017). Another important regulatory mechanism of RIP1 is phosphorylation. One study identified MK2 (MAPKAP kinase-2) as able to phosphorylate RIP1 at serine 321 upon infection or pro-inflammatory stimulation. This phosphorylation blocks autophosphorylation of RIP1 and consequently inhibits its kinase activity, resulting in the promotion of cell survival (Menon et al., 2017). Furthermore, IKKα, IKKβ, IKKε and TBK1 were found to phosphorylate RIP1 in complex I upon TNF induced signalling. These phosphorylations also confer protection from RIP1 kinase-activity dependent cell death (Dondelinger et al., 2015, Lafont et al., 2018).

Another important regulator of cell fate is **caspase-8**. Besides its traditional role as an initiator for apoptosis, caspase-8 was found to regulate a variety of cell death related signalling pathways. Different studies identified RIP1 as a substrate of caspase-8 mediated cleavage. This cleavage results in inhibition of RIP3- and MLKL-mediated necroptosis and overall blocks excessive cell death through RIP1 signalling. It also plays an important role during embryonic development (Newton et al., 2019, Lalaoui et al., 2020).

Detailed ways of crosstalk between the three main forms of PCD are in the following separately described in pairs of interacting pathways.

Connections between **apoptosis and necroptosis** were already mentioned in 1.4.2. as absence of apoptotic caspase-8 leads to RIP1 being recruited to the necroptosome with RIP3 (Ketelut-Carneiro and Fitzgerald, 2022). Thus, overall crosstalk between these pathways is highly dependent on the master regulator caspase-8. Deficiency of caspase-8 in mouse embryos is lethal, but deletion of both caspase-

8 and RIP3 promotes survival which demonstrates that caspase-8-mediated inhibition of necroptosis is crucial for embryonic development (Kaiser et al., 2011). Studies showed that this inhibition depends on the catalytic activity of caspase-8 and on its ability to cleave RIP1 at Asp-324 which stops the formation of a death-inducing complex (Newton et al., 2019). Cleavage of RIP1 has been shown to inhibit NF-κB activation which may promote TNF-induce apoptosis (Lin et al., 1999). Additionally, RIP3 was identified as a target of caspase-8-mediated cleavage when apoptosis is induced (Feng et al., 2007). Another study focused on small-molecule inhibitors of necroptosis and found that these compounds trigger interaction of RIP3 with RIP1 which in turn leads to activation of caspase-8 and the assembly of a pro-apoptotic complex comprised of caspase-8, FADD and cFLIP (Mandal et al., 2014). In summary, these pathways are tightly connected and RIP1 and caspase-8 strongly influence if cells undergo necroptosis or apoptosis. It has recently been suggested that the cell fate might also depend on the levels of RIP1 expression, with high levels corresponding to necroptosis and low levels to apoptosis (Li et al., 2021).

Apoptosis and pyroptosis also exhibit areas of overlap. As described in 1.4.4, the apoptotic caspase-8 is able to cleave GSDMD, the executioner of pyroptosis, while caspase-3 can not only activate the related GSDME but also inhibit GSDMD (Wang et al., 2017, Rogers et al., 2017, Sarhan et al., 2018, Taabazuing et al., 2017). But the crosstalk between these pathways does not end there. For one, it has been shown that in absence of GSDMD, caspase-1, a key player in canonical inflammasome formation, is able to cleave BID, a member of the Bcl2 family. As upon intrinsic apoptotic signalling, cleavage of BID leads to MOMP and activation of caspases-9 and -3 which results in apoptosis and GSDME-mediated secondary necrosis. This study also found that apoptosis can be triggered in a similar manner in cells that have low GSDMD expression (Tsuchiya et al., 2019). A similar study also found that caspase-1 mediated BID truncation leads to MOMP when GSDMD is absent in murine macrophages. But while this work illustrated that caspase-1, BID and caspase-3 are necessary in this case, they reported a redundancy for caspase-8 and caspase-9 in processing caspase-3 and did not find GSDME to play a role in consequent secondary necrosis (Heilig et al., 2020).

Additionally, the apoptotic effector caspase-7 was identified as a substrate for caspase-1 mediated cleavage. Mapping of the cleavage site suggests that caspase-1 is able to activate caspase-7 to trigger apoptosis (Lamkanfi et al., 2008). Furthermore, the interactions between caspase-8 and the formation of different inflammasomes showed additional points of intersection between apoptosis and pyroptosis. One study showed that the Naip5 / NLRC4 /ASC inflammasome can recruit caspase-8 after infection with bacteria positive for flagellin. This recruitment can result in activation of caspase-8, but only in the absence of caspase-1 or GSDMD, which suggests that this interaction acts as a back-up mechanism for cell death when important molecules of pyroptosis are blocked (Mascarenhas et al., 2017). Caspase-8

was also described as being able to promote ASC inflammasome formation and thus caspase-1 mediated pyroptosis when necroptosis and apoptosis are inhibited. This function was independent from the catalytic activity of caspase-8 (Fritsch et al., 2019). Another study found that absence of caspase-8 also impairs activation of caspases-1 and -11 downstream of NLRP3 inflammasome formation and that deletion of caspase-8 and FADD decreases IL-1β release in mice. These results suggest another area of overlap and cross regulation (Gurung et al., 2014). Lastly, one study found a connection between these two pathways based on the channel-forming protein Pannexin-1. This glycoprotein can be activated through cleavage mediated by caspases-3 and -7. Its activity is responsible for triggering formation of the NLRP3 inflammasome in the course of apoptosis (Chen et al., 2019).

Pyroptosis and necroptosis are comparable as they both are lytic ways of cell death. Studies have shown that cells undergoing necroptosis still exhibit activation of IL-1β and IL-18, which is a traditional characteristic of pyroptosis. This finding indicates that there are connections between these two pathways. Necroptosis-mediated MLKL pore formation leads to potassium efflux which in turn triggers formation of the NLPR3 inflammasome and consequently maturation of interleukins through caspase-1. This results in GSDMD-independent release of these cytokines (Gutierrez et al., 2017, Kang et al., 2013). Additionally, in absence of caspase-8, NLRP3 inflammasome formation can be triggered by LPS in a manner that is dependent on the necroptotic key molecules RIP3 and MLKL (Kang et al., 2013).

Overall, crosstalk between forms of PCD is extensive and still an active field of study. These connections between cell death pathways are especially important in situations where one or more pathways are blocked due to pathogen infection (Snyder and Oberst, 2021).

1.5 *Yersinia* induced cell death

Infection with *Yersinia* leads to inhibition of the host immune signalling and triggers programmed cell death, though the exact mechanisms and the question whom this cell death benefits, remain the focus of various studies. The bacterium is overall commonly used to study the crosstalk between cell death pathways, as it has become apparent that *Yersinia* mediated cell death is reliant on components connected to different forms of PCD (Snyder and Oberst, 2021). So far, the majority of studies has been conducted in mouse immune cells, mostly macrophages.

Early research into this field reported, that infection with *Y. enterocolitica* leads to apoptosis in murine macrophages as dying cells exhibited typical signs of this form of cell death, like cellular and nuclear shrinking and the formation of apoptotic bodies. They also found, that YopP is responsible for these effects as infection with YopP deficient bacteria did not lead to cell death (Mills et al., 1997).

In general, *Yersinia* infection triggers cell death through recognition of LPS in the bacterial outer membrane by TLR4 and consequently the adapter molecules FADD and TRIF. It has been shown that absence

of TLR4 protects cells from *Yersinia* induced cell death (Haase et al., 2003, Ruckdeschel et al., 2004, Weng et al., 2014). Downstream, the receptor signalling triggers recruitment of RIP1 to complex I which can then lead to activation of cell survival pathways, namely NF-κB and MAPK signalling (Kelliher et al., 1998). However, blockage of these signalling pathways leads to formation of the death inducing complex IIa with caspase-8. In the case of *Yersinia* infection, this blockage is conferred by the effector protein YopP, which is able to acetylate TAK1 and thus inhibits its activating auto-phosphorylation at Thereonin-184 and Threonin-187. As TAK1, in complex with TAB1 and TAB2, is responsible for activating MAPK and NFκB pathways, its inhibition leads to blockage of cell survival signalling (Haase et al., 2005, Paquette et al., 2012, Sakurai et al., 2000). Consequently, *Yersinia* infection decreases cytokine production and release and triggers programmed cell death in a YopP-dependent manner (Peterson et al., 2017, Philip et al., 2014, Monack et al., 1997). Disassociation of RIP1 from complex I can either lead to formation of complex IIa and apoptosis, or RIP1 can form complex IIb with RIP3 and trigger MLKL mediated necroptosis. Studies showed that YopP mediated cell death is dependent on RIP1, caspase-8 and FADD but not on RIP3 (Philip et al., 2014, Malireddi et al., 2020a). In line with that, deletion of RIP3 and MLKL does not protect cells from *Yersinia* induced cell death, however absence of both RIP3 and caspase-8 confers a protective effect. Additionally, RIP1 deficiency leads to an increase in active, phosphorylated MLKL, indicating that RIP1 inhibits the necroptotic pathway. These results suggest that necroptosis is not the main pathways activated upon infection but merely a backup if other key molecules are blocked (Sarhan et al., 2018, Malireddi et al., 2020a). Traditionally, RIP1, caspase-8 and FADD are connected to extrinsic apoptosis, however studies found that activation of these molecules upon *Yersinia* infection leads to cleavage of GSDMD, producing its active fragment. The inactive fragment produced by caspase-3 cleavage could also be detected. Under TAK1 inhibition, GSDMD has been shown to trigger morphologically pyroptotic cell death as well as release of interleukins. GSDMD-deficient macrophages exhibited delayed *Yersinia* induced cell death, as measured by PI (propidium iodide) uptake. The fact, that cell death is not completely blocked indicates that other cell death pathways might be activated when GSDMD is absent (Sarhan et al., 2018). Interestingly, *Yersinia* infection also triggered activation of GSDME. However, GSDME deficiency, either alone or in combination with GSDMD deficiency, did neither affect cell death nor secretion of IL-1β, which indicates that this molecule is not required for triggering pyroptosis in infected macrophages (Chen et al., 2021, Sarhan et al., 2018). In contrast, GSDME was identified as being the executioner of pyroptosis in neutrophils upon *Yersinia* infection. In these cells, infection and subsequent YopP mediated TAK1 inhibition leads to RIP1 and caspase-3 dependent cleavage of GSDME, which is in turn responsible for interleukin release and cell death. GSDMD has been shown to be activated by caspases-1 and -8, however it does not play a role in neutrophil cell death (Chen et al., 2021). Another function of TAK1 in uninfected cells is blockage

of the formation of the NLRP3 inflammasome and subsequent pyroptosis (Malireddi et al., 2018). YopP dependent blockage during *Yersinia* infection has been shown to induce activation of caspase-1 in macrophages. This activation was dependent on RIP1, caspase-8 and FADD, while RIP3 did not affect it (Philip et al., 2014). It is suggested that GSDMD pore-formation leads to potassium efflux which subsequently triggers formation of the NLRP3 inflammasome and maturation of cytokines through active caspase-1. Deletion of caspase-1 or NLRP3, however, does not influence *Yersinia* mediated cell death significantly (Orning et al., 2018).

In summary, infection of murine macrophages with *Yersinia* triggers YopP-dependent cell death that requires RIP1, caspase-8 and FADD and that results in GSDMD pore formation. It is suggested that this complex connection of different pathways is part of the host's defense against bacterial infection.

1.6 Aim of this study

Infection of macrophages with *Y. enterocolitica* leads to cell death. This process is dependent on YopP which inhibits TAK1 and thus blocks downstream cell survival promoting signalling through the MAPK and NFκB pathways. In consequence, cell death mediated by RIP1, caspase-8 and GSDMD is triggered. This illustrates that crosstalk between different forms of cell survival and PCD signalling is essential in *Yersinia* infection. Nevertheless, relevant details of these processes remain still unclear. Therefore, the *Yersinia* infection model is the focus of many studies. However, the majority of research has so far been conducted in murine macrophages. One of the aims of this study was therefore to investigate the effects of *Y. enterocolitica* infection, and especially YopP, in primary human macrophages and to compare the results to what is already known from murine macrophages. An emphasis was placed on examining the role of GSDME by generating GSDME deficient human macrophages.

The second part of this study focused on the involvement of BID in *Yersinia* induced cell death of murine macrophages. It has been shown that BID not only plays a role in mediating intrinsic apoptosis, but that it is also involved in pyroptotic processes as it can be cleaved by caspase-1 and trigger MOMP. Here, different knockout cell lines were produced and studied with the aim to elucidate how BID might be involved in mediating cell death upon infection with *Y. enterocolitica.*

Overall, the aim of this study was to further dissect the mechanisms that regulate cell death in macrophages upon *Yersinia* infection in order to gain more insights into the control of these pathways in eukaryotic cells.

2 Material and Methods

2.1 Materials

2.1.1 Devices

Table 1: Used devices

Device	Manufacturer
Accu-Jet pro	Brand (Wertheim, Germany)
Blotting chamber: OWL HEP-1	Thermo Fisher Scientific (Waltham, USA)
Blotting chamber	Hartenstein GmbH (Würzburg, Germany)
Cell counting chamber: Neubauer improves	Hartenstein GmbH (Würzburg, Germany)
Cell incubator: CB Series	Binder (Tuttlingen, Germany)
Centrifuge: 3K30 (Rotor 19776-H)	Sigma (Osterode am Harz, Germany)
Centrifuge: 5417 R (Rotor F45-30-11)	Eppendorf (Hamburg, Germany)
Centrifuge: 5424 R (Rotor FA-45-24-11)	Eppendorf (Hamburg, Germany)
Centrifuge: 5810 R (Rotor A-4-81)	Eppendorf (Hamburg, Germany)
Clean bench: Hera Safe	Thermo Fisher Scientific (Waltham, USA)
Cryco freezing container “Mr. Frosty”	Nalgene Scientific (Rockford, USA)
Developer for X-ray films: Curix 60	Agfa (Mortsel, Belgium)
Film cassette	Hartenstein GmbH (Würzburg, Germany)
Freezer: -20 °C	Liebherr (Biberach an der Riß, Germany) Bosch (Gerlingen-Schillerhöhe, Germany)
Freezer: -80 °C, Hera freeze	Thermo Fisher Scientific (Waltham, USA)
Imager: ImageQuant 800	Amersham Bioscience / Cytiva Europe GmbH (Freiburg im Breisgau, Germany)
Incubator: B 5090 E	Heraeus (Hanau, Germany)
Incubator: Certomat BS-1	Sartorius (Göttingen, Germany)
Incubator: Multitron Pro	Infors HAT (Bottmingen, Schweiz)
Magnetic stirrer RCT basic	IKA (Staufen, Germany)
Magnetic rack: QuadriMACS™ Seperator	Miltenyi Biotec (Bergisch Gladbach, Germany)
Microscope: Axiovert 25	Zeiss (Jena, Germany)
Microscope: Eclipse TS100	Nikon (Düsseldorf, Germany)
Photometer: Ultrospec 3100 Pro	Amersham Biosciences (Freiburg, Germany)
pH meter: Seven Easy	Mettler Toledo (Gießen, Germany)
Pipettes 10, 20, 100, 200, 1000 µl, Research Plus	Eppendorf (Hamburg, Germany)
Plate reader: Infinite M200	Tecan (Männedorf, Switzerland)
Plate reader: Synergy H1	BioTek (Vermont, USA)
Power supply: BluePower 500	Serva (Heidelberg, Germany)
Refrigerators	Liebherr (Biberach an der Riß, Germany)
Scale	Sartorius (Göttingen, Germany)
SDS-PAGE chamber: HoeferTM SE 400	Thermo Fisher Scientific (Waltham, USA)
SDS-PAGE electrophoresis cell: Mini-Protean II	Biorad (Munich, Germany)

Thermoblock: Rotilabo-Block-Heater H250	Roth (Karlsruhe, Germany)
Vortex	Hartenstein GmbH (Würzburg, Germany)
Water bath GFL Type 1013	GFL (Burgwedel, Germany)

2.1.2 Disposables

Table 2: Used disposables

Item	**Manufacturer**
Cell culture dishes: 100 mm / 150 mm	Sarstedt (Nümbrecht, Germany)
Cell culture flasks: T-25 / T-75	Sarstedt (Nümbrecht, Germany)
Cryo vials 1.6 ml	Sarstedt (Nümbrecht, Germany)
Disposable inoculation loop	Sarstedt (Nümbrecht, Germany)
Multi-well-plates: 6-/12-/24-/96-wells	Sarstedt (Nümbrecht, Germany)
Multi-well-plates: 96-wells µCLEAR®	Greiner Bio-One (Kremsmünster, Austria)
Pre-Separation Filters	Miltenyi Biotec (Bergisch Gladbach, Germany)
Pipette tips (10, 20, 100, 200, 1000 µl)	Sarstedt (Nümbrecht, Germany)
Pipette tips: Gelloader	Hartenstein GmbH (Würzburg, Germany)
PVDF-membrane (0.45 µm pore size)	Roth (Karlsruhe, Germany)
Reaction tubes: 15 ml / 50 ml (sterile)	Sarstedt (Nümbrecht, Germany)
Reaction tubes: 0.5 ml / 1.5 ml / 2 ml	Sarstedt (Nümbrecht, Germany)
Serological pipettes: 5 ml / 10 ml / 25 ml	Sarstedt (Nümbrecht, Germany)
Serological pipettes: 5 ml / 10 ml / 25 ml (sterile)	Sarstedt (Nümbrecht, Germany)
Serparation columns, LS columns	Miltenyi Biotec (Bergisch Gladbach, Germany)
Sterile filter units	Merck Millipore (Darmstadt, Germany)
Whatman paper 0.35 mm	Hartenstein GmbH (Würzburg, Germany)
X-ray films	Fuji-Film Europe (Düsseldorf, Germany)

2.1.3 Enzymes, Kits and reagents

Table 3: Used enzymes, kits and reagents

Name	**Manufacturer**
Acryl-Bisacrylamid	Roth (Karlsruhe, Germany)
Albumin bovine Fraction V (BSA)	Serva (Heidelberg, Germany)
Amino hexanoic acid	Merck Millipore (Darmstadt,Germany)
Ammonium persulphate (APS)	Sigma-Aldrich (Steinheim, Germany)
Aqua	Braun (Melsungen, Germany)
Adenosintriphosphat (ATP)	Hartmann Analytic (Braunschweig, Germany)
β-Mercaptoethanol	Sigma-Aldrich (Steinheim, Germany)
Bromphenol blue	Merck Millipore (Darmstadt,Germany)
CD14 MicroBeads, human	Miltenyi Biotec (Bergisch Gladbach, Germany)
Chloroform	J.T. Baker (Arnheim, Netherlands)

Color Prestained Protein Standard	New England BioLabs (Frankfurt am Main, Germany)
Complete Protease Inhibitor Cocktail Tablets	Roche (Mannheim, Germany)
DOC	Merck Millipore (Darmstadt, Germany)
CutSmart® Buffer	New England BioLabs (Frankfurt am Main, Germany)
DTT	Thermo Fisher Scientific (Waltham, USA)
FastDigest Esp3I	Thermo Fisher Scientific (Waltham, USA)
femtoLUCENT™ Plus HRP Kit	G-Bioscience (St Louis, USA)
Glycerin	Roth (Karlsruhe, Germany)
Glycine	Roth (Karlsruhe, Germany)
Human serum albumin	Sigma-Aldrich (Steinheim, Germany)
Hydrochloric acid (HCl)	Roth (Karlsruhe, Germany)
IL-1β Human Uncoated ELISA Kit	Thermo Fisher Scientific (Waltham, USA)
Isopropanol	ChemSolute (Renningen, Germany)
Lipopolysaccharide (LPS)	Sigma-Aldrich (Steinheim, Germany)
Methanol (MeOH)	Roth (Karlsruhe, Germany)
Natriumchlorid (NaCl)	Roth (Karlsruhe, Germany)
Natriumhydroxid (NaOH)	Merck Millipore (Darmstadt, Germany)
Non-fat dry milk	Roth (Karlsruhe, Germany)
NP-40	Thermo Fisher Scientific (Waltham, USA)
Passive Lysis 5X Buffer	Promega (Madison, Wisconsin, USA)
Polyethylenimin (PEI)	Polyscience Inc. (Washington, USA)
PeqGold Plasmid Miniprep Kit	VWR (Darmstadt, Germany)
PhosSTOP Phosphatase Inhibitor Cocktail Tablets	Roche (Mannheim, Germany)
Polybrene®	Sigma (München, Germany)
PureLinkTM HiPure Plasmid Maxiprep Kit	Thermo Fisher Scientific (Waltham, USA)
Resolving Gel Buffer pH 8,8	Bio-Rad Laboratories (München)
Restore™ Western Blot Stripping Buffer	Thermo Fisher Scientific (Waltham, USA)
Stacking Gel Buffer pH 6,8	Bio-Rad Laboratories (München, Germany)
SYTOX® Green Nucleic Acid Stain	Thermo Fisher Scientific (Waltham, USA)
T4-DNA-Ligase	New England BioLabs (Frankfurt am Main, Germany)
TCA	Sigma-Aldrich (Steinheim, Germany)
TEMED	Roth (Karlsruhe, Germany)
TNF-α Human Uncoated ELISA Kit	Thermo Fisher Scientific (Waltham, USA)
Triton X-100	Roth (Karlsruhe, Germany)
Trizma Base	Sigma-Aldrich (Steinheim, Germany)
Trizma HCl	Sigma-Aldrich (Steinheim, Germany)
Trypan Blue Solution	Gibco (Waltham, USA)
Tween20®	Merck Millipore (Darmstadt,Germany)

2.1.4 Plasmids and Oligonucleotides

Table 4: Used plasmids

Name	Description / Use	Manufacturer / Provider
lentiCas9_Blast	- encoding Cas9 - encoding blasticidin resistance	Addgene (Teddington, UK)
new_cassette_lego_puro	- Used to insert sequence for gRNA against GSDME - EGFP - lentiviral plasmid	Provided by Dr. Weißmann, Simon (LIV, Hamburg)

Table 5: Used DNA and RNA oligonucleotides

Name	Sequence	Description / Use	Manufacturer
Bid_m_1_fw_lenti	CACCTGGCTG-TACTCGCCAAGAGCTGG	For cloning into new_cassette_lego_puro - encoding gRNA binding to murine *Bid*	Sigma (München, Germany)
Bid_m_1_rc_lenti	AAACCCAGCTCTT-GGCGAGTACAGCCA	"	Sigma (München, Germany)
Bid_m_2_fw_lenti	CAC-CGGTCCATCTCATCGCC-TATTTGG	"	Sigma (München, Germany)
Bid_m_2_rc_lenti	AAACCCAAA-TAGGCGATGAGATGGACC	"	Sigma (München, Germany)
Gsdme_L_1	CACCGTCGGACTTT-GTGAAATACG	For cloning into new_cassette_lego_puro - encoding gRNA binding to human *Gsdme*	Sigma (München, Germany)
Gsdme_L_1_rc	AAACCG-TATTTCACAAAGTCCGAC	"	Sigma (München, Germany)

Gsdme_L_2	CACCG-TATAACTCAATGACACCG-TAGG	"	Sigma (München, Germany)
Gsdme_L_2_rc	AAACCCTACGGTGTCATT-GAGTTATAC	"	Sigma (München, Germany)
Mm.Cas9.BID.1.AA	rUrGrGrCrUrGrU-rArCrUrCrGrCrCrArArGrAr-GrCrGrUrUrUrUrArGrAr-GrCrUrArUrGrCrU	crRNA Used as part of the Alt-R® CRISPR-Cas9 System to generate *Bid* knock-outs	IDT (Leuven, Belgium)
Mm.Cas9.DFNA5.1.AA	rCrArCrGrGrArCrArCrCrA-rArUrGrU-rArGrUrGrCrGrUrUrUrU-rArGrArGrCrUrArUrGrCrU	crRNA Used as part of the Alt-R® CRISPR-Cas9 System to generate *Gsdme* knockouts	IDT (Leuven, Belgium)
Mm.Cas9.GSDMD.1.AA	rGrUrCrGrUrCr-GrArUrGrGrGrArArCrA-rUrUrCrArGrUrUrUrU-rArGrArGrCrUrArUrGrCrU	crRNA Used as part of the Alt-R® CRISPR-Cas9 System to generate *Gsdmd* knockouts	IDT (Leuven, Belgium)

2.1.5 Antibiotics

Table 6: Used antibiotics

Antibiotic	**Dissolved in**	**Final concentration [µg/ml]**
Blasticidin (Blast)	ddH_2O	32
Chloramphenicol (Chlor)	70 %EtOH	20
Gentamycin (Genta)	ddH_2O	100
Kanamycin (Kana)	ddH_2O	50
Nalidixic acid (Nal)	1 M NaOH	60

2.1.6 Buffers and solutions

Table 7: Buffer compositions of general buffers and solutions

Name	Composition
Annealing buffer	10 mM Tris (pH 7,5 - 8) 50 mM NaCl 1 mM EDTA
MES buffer	19.8 mM EGTA 19.8 mM EDTA 0.25 M D-Mannitol 19.8 mM MES 1 tablet Complete Protease Inhibitor Cocktail per 50 ml
Monocyte buffer	2 mM EDTA pH 7.4 0.5 % human serum albumin in DPBS
PBS pH 7,4 (Phosphate Buffered Saline)	10 mM Na2HPO4 140 mM NaCl 2.5 mM KCl 1.8 mM KH2PO4
RIPA buffer	50 mM Tris HCl pH 8,0 150 mM NaCl 1 mM EDTA 1 mM EGTA 1 % (v/v) NP-40 0.5 % (w/v) DOC 0.1 % (w/v) SDS 1 mM NaF 20 mM β-Glycerolphosphat 1 mM Na3VO4 0.4 mM PMSF 1 tablet Complete Protease Inhibitor Cocktail per 50 ml 1 tablet PhosSTOP per 10 ml
TBS pH 7,6	15 mM Tris-HCl 140 mM NaCl
TBS-T	15 mM Tris-HCl 140 mM NaCl 0.1 % (v/v) Tween20®

Table 8: Buffer compositions of buffers used for SDS-PAGE and western blotting

Name	Composition
4 x sample buffer for SDS-PAGE	12 % (w/v) SDS 40 % (v/v) Glycerol (86 %) 200 mM Tris HCl, pH 7,0 0.004 % (w/v) Bromphenolblau 5 % (v/v) β-Mercaptoethanol
Resolving gel	10-15 % (v/v) Acryl-Bisacrylamid 375 mM Tris-HCl, pH 8.8 (Resolving Gel Buffer) 0.1 % (w/v) SDS 0.1 % (w/v) Ammonium persulphate 0.04 % (v/v) TEMED
SDS-PAGE running buffer	25 mM Tris 192 mM Glycin 3.5 mM SDS
Stacking gel	5 % (v/v) Acryl-Bisacrylamid 125 mM Tris-HCl, pH 6.8 (Stacking Gel Buffer) 0.1 % (w/v) SDS 0.1 % (w/v) Ammonium persulphate 0.1 % (v/v) TEMED
Transfer buffer	150 mM Tris 25 mM Glycine 20 % (v/v) Methanol

2.1.7 Antibodies

Table 9: Used primary antibodies (NFDM = non fat dry milk)

Name / Order number	Dilution	Source	Manufacturer
Anti-Actin, clone C4 #MAB1501	1:2000 in TBST	Mouse IgG	Merck Millipore (Darmstadt, Germany)
BID #2003	1:1000 in 5 % BSA-TBST	Rabbit IgG	Cell Signaling Technology (Leiden, Netherlands)
Caspase-3 (D3R6Y) #14220	1:1000 in 5 % BSA-TBST	Rabbit IgG	Cell Signaling Technology (Leiden, Netherlands)
Caspase-3 #9662	1:1000 in 5 % BSA-TBST	Rabbit IgG	Cell Signaling Technology (Leiden, Netherlands)
Cleaved Caspase-8 (Asp384) #9748	1:1000 in 5 % BSA-TBST	Rabbit IgG	Cell Signaling Technology (Leiden, Netherlands)
Caspase-9 #9504	1:1000 in 5 % BSA-TBST	Rabbit IgG	Cell Signaling Technology (Leiden, Netherlands)

Gasdermin D (E8G3F) #97558	1:1000 in 5 % BSA-TBST	Rabbit IgG	Cell Signaling Technology (Leiden, Netherlands)
GSDMD [ERP19828] #ab209845	1:1000 in 5 % NFDM-TBST	Rabbit IgG	abcam (Cambride, GB)
GSDME [ERP19859] #ab215291	1:1000 in 5 % NFDM-TBST	Rabbit IgG	abcam (Cambride, GB)
HSP90 (C45G5) #4877	1:1000 in 5 % NFDM-TBST	Rabbit IgG	Cell Signaling Technology (Leiden, Netherlands)
RIP (D94C12) XP #3493	1:1000 in 5 % BSA-TBST	Rabbit IgG	Cell Signaling Technology (Leiden, Netherlands)
RIP (Phospho Ser166)(D1L3S) #65746	1:1000 in 5 % BSA-TBST	Rabbit IgG	Cell Signaling Technology (Leiden, Netherlands)
TAK1 #4505	1:1000 in 5 % BSA-TBST	Rabbit IgG	Cell Signaling Technology (Leiden, Netherlands)
TAK1(Phospho Thr184/187) #4508	1:1000 in 5 % BSA-TBST	Rabbit IgG	Cell Signaling Technology (Leiden, Netherlands)

Table 10: Used secondary antibodies (NFDM = non fat dry milk)

Name / Order number	**Dilution**	**Source**	**Manufacturer**
Anti-rabbit IgG, HRP-linked Antibody #7074	1:10.000 in 5 % NFDM-TBST	Goat IgG	Cell Signaling Technology (Leiden, Netherlands)
Peroxidase-conjugated AffiniPure Goat Anti-Mouse IgG (H+L)	1:20.000 in 5 % NFDM-TBST	Goat IgG	Jackson ImmunoResearch Laboratories Inc. (West Grove, USA)

2.1.8 Growth media and additives

Table 11: Used cell culture media

Medium	**Manufacturer**
Dulbeco's Modified Eagle Medium (DMEM)	Gibco (Waltham, USA)
Opti-MEM®	Gibco (Waltham, USA)
Roswell Park Memorial Institute Nr. 1640 Medium (RPMI)	Gibco (Waltham, USA)

Table 12: Used cell culture additives

Name	Description	Manufacturer
Accutase	400 – 600 units/ml	Sigma-Aldrich (Steinheim, Germany)
DPBS	Dulbeccos' Phosphate Buffered Saline, w/o CaCl2, w/o MgCl2, 1x	Thermo Fisher Scientific (Waltham, USA)
FCS	Fetal Bovine Serum, heat-inactivated	Thermo Fisher Scientific (Waltham, USA)
GM-CSF	Granulocyte-Macrophage Colony-Stimulating Factor, Human, 100 ng/ml in ddH_2O	Peprotech (Hamburg, Germany)
HEPES	HEPES Buffer Solution, 1 x	Thermo Fisher Scientific (Waltham, USA)
L-Glutamin	L-Glutamin, 200 mM, 100 x	Thermo Fisher Scientific (Waltham, USA)
MCSF	L929- cell culture supernatant, sterile filtered	Produced in lab
MEM NEAA	MEM Non-Essential-Aminoacids, 100 ×	Thermo Fisher Scientific (Waltham, USA)
Pen/Strep	Penicilline/Streptomycine, 5.000 Units/ml; 5.000 µg/ml	Thermo Fisher Scientific (Waltham, USA)
PMA	Phorbol-12-myristat-13-acetat	Abcam (Cambridge, GB)

2.1.9 Inhibitors and stimulators

Table 13: Used inhibitors and stimulators

Name	Working concentration	Manufacturer
LPS	1 µg/ml	Sigma-Aldrich (Steinheim, Germany)
Necrostatin-1s	50 µM	Focus Biomolecules (Plymouth Meeting, USA)
NG25	15 µM	Hycultec (Beutelsbach, Germany)

2.1.10 *E. coli* strains

Table 14: Used *E. coli* strains

Name	Description	Reference
TOP 10	*F- mcrA*, Δ(*mcr*BC-*hsd*RMS-*mrr*), *end*A1, *rec*A1, *rel*A1, *gyr*A96, Φ80*lac*ZΔM15, *deo*R, *nup*G, *ara*D139, F(*lac*Iq, Tn10 (Tetr)), *gal*U, Δ*lac*X74, *gal*K, Δ(*araleu*)7697 Used for transformation	Thermo Fischer Scientific (Waltham, USA)

2.1.11 *Yersinia* strains

Table 15: Used *Yersinia enterocolitica* strains

Name	Description	Reference
WAP	WA-314 O:8, pYVO8 virulence plasmid, bio group 1B, intrinsic Nalidixic acid resistance	(Heesemann and Laufs, 1983)
ΔP	WA-ΔyopP, yopP-gene replaced by Chlor cassette	(Trülzsch et al., 2004)
ΔPQ	WA-ΔyopP ΔyopQ, yopP-gene replaced by Chlor cassette, yopQ-gene replaced by Kana cassette	(Leibiger et al., 2008)

2.1.12 Eukaryotic cells

Table 16: Used eucaryotic cell lines and cells

Name	Description / Reference	Cultivating condition
i*Bid*$^{-/-}$	Immortalised mouse bone marrow derived macrophages, *Bid* knockout generated using the genome editing system Alt-R-CRISPR/Cas (IDT).	DMEM, 10 % FCS, 10 % MCSF, 1 % NEAA, 1 % Pen/Strep, 1 % HEPES
i*Gsdmd*$^{-/-}$	Immortalised mouse bone marrow derived macrophages, *Gsdmd* knockout generated using the genome editing system Alt-R-CRISPR/Cas (IDT).	DMEM, 10 % FCS, 10 % MCSF, 1 % NEAA, 1 % Pen/Strep, 1 % HEPES

i*Bid*$^{-/-}$ *Gsdmd*$^{-/-}$	Immortalised mouse bone marrow derived macrophages, *Bid* and *Gsdmd* knockout generated using the genome editing system Alt-R-CRISPR/Cas (IDT).	DMEM, 10 % FCS, 10 % MCSF, 1 % NEAA, 1 % Pen/Strep, 1 % HEPES
iWT	Immortalised mouse macrophages, isolated from bone marrow of wildtype mice. (Heilig et al. 2020)	DMEM, 10 % FCS, 10 % MCSF, 1 % NEAA, 1 % Pen/Strep, 1 % HEPES
iWT Cas9	Immortalised mouse macrophages stably expressing Cas9.	DMEM, 10 % FCS, 10 % MCSF, 1 % NEAA, 1 % Pen/Strep, 1 % HEPES
i*Bid*$^{-/-}$ Cas9	Immortalised mouse macrophages stably expressing Cas9. *Bid* knockout generated using CRISPR / Cas9.	DMEM, 10 % FCS, 10 % MCSF, 1 % NEAA, 1 % Pen/Strep, 1 % HEPES
L929	Used for production of MCSF supernatants.	DMEM, 10 % FCS, 1 % Pen/Strep
Lenti-X™ 293T	Used to produce lentiviral particles. Clontech Catalog No. 632180	DMEM, 10 % FCS, 1 % Pen/Strep
Primary human macrophages	Isolated peripheral blood mococytes, differentiated to macrophages through addition of human GM-CSF for 7 days.	RPMI, 10 % FCS, 1 % L-Glumatin, 20 ng/ml human GM-CSF
THP-1	Human monocytic cell line (DSMZ, ACC 16)	RPMI, 20 % FCS, 1 % L-Glutamin
THP-1 *Gsdme*$^{-/-}$	*Gsdmd* knockout generated using CRISPR / Cas9	RPMI, 20 % FCS, 1 % L-Glutamin

2.1.13 Software

In the course of this study, Microsoft Office (Word, Excel, PowerPoint) was used as well as GraphPad Prism 9.

2.2 Methods

2.2.1 Molecular biology methods

2.2.1.1 Plasmid preparation and sequencing

For small scale plasmid preparation for analysis and sequencing, 2 ml of LB medium containing selective antibiotics were incoculated with bacteria of interest and incubated overnight at 180 rpm and either 37 °C or 30 °C if expressing lentiviral plasmids. The next day, plasmids were isolated using PeqGold Plasmid Miniprep Kit according to the manufacturer's instructions. For larger scale preparations, i.e. for transfecting Lenti-X™ 293T cells, 200 ml of bacteria culture were prepared, incubated as described and isolation was conducted using PureLinkTM HiPure Plasmid Maxiprep Kit according to the manufacturer's instructions. Concentrations of purified plasmids were determined photometrically using MESSGerat by measuring the optical density at 260 nm (OD 260). Sequencing to check for successful cloning was performed by SeqLab (Göttingen, Germany).

2.2.1.2 Cloning and transformation

To generate lentiviral plasmids coding for target-specific gRNA, oligonucleotides of the region of interest were first annealed by mixing 1 µl of forward and reverse oligonucleotides with 98 µl annealing buffer (see Table 7). This mixture was heated to 95 °C for 5 min and then slowly cooled down to room temperature. The now annealed oligonucleotides were then introduced into the vector of choice, in this case new_cassette_lego_puro, in a one-step reaction. The components were as follows:

Component	**Amount**
Annealed Oligonucleotides	1 µl
ATP (10 mM)	1 µl
DTT (10 mM)	1 µl
CutSmart® Buffer	1 µl
Esp3I FastDigest	0.1 µl
Ligase	0.1 µl
Plasmid	25 ng
Total	10 µl

The mixture was incubated at 37 °C for 20 min and then directly used for heat shock transformation into chemically competent *E. coli* TOP10 cells. First, cells were thawed on ice, then the ligation mix was added and carefully mixed in. After incubation on ice for 30 min, bacteria were heat shocked for 42 s at 42 °C and then incubated again on ice for 2 min. Next, 1 ml of LB medium was added, and the suspension was incubated at 37 °C for 1 h with light shaking. Afterwards, 200 µl of the suspension were

plated onto LB plates containing selective antibiotics. Plates were incubated overnight at 37 °C and single colonies were consequently used to prepare for plasmid preparation and sequencing (see above).

2.2.2 Microbiological methods

2.2.2.1 Cultivation of Yersinia enterocolitica strains

All strains used in this study were cultivated on Lurian-Bertani (LB) plates containing selective antibiotics. After inoculation from frozen glycerol stocks, plates were incubated at 27 °C for 24 – 48 h and consequently stored at 4 °C for up to one month.

2.2.2.2 Yersinia infection

For infection experiments, 3 ml of liquid LB medium with selective antibiotics were inoculated with bacteria and incubated at 27 °C overnight. Next, overnight cultures were diluted 1:10 in fresh LB medium and incubated at 37 °C and 180 rpm for 90 min. This step activates expression of the virulence plasmid. Thereafter, cultures were centrifuged (3000 x g, 5 min, 4 °C) and supernatants were discarded. The bacteria pellet was resuspended in 1 – 3 ml PBS and the optical density of a 1:10 dilution was measured (OD_{600}) and adjusted to 0.36 with the following formular:

$$\text{Missing Volume [ml]} = \frac{\text{measured } OD_{600} \cdot \text{suspension volumen [ml]}}{0{,}36} - \text{suspension volumen [ml]}$$

The adjusted bacteria suspension was then used for infection of cells. Infections were stopped after 90 to 120 min by adding Gentamycin.

2.2.3 Cell culture methods

2.2.3.1 Isolation and cultivation of primary human macrophages

Human peripheral blood monocytes were isolated from buffy coats provided by the Institute of Transfusion Medicine (UKE) and differentiated into macrophages using GM-CSF.

First, three 50 ml tubes with 15 ml LSM each were prepared and carefully layered with 20 ml blood sample per tube. The tubes were centrifuged (1500 rpm, 4 °C, 30 min) which led to a separation of the fluids into three phases: erythrocytes at the bottom, then a milky phase of so-called buffy coats, containing the wanted monocytes, and blood plasma on top. The milky phase from each of the three tubes was transferred to a new tube each with 10 ml ice-cold RPMI and subsequently filled up to 50 ml with ice-cold RPMI. After centrifugation (1500 rpm, 4 °C, 10 min) the supernatant of each tube was discarded, pellets were resuspended in 10 ml RPMI and the content of all three tubes was pooled into

two tubes. These were again filled up to 50 ml with RPMI and centrifuged as before. The supernatants were again discarded, the pellets were resuspended, and both tubes were pooled into one and filled up to 50 ml with RPMI. After a final centrifugation, the resulting pellet was resuspended in 1.5 ml monocyte buffer, mixed with 250 µl CD14 microbeads and incubated on ice for 15 min. In that time, a lymphocyte separation column with a pre-separation filter was fitted into a magnetic rack and prepared by equilibrating with 900 µl monocyte buffer. Thereafter, the cell sample was added onto the column and washed twice with 1 ml monocyte buffer. Then, 3 ml monocyte buffer were added to the column, the column was removed from the magnetic rack and cells were pressed out of the column into a tube containing 20 ml cold RPMI using a stamp. The volume of the cell suspension was adjusted to 30 ml and cells were counted. Finally, the cell concentration was adjusted to 2 x 10^6 / ml and 1 ml was added to each well of a 6-well plate.

Isolated cells were incubated at 37 °C and 5 % CO_2 for 3 – 5 h or until adherent. Then, medium was changed to RPMI containing 10 % (v/v) FCS and 20 ng/ml GM-CSF in order to start differentiation into macrophages. After 3 days of incubation, the medium was renewed and after 7 days, differentiation was completed.

To seed the now differentiated primary macrophages, the medium was removed, and cells were washed with 1 ml DPBS per well. After, 0.5 ml accutase was added to each well and cells were left to detach for 20 – 30 min at room temperature until visibly rounded and mostly detached. Wells were carefully scraped with a cell scraper and the cell suspension was transferred into tubes and counted using a Neubauer cell counting chamber. Depending on the experiments, cells were then seeded in different multi-well plates according to the following table:

Table 17: Overview – number of seeded human macrophages in different multi plates

Plate size	**Cells seeded per well**
96-well plate	0.09 x 10^6
12-well plate	0.5 x 10^6

2.2.3.2 Cultivation and differentiation of THP-1 cells

THP-1 cells are human monocytic suspension cells. They were cultivated in T75 flasks stored upright at 37 °C and 5 % CO_2. They were passaged every 2 – 3 days in a 1:3 ratio. For infection or stimulation experiments, cells were counted and seeded according to the following table.

Table 18: Overview – number of seeded THP-1 cells in different multi plates

Plate size	Cells seeded per well
96-well plate	0.12 x 10^6
24-well plate	0.2 x 10^6
12-well plate	0.4 x 10^6

In order to start differentiation into macrophages, 10 ng/ml PMA was added to each well for 24 h. Thereafter, the medium was discarded and replaced with medium without PMA for another 24 h. Then, cells were fully differentiated into macrophages and ready for experiments.

2.2.3.3 Generation of THP-1 knockout cell lines using CRISPR/CAS9 and lentiviral transduction

To further study the role of GSDME in human macrophages, lentiviral transduction was used to generate GSDME-deficient THP-1 cells.

First, lentiviral particles were produced. The packaging cell line Lenti-X™ 293T was seeded into 10 cm cell culture dishes at a density of 5 x 10^6 cells / dish and incubated overnight. Next, the following transfection mix, containing the third-generation packaging plasmids phCMV-gag-pol, phCMV-rev and phCMV-VSV-g env as well as the plasmid of interest was prepared, mixed and incubated for 30 min at room temperature:

Component	Amount for 10 cm cell culture dish
DMEM	1 ml
phCMV-gag-pol	10 µg
phCMV-rev	5 µg
phCMV-VSV-g env	2 µg
LeGo plasmid of interest	10 µg
PEI	270 µl

The transfection mix was then added to the cells and distributed evenly in the medium. 6 – 8 h later, the medium was discarded and replaced by DMEM (10 % FCS, 1 % Pen/Strep, 1 % HEPES). After further incubation for 72 h, cell culture supernatants now containing lentiviral particles were removed, sterile-filtered and frozen at -80 °C until further use.

To generate THP-1 cells that stably express the enzyme Cas9, lentiviral transduction was used. First, THP-1 cells well seeded into a 24-well plate at a density of 1 x 10^5 cells/well. Then polybrene was added (1:1000) as well as lentiviral particles containing the plasmid encoding Cas9 and a blasticidin resistance. The plate was centrifuged at 1000 x g and 37 °C for 1 h. After 24 h of incubation, the medium was

changed to RMPI without antibiotics and after another 24 h changed again to RPMI containing blasticidin (32 µg/ml). This started the selection, as only cells that integrated the plasmid could express Cas9 and the blasticidin resistance and therefore survive. Selection was continued for 8 days with media changes every 2 days. Then, samples of cell suspensions from each well were transferred into 1.5 ml reaction tubes and centrifuged (200 x g, 5 min). Pellets were resuspended in 30 µl 2 x sample buffer and incubated at 95 °C. SDS-PAGE, western blotting and immunodetection were carried out as described below with a primary antibody against the FLAG-tag fused to Cas9. Samples that showed a strong FLAG signal were further cultivated and used in the next transduction steps.

THP-1 cells expressing Cas9 were subsequently used to introduce target-specific gRNA via lentiviral transduction. The plasmid introduced in this step also contains a GFP sequence to enable sorting via fluorescence. Cells were seeded and transduced as described above. After 24 h, medium was changed to RPMI without antibiotics and after further incubation for 24 h, cells were prepared for sorting by transferring them into a tube, centrifuging (700 rpm, 3 min) and then resuspending the pellet in 200 µl DPBS containing 0.5 % (v/v) FCS. Sorting of GFP-positive cells was carried out by the FACS Core Unit (UKE) using BD FACSAria™ Fusion (BD Biosciences, Heidelberg, Germany). As single-cell sorting had shown to not work for THP-1 cells, one GFP positive cell was sorted to a well of a 96-well plate already containing 500 THP-1 wildtype cells. These mixed cultures were cultivated in increasingly large cell culture dishes for 3 weeks. Then, cells were sorted again as described before. This time, all GFP-positive cells from one sample, which consequently are all clones of one cell, were sorted into the same well of a 96-well plate. Once wells were sufficiently full, 60 µl of each cell suspension were transferred into a 1.5 ml reaction tube and prepared for western blotting and immunodetection as described below. GSDME-specific antibodies were used to determine which cell clones were GSDME-deficient. These cells were then cultivated further and used for cryoconservation and experiments.

2.2.3.4 Cultivation of iWT

Murine bone marrow derived macrophages were kindly provided by Broz () The wildtype cell line and all generated knockout cell lines based on it were cultivated in T-75 flasks in DMEM (10 % FCS, 10 % MCSF, 1 % NEAA, 1 % Pen/Strep, 1 % HEPES) at 37 °C and 5 % CO_2. Every 2 – 3 days cells were passaged by removing the medium and adding 5 ml cold DPBS per flask. Cells were detached using a cell scraper, transferred into 50 ml tubes and centrifuged (200 x g, 5 min). Supernatants were removed, pellets were resuspended in 4 – 6 ml fresh medium and transferred at a ratio of 1:6 to 1:12 into new T-75 flasks containing 12 ml medium.

For experiments, cell suspensions were counted, and cells were seeded in multi-well plates according to the following table:

Table 19: Overview – number of seeded murine bone marrow derived macrophages in different multi plates

Plate size	Cells seeded per well
96-well plate	0.12 x 10^6
24-well plate	0.2 x 10^6
12-well plate	0.4 x 10^6

2.2.3.5 Generation of knockout cell lines using the Alt-R® CRISPR-Cas9 system

To further study the role and involvement of specific proteins in *Yersinia*-induced cell death in murine macrophages, different knockout cell lines based on iWT cells were generated in the course of this study. For this the genome editing system Alt-R® CRISPR-Cas9 from IDT was used. In this system, first a target-specific crRNA is mixed with a so called tracrRNA. This RNA mixture then hybridizes with the Cas9 endonuclease of choice and the entire complex is then reverse transfected into the cell line of interest. In this study the Cas9 Alt-R *S.p.* Cas9-RFP V3 (IDT) was chosen to enable sorting of cells by fluorescence.

Preparation of RNA Oligos and formation of the RNP complex were carried out according to the manufacturer's protocol (Alt-R® CRISPR-Cas9 System: Cationic lipid delivery of CRISPR ribonucleoprotein complexes into mammalian cells / IDT).

The resulting RNP complex was then reverse transfected into either iWT cells or previously generated knockout cell lines. To transfect one well of a 24-well plate, the following transfection mix was prepared:

Component	Amount
RNP complex	100 µl
RNAiMax	4,8 µl
Opti-MEM Media	95,2 µl
Total	200 µl

This mixture was incubated for 20 min at room temperature. Meanwhile, cells to be transfected were prepared for seeding as described above and diluted to a concentration of 0.4 x 10^6 cells/ml in media without antibiotics. After incubation, the transfection mix was transferred into a 24-well and 400 µl of cell suspension were added. Then, cells were incubated for 48 h at 37 °C and 5 % CO_2.

Next, cells were detached, transferred into tubes and centrifuged (200 x g, 5 min). Pellets were resuspended in 100 – 200 µl DPBS containing 0.5 % (v/v) FCS and transferred into fresh tubes. Sorting of RFP-positive cells was carried out by the FACS Core Unit (UKE) using BD FACSAria™ Fusion (BD Biosciences, Heidelberg, Germany). One RFP-positive cell was sorted into each well of a 96-well plate containing 180 µl complete medium. Cells were incubated at 37 °C and 5 % CO_2 until wells were at least 50 % filled.

Then, cells were detached using pipette tips and half of each well's volume was transferred into 1.5 ml tubes and centrifuged (400 x g, 5 min). Pellets were resuspended in 30 µl 2 x protein sample buffer and heated to 95 °C for 10 min. SDS-PAGE, western blotting and immunodetection were carried out as described below. In case a cell clone showed the desired knockout, the cell population was transferred into a bigger cell culture flask and further cultivated until ready for cryoconservation and experiments.

2.2.3.6 Generation of iWT based knockout cell lines using CRISPR/CAS9 lentiviral transduction

In addition to generation of murine knockout cell lines based on iWT cells as described above, BID deficient macrophages were also produced using CRISPR/CAS9 and lentiviral transduction. Procedures were carried out as described in for THP-1 cells (2.2.3.3). The only difference was that after transduction of the plasmid encoding the gRNA sequence, cells were sorted into empty wells, so that each well only contained one cell. This way, the second sorting step was superfluous. Clones were screened and knockout cell lines were validated using immunodetection.

2.2.3.7 Infection and stimulation experiments

To study the effects of *Yersinia* infection and subsequent cell death on different cell lines, infection experiments were conducted in the course of this study.

Cells were seeded and bacteria suspensions were prepared as described previously. Before infection, cell culture medium was changed to medium not containing antibiotics. In case inhibitors were used, they were added one hour before infection. Cells were then infected with the appropriate MOI and incubated for 90 to 120 min at 37 °C and 5 % CO_2. After this time period, gentamycin was added to stop the proliferation of bacteria in the medium. Alternatively, cells were stimulated with LPS (1 µg/ml) and treated with TAK-1 inhibitor (NG25) simultaneously to simulate *Yersinia* infection. Cell lysates of infected cells were consequently produced at given time points as described below.

2.2.3.8 Measurement of cell death rates using SYTOX® Green

To quantify and compare *Yersinia*- or stimulation induced cell death in different cell lines, SYTOX® Green Nucleic Acid Stain was used. While this dye cannot pass through intact membranes of living cells, it can penetrate damaged membranes of dead cells. Once it enters the nucleus of a dead cell, it binds to nucleic acids which leads to a 500 fold increase in fluorescence with an emission peak at 523 nm when excited with a wavelength of 488 nm. Using a plate reader, this signal can be measured and used to quantify the relative cell death of different infection conditions and over multiple time points.

For these experiments, cells were seeded the day before in 96-well plates with clear bottoms and black walls. They were cultivated overnight at 37 °C and 5 % CO_2. Next, cells were either infected with *Yersinia* or stimulated as indicated. 90 min after infection or stimulation, SYTOX® Green was added at a

concentration of 0.5 µM. Cells treated with Triton X-100 were used as a control for maximum cell death rates, while untreated cells served as a control for background cell death. After a minimum of 30 min of incubation with SYTOX® Green, fluorescence was measured at different time points for up to 24 h. Finally, the following formular was used to calculate the percentage of dead cells for each condition and time point:

$$\text{cell death } [\%] = \frac{\text{induced cell death} - \text{background cell death}}{\text{maximum cell death} - \text{background cell death}}$$

2.2.3.9 Cryoconservation and re-cultivation of eukaryotic cell lines

For long term storage, cells can be transferred into specialised cryo vials and frozen at -196 °C. First, cells were transferred from their culture flasks into 50 ml tubes and centrifuged for 5 min at 200 x g. The supernatant was removed, and cell pellets were resuspended in FCS with 10 % (v/v) DMSO and transferred into cryo vials. These vials were subsequently placed into a "Mr. Frosty" cryo container, stored overnight at -80 °C and then transferred to liquid nitrogen storage containers.

To r-cultivate frozen cells, cryo vials were quickly thawed in a 37 °C degree water bath and resuspended in pre-warmed cell culture medium. After centrifugation for 5 min at 200 x g, the supernatant was discarded to remove all DMSO and the cell pellet was resuspended in fresh medium and transferred into the appropriate cell culture flask for further cultivation.

2.2.4 Proteinbiochemical methods

2.2.4.1 Production of cell lysates

In order prepare cells for analysing with SDS-PAGE and immunoblotting, cell lysates were produced using different lysis buffers.

For human macrophages and THP-1 cells, RIPA lysis buffer was used. The whole process was carried out on ice. First, supernatants were transferred into 1.5 ml reaction tubes and centrifuged at 400 x g and 4 °C for 5 min to collect any cells that might have become detached during the experiment. The supernatant was either discarded or removed and stored for further analysis while cell pellets were stored on ice until further use. Meanwhile RIPA lysis buffer was added to each well of the plate and pipette tips were used to detach the cells from the surface. This sample was consolidated with the cell pellets from the supernatant and incubated on ice for 5 min. Thereafter, samples were centrifuged (15.000 x g, 4 °C, 10 min) to remove any cell debris. Supernatants of each sample were then transferred into new reaction tubes, mixed with the appropriate amount of 4 x sample buffer and then incubated for 10 min at 95 °C to linearise the proteins and allow the incorporation of SDS. Samples were subsequently stored at -20 °C until further use.

All murine bone marrow derived macrophages (iWT and knockouts based on iWT) were lysed using Passive Lysis 5X Buffer (Promega) according to the manufacturer's protocol. Cells were detached from plates using pipette tips or cell scrapers and transferred to 1.5 ml reaction tubes and centrifuged (400 x g, 5 min, RT). Supernatants were removed and pellets were resuspended in appropriate volumes of 1 x Passive Lysis Buffer. Samples were incubated at RT for 20 min with slight shaking and then centrifuged (11.000 x g, 4 °C, 15 min). Supernatants were transferred into new reaction tubes, mixed with the appropriate amount of 4 x sample buffer and then incubated for 10 min at 95 °C. Samples were stored at -20 °C.

2.2.4.2 SDS-polyacrylamide gel electrophoresis (SDS-PAGE)

Sodium dodecyl sulphate polyacrylamide gel electrophoresis is a method used to separate proteins from a sample by size. First, samples are heated to 95 °C which leads to denaturation of the proteins. Furthermore, negatively charged SDS binds to the linearised proteins in a size dependent manner, making it overall negatively charged. Applying a current to an acrylamide gel with protein samples loaded, makes the proteins move towards the positively charged anode. As the gel works like a molecular sieve, smaller proteins move faster than larger proteins, leading to a separation by size.

In this study, acrylamide gels (13x15 cm) were used and put into a chamber with 1 x running buffer. A current of 30 mA was applied for 1 h to the empty gel. Thereafter, 40 – 100 µl of sample were loaded onto the gel and a current of 30 mA was applied until all samples were at the border between stacking and resolving gel. Then, the current was increased to 40 mA until the run finished.

2.2.4.3 Western Blotting and immunodetection

After proteins are separated by size via SDS-PAGE, they can be transferred onto a membrane and incubated with specific antibodies for immunodetection.

Here, western blotting was prepared by soaking 6 pieces of Whatman paper in transfer buffer and activating a piece of PVDF membrane in methanol before transferring it into transfer buffer. The acrylamide gel was also shortly incubated in transfer buffer before setting up the blot. 3 layers of Whatman paper were placed on the anode of the blotting chamber, then the membrane was layered over that, followed by the gel and another 3 layers of Whatman paper. After ensuring that there were no air bubbles between the layers and adding the cathode part of the chamber, a current of 400 mA was applied for 50 min to transfer all proteins out of the gel and onto the membrane.

After transfer, the membrane was incubated for 1 h in 5 % (v/v) BSA in TBST on a shaker to block all unspecific protein-binding domains. Then, a specific primary antibody was added, and the membrane was incubated overnight at 4 °C while shaking. Next, the primary antibody was removed and the

membrane was washed three times for 15 min each with TBST before the secondary antibody was added for 1 h at room temperature. The secondary antibodies used in this study are coupled with horseradish peroxidase (HRP), which allows for immunodetection when adding an appropriate substrate. The membrane was then washed again as described before in TBST.

For immunodetection, femtoLUCENT™ PLUS-HRP was added to the membrane according to the manufacturer's protocol. As this substrate is processed by HRP, it emits a chemiluminescent signal. This signal was either directly detected by the imaging system ImageQuant 800 or used to expose X-ray films that were consequently developed using Curix 60.

2.2.4.4 Enzyme-linked immunosorbent assay (ELISA)

ELISA can be used to quantify the concentration of different released cytokines in cell culture supernatants.

In this study, assays to determine concentrations of TNF-α and IL-1β were used according to manufacturer's instructions (Thermo Fisher). Cell culture supernatants from infected and uninfected primary human macrophages were diluted 1:2 and used as samples. The resulting fluorescent signals were detected using microplate reader Infinite M200 (Tecan) and measured values were compared to an included standard curve.

3 Results

3.1 *Yersinia*-induced cell death in primary human macrophages

As previously described, the pathways activated upon *Yersinia* infection, including YopP dependent blockage of TAK1 phosphorylation, activation of RIP1, and finally GSDMD pore formation, are well studied in murine macrophages but have not yet been extensively investigated in human macrophages. Therefore, this was one of the focus points of this study. Primary human macrophages were infected with different *Yersinia* strains and the effects on various important proteins involved in cell death, especially GSDMD and GSDME, as well as the role of YopP specifically, were investigated.

3.1.1 *Yersinia*-infected human macrophages die in a YopP-dependent manner

To first determine if and when *Yersinia* infection leads to cell death, primary human monocyte-derived macrophages were infected with wild type *Y. enterocolitica* (WAP) or a strain lacking YopP (ΔP) for 5 h or 23 to 24 h. Furthermore, Necrostatin-1s (Nec1s), a RIP1 kinase inhibitor, was added to WAP infection in order to investigate, whether RIP1 is involved in mediating cell death. SYTOX® Green was used to quantify cell death rates and cells treated with TritonX were used as a reference for 100 % cell death (Figure 4).

After 5 h of infection, no difference between cell death rates could be detected, whereas after 24 h of infection, macrophages infected with WAP showed significantly higher cell death rates compared to those infected with ΔP. This shows not only that human macrophages die when infected with *Y. enterocolitica,* but also that cell death seems to be dependent upon YopP. Furthermore, these results show, that addition of the RIP1 inhibitor Nec1s did not affect cell death rates, indicating that RIP1 kinase activity might not be involved in mediating cell death in human macrophages.

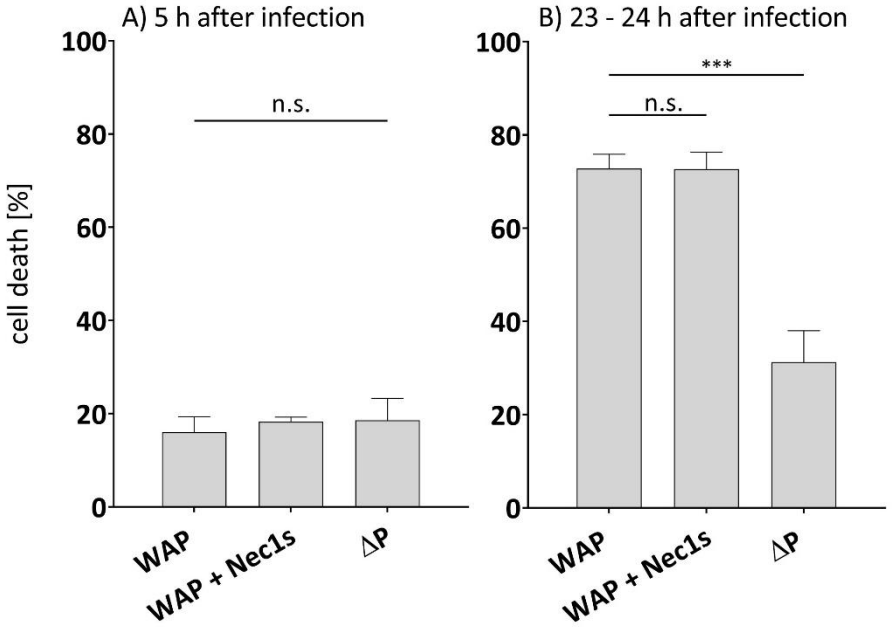

Figure 4: Relative cell death rates of primary human macrophages upon *Yersinia* infection after (A) 5 h and (B) 23-24 h. Primary human macrophages were treated with Nec1s and infected with WAP or ΔP (MOI 20:1) as indicated. 120 min after infection, gentamycin was added as well as SYTOX® Green. Fluorescence was measured multiple times for up to 24 h. Cells treated with Triton-X were used as a maximum cell death value and untreated cells were used as background cell death value. Bars for WAP and ΔP infection represent mean values ± SEM of n = 5 experiments. Bars for WAP + Nec1s infections represent mean values ± SEM of n = 3 experiments. (n.s. = not significant, *** $p < 0.001$, unpaired t-test).

3.1.2 YopP inhibits TAK1 phosphorylation

TAK1 is an important signalling molecule in *Yersinia* mediated cell death. In murine macrophages cell death can be induced by YopP inhibiting autophosphorylation of TAK1 at two threonine residues (Thr-184/Thr-187). Unphosphorylated TAK1 remains inactive, which leads to a disruption of MAPK- and NFκB signalling pathways as well as activation of RIP1 dependent cell death (Paquette et al., 2012, Philip et al., 2014).

Therefore, phosphorylation of TAK1 in primary human macrophages was investigated by infecting cells with either WAP or ΔP. Cells were lysed 3 h and 6 h after infection and phosphorylation was investigated using antibodies specifically binding TAK1 phosphorylated at Threonin-184/Threonin-187 in comparison to antibodies binding to unphosphorylated TAK1 (Figure 5) Phosphorylation of TAK1 could only be detected in cells infected with YopP-deficient *Yersinia* after 3 h of infection, whereas TAK1 could be detected under all conditions. This implies that blockage of TAK1 phosphorylation in human macrophages is YopP- dependent and might lead to disruption of downstream pathways, similar as in murine macrophages.

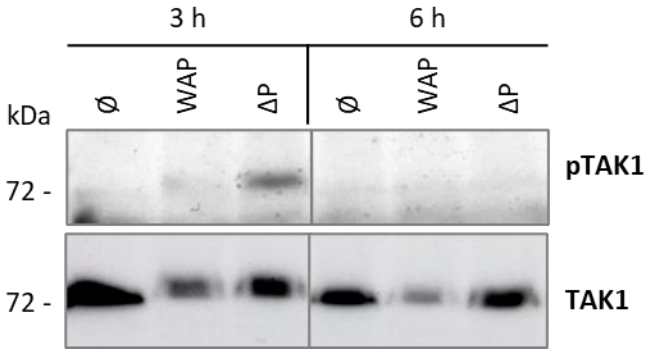

Figure 5: TAK1 and its phosphorylation in infected primary human macrophages. Primary human macrophages remained either untreated or were infected with *Y. enterocolitica* strains WAP or ΔP (MOI 50:1). Gentamycin was added after 120 min of infection and cells were lysed after 3 h or 6 h. Lysates were analysed via SDS-PAGE (9 %) and immunoblotting using antibodies against phosphorylated TAK1 (Thr-184/Thr-187) and TAK1.

3.1.3 YopP triggers RIP1 phosphorylation

RIP1 is a key component of signalling pathways involved in promoting cell death or cell survival. During *Yersinia* infection, YopP-dependent acetylation and thereby blockage of TAK1 leads to RIP1 disassociating from complex I, which is important for cell survival signalling. RIP1 can then form a complex with caspase-8 and FADD and thus promote apoptosis. Or it can form a complex with RIP3 and induce necroptosis via MLKL. Studies have showed that auto-phosphorylation of RIP1 at Ser166 is essential in order for it to form these cell death inducing complexes (Laurien et al., 2020).

To study the phosphorylation of RIP1 in human macrophages, cells were again infected with either WAP or ΔP, and additionally treated with RIP1 inhibitor Nec1s where indicated. Cell lysates generated 3, 6 and 18 h after infection were then analysed using immunodetection with specific antibodies either against RIP1 or against RIP1 auto-phosphorylated at Ser-166 (Figure 6). A clear signal of phosphorylated RIP1 was only detectable in cells infected with WAP for 6 h. Absence of YopP or addition of Nec1s seemed to prevent autophosphorylation and thus likely activation of downstream molecules. Hence, auto-phosphorylation of RIP1 was triggered by infection with *Y. enterocolitica* in a YopP dependent manner, comparably with what has been shown for murine macrophages before.

Unphosphorylated RIP1 seemed to disappear in cells infected with WAP with or without Nec1s for 18 h. As shown previously (Figure 4), cells infected for such long time spans exhibited high rates of cell death under both of these conditions so it is possible that RIP1 was already disintegrated at this time point and therefore no longer detectable here.

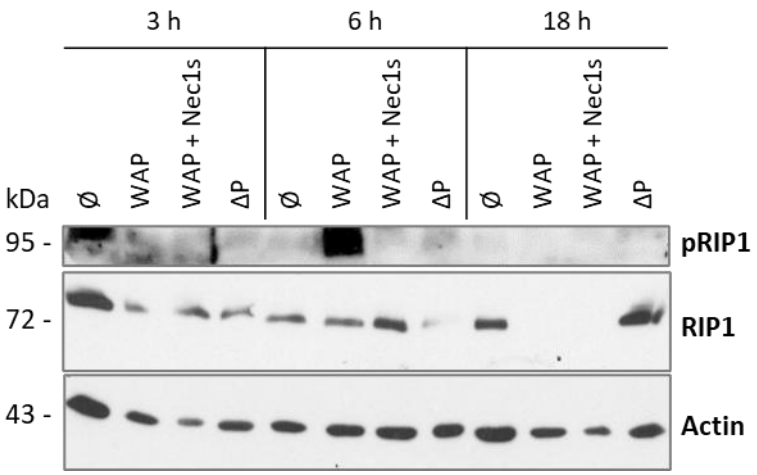

Figure 6: RIP1 and its phosphorylation in infected primary human macrophages with Actin control. Primary human macrophages remained either untreated or were infected with *Y. enterocolitica* strains WAP or ΔP (MOI 30:1). Where indicated, cells were treated with RIP1 kinase inhibitor Nec1s 1 h prior to infection. Gentamycin was added after 120 min of infection and cells were lysed after 3 h, 6 h and 18 h. Lysates were analysed via SDS-PAGE (9 %) and immunoblotting using antibodies against phosphorylated RIP1 (Ser-166), RIP1 and Actin as a loading control.

3.1.4 *Yersinia* infection leads to activation of caspases-3 and -8

Initiator Caspase-8 plays an important role in signalling of cell death upon *Yersinia* infection in murine macrophages. It is cleaved into different fragments when activated. First, caspase-8 is cleaved into two intermediates: p43/p41 and p12. While p12 is further processed into the p10 fragment, the lager intermediate gets processed into the inactive pro-domain p26/p24 and the active enzyme fragment p18 (Lavrik et al., 2003). Active caspase-8 can then cleave the pore-forming protein GSDMD and consequently trigger pyroptosis, or it can activate caspase-3, an effector-caspase (Sarhan et al., 2018, Kesavardhana et al., 2020). Pro-caspase-3 is first cleaved into a p12 and a p20 fragment. The latter is then further processed into the active p17 fragment (Han et al., 1997). Active caspase-3 can trigger apoptosis as well as process GSDME into its active, pore-forming subunit. Furthermore, it can inactivate GSDMD through cleavage at a site distinct from where caspase-8 cleaves it (Taabazuing et al., 2017, Wang et al., 2017).

Here, activation of caspase-8 and caspase-3 upon *Yersinia* infection was examined by infecting primary human macrophages with either WAP or ΔP, and generating lysates at the indicated time points. SDS-PAGE and immunodetection were then performed with antibodies binding either processed caspase-8 or full-length and processed caspase-3. Thus, cleavage of these molecules could be examined (Figure 7). Caspase-8 was processed into its active fragment at every time point when cells were infected with wildtype *Y. enterocolitica* with notably the strongest signal after 6 h of infection. The processed fragments p43/p41 were also detectable under these conditions. Meanwhile, infection with the YopP deficient strain mostly led to cleavage of caspase-8 into the not fully active p43/p41 fragments. WAP

infection for 6 h or longer also led to activation of caspase-3. The active fragment was clearly detectable with the strongest signal after 18 h of infection. Full-length caspase-3 was detectable in all samples but absence of YopP did not trigger any cleavage into active fragments. As active caspase-8 was present in infected human macrophages, it is likely that that these fragments were consequently responsible for cleavage and activation of caspase-3 following infection with WAP.

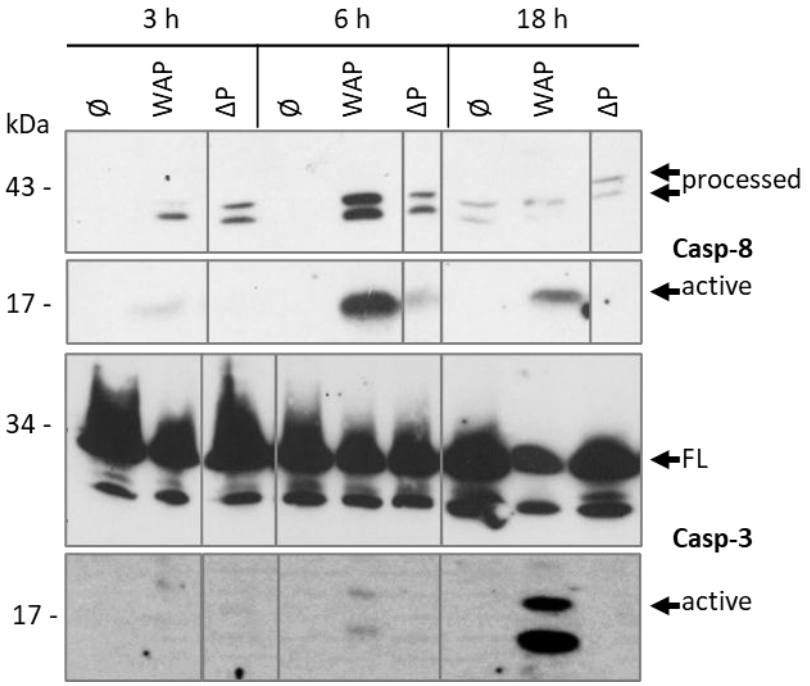

Figure 7: Processing of caspase-3 and -8 in infected primary human macrophages. Primary human macrophages remained either untreated or were infected with *Y. enterocolitica* strains WAP or ΔP (MOI 30:1). Gentamycin was added after 120 min of infection and cells were lysed after 3 h, 6 h and 18 h. Lysates were analysed via SDS-PAGE (12 %) and immunoblotting. Antibodies were used to detect (A) processed caspase-8 fragments or (B) full-length caspase-3 as well as processed caspase-3 fragments. (FL = full-length)

3.1.5 GSDME but not GSDMD is activated after infection

In murine macrophages, *Yersinia* infection can lead to cleavage of the pore-forming protein GSDMD by caspase-8 into its active p30 fragment. This activation then leads to pyroptosis and release of interleukin IL-1β, which overall indicates that GSDMD plays an important role in modulating the cellular immune response upon infection (Sarhan et al., 2018). GSDMD can be inactivated by caspase-3 dependent cleavage into the p43 fragment (Taabazuing et al., 2017). The related protein GSDME, on the other hand, does not seem to have similar effects to GSDMD. Studies showed that while GSDME is processed into its active fragment p31 by caspase-3, it does not seem to influence either cell death or IL-1β release in murine macrophages infected with *Yersinia* (Wang et al., 2017, Chen et al., 2021).

To determine, whether GSDMD and GSDME are activated upon *Y. enterocolitica* infection in primary human macrophages, cells were infected with three different strains of bacteria for either 3, 6 or 18 h. Besides infection with WAP and ΔP as described in previous experiments, macrophages were additionally infected with the strain ΔPQ, which lacks YopP and YopQ. This strain has been shown to induce pyroptosis via caspase-1 activation and was therefore used as a positive control for GSDMD cleavage (Brodsky et al., 2010). Cell lysates were analysed using antibodies binding either full-length GSDMD and its fragments, or full-length GSDME and its fragments (Figure 8). The results here indicate that infection with WAP did not lead to activation of GSDMD in human macrophages, as only the full-length protein and the inactive p43 fragment could be detected. The pore-forming subunit p31 could only be detected when infecting cells with *Yersinia* strain ΔPQ. As caspase-1 is likely to be active under this condition, GSDMD might have been processed by that. Full-length protein could be detected at any condition as well as the inactive p43 fragment with strongest signals after 6 and 18 h of WAP infection. Opposed to that, signals for the active fragment of GSDME could be detected 6 h and 18 h after infection with WAP, likely processed by caspase-3 which was previously shown to be in its active state at these time points (Figure 7). Full-length GSDME was detectable under all conditions. The results of this experiment indicate that there might be differences in the execution of cell death upon *Yersinia* infection between murine and human macrophages, though it remains to be examined which role active GSDME plays in this case and if it induces pyroptosis downstream.

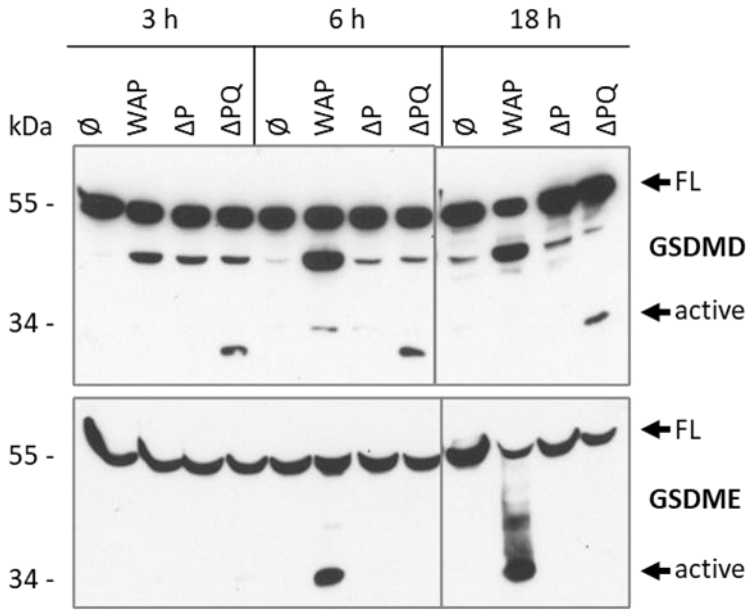

Figure 8: Processing of GSDMD and GSDME upon *Yersinia* infection in human macrophages. Primary human macrophages remained either untreated or were infected with *Y. enterocolitica* strains WAP, ΔP or ΔPQ (MOI 30:1). Gentamycin was added after 120 min of infection and cells were lysed after 3 h, 6 h and 18 h. Lysates were analysed via SDS-PAGE (10 %) and immunoblotting. Antibodies were used to detect (A) GSDMD in its full length as well as processed fragments, or (B) full-length GSMDE as well as its active fragment.

3.1.6 YopP inhibits release of cytokines

Finally, primary human macrophages were analysed regarding their release of the pro-inflammatory cytokines TNF-α and IL-1β. Examining this can give further insight into how these cells die upon *Y. enterocolitca* infection. Studies have shown that release of TNF-α can be suppressed in a YopP dependent manner in murine macrophages while IL-1β is reportedly released in a GSDMD-dependent manner during pyroptosis (Palmer et al., 1998, Chen et al., 2021).

Primary human macrophages were infected with either WAP, ΔP or ΔPQ. Supernatants were removed 17 h later and then used to determine concentrations of cytokines by ELISA (Figure 9). Cells infected with WAP released significantly more TNF-α than uninfected cells (on average 1871 pg/ml), but concentrations of released cytokine increased about 4-fold when cells were infected with either ΔP or ΔPQ (on average 8154 pg/ml and 7974 pg/ml respectively). As TAK1 is normally responsible for TNF-α production, YopP-dependent TAK1 inhibition consequently seemed to lead to reduced cytokine levels in supernatants.

Similar results were obtained when measuring IL-1β concentrations. While cells infected with WAP released significantly higher amounts of IL-1β (on average 56 pg/ml), concentrations were also significantly lower when compared to supernatants of cells infected with *Yersinia* lacking either YopP or YopP and YopQ (on average 296 pg/ml and 321 pg/ml respectively). This indicates that release of IL-1β also seems to be inhibited by YopP in human macrophages. GSDMD has been described as playing an important role in IL-1β release in murine macrophages but has been shown previously to not be activated in human macrophages upon WAP infection. Therefore, the release of IL-1β detected here might be GSDMD-independent.

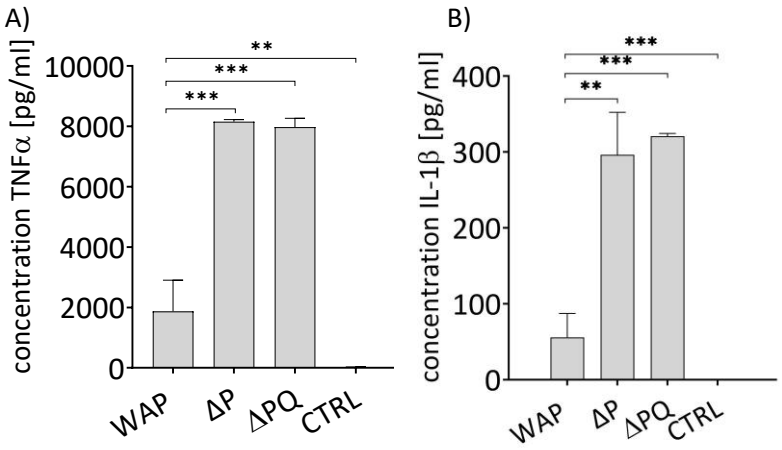

Figure 9: Concentration of inflammatory cytokines in cell culture supernatants of untreated and *Y. enterocolitca* infected primary human macrophages. Primary human macrophages remained either untreated or were infected with *Y. enterocolitica* strains WAP, ΔP or ΔPQ (MOI 30:1). Gentamycin was added after 120 min of infection. 17 – 18 h after infection, cell culture supernatants were collected and used to determine (A) TNF-α concentrations [pg/ml] and (B) IL-1β concentrations [pg/ml] by ELISA. Bars represent mean values ± SEM of n = 5 independent experiments (** $p < 0.01$, *** $p < 0.001$, unpaired t-test).

3.2 THP-1 cells as a human macrophage model for *Yersinia* infection

3.2.1 *Yersinia*-induced cell death in THP-1 macrophages

As shown above, experiments with primary human macrophages suggest a role for GSDME in *Y. enterocolitica* mediated cell death. Therefore, THP-1 cells were used to create and subsequently study a GSDME-deficient human cell line. THP-1 cells are a human monocyte cell line that can be differentiated into macrophages with PMA.

First, processing of key signalling molecules in THP-1 macrophages was investigated to ensure comparability to primary human macrophages (Figure 10). After differentiation using PMA, cells were infected with wild type *Y. enterocolitica* and the strain lacking YopP. As can be seen in Figure 10, TAK1 phosphorylation was inhibited in a YopP-dependent manner upon infection, exactly like shown previously for primary macrophages (Figure 5). Next, processing of capase-3 was investigated. The active fragment of caspase-3 could be detected after 17 h of infection with WAP, whereas only little caspase-3 processing was obvious after infection with YopP deficient bacteria. Finally, immunodetection showed that, just like in primary macrophages, active GSDME fragments were detected in WAP-infected THP-1 macrophages 6 h and 18 h after infection. As no active GSDME fragments were detected in lysates of cells infected with ΔP, cell death seems to be mediated by YopP here too.

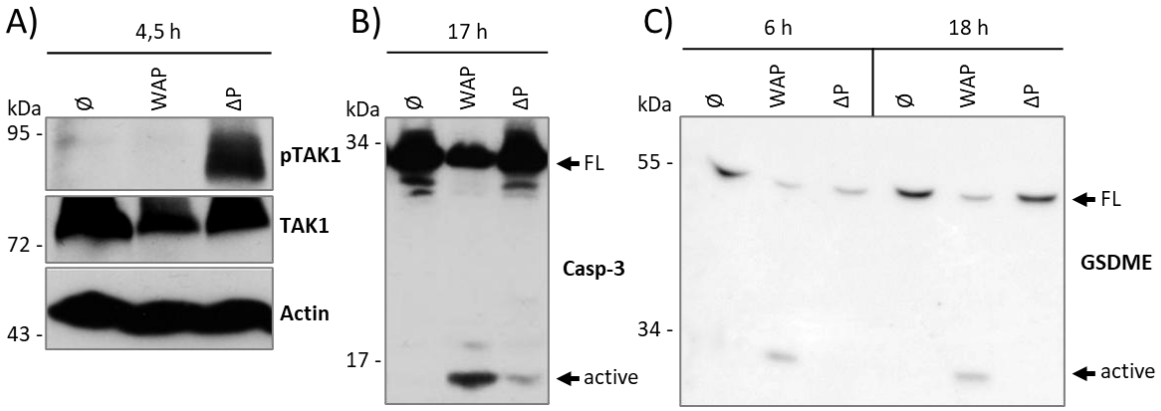

Figure 10: Investigating TAK1 phosphorylation and processing of caspase-3 and GSDME in THP-1 macrophages. THP-1 cells were differentiated with PMA (20 ng/ml) and remained either untreated or were infected with *Y. enterocolitica* strains WAP or ΔP (MOI 30:1). Gentamycin was added after 120 min of infection and cells were lysed at the indicated time points. Lysates were analysed via SDS-PAGE and immunoblotting. Antibodies were used to detect (A) phosphorylated TAK1, TAK1 and actin as a control, (B) full-length caspase-3 as well as processed caspase-3 fragments, or (C) full-length GSMDE as well as its active fragment. (FL = full-length)

3.2.2 Generation of GSDME-deficient THP-1 cells

As the results presented above were comparable to those obtained from studying primary human macrophages, THP-1 cells were next used to create a GSDME-deficient human cell line. This knockout-cell line was generated using the CRISPR / Cas9 system and lentiviral transduction. GSDME-deficiency was confirmed using western blotting and immunodetection (Figure 11).

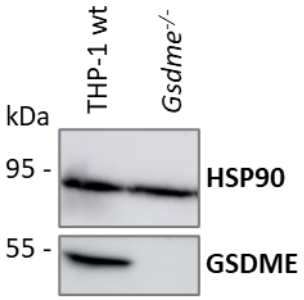

Figure 11: Validation of the Gsdme knock-out in THP-1 cells using immunodetection. THP-1 cells were used to generate a GSDME deficient cell line using the CRISPR / Cas9 system and lentiviral transduction as described above. Wildtype cells (control) and individual clones were lysed and lysates were analysed via SDS-PAGE and immunoblotting with antibodies against GSDME or HSP90 as a loading control.

3.2.3 Absence of GSDME leads to reduction of *Yersinia*-induced cell death

To investigate whether absence of GSDME affects cell death rates after *Y. enterocolitica* infection, SYTOX® Green assays were conducted. THP-1 wild type cells and THP-1 cells lacking GSDME were

infected with wild type *Y. enterocolitica* (WAP) or a strain lacking YopP (ΔP) for 5 h or 18 – 20 h. Fluorescence of SYTOX® Green was measured and cell death rates were calculated using cells treated with TritonX as a reference for 100 % cell death (Figure 12).

5 h after infection, no difference between neither cell lines nor infection conditions could be observed. After 18 – 20 h of infection, however, cells lacking GSDME showed significantly reduced cell death compared to wild type cells. This implies that GSDME might be involved in *Yersinia*-induced cell death in human macrophages. As cell death rates upon infection with ΔP remained lower compared to WAP infection, it is likely that the cell death observed here is YopP dependent, like it is in primary macrophages.

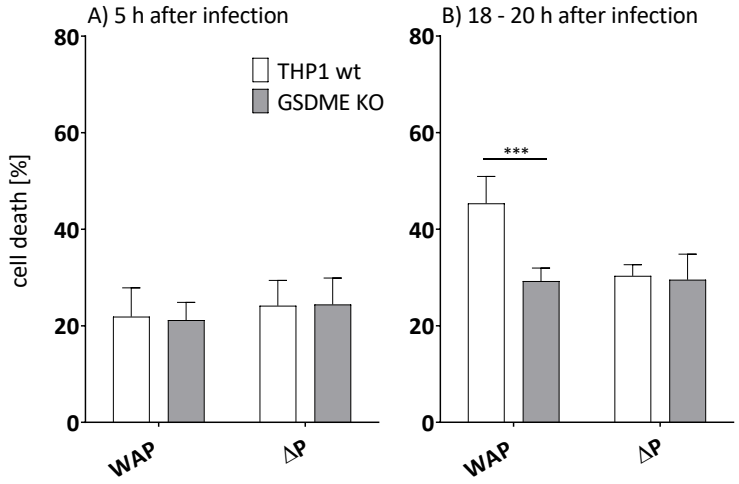

Figure 12: Relative cell death rates of wildtype THP-1 cells and GSDME-deficient THP-1 cells upon *Yersinia* infection after (A) 5 h and (B) 18 - 20 h. Differentiated THP-1 macrophages were infected with WAP or ΔP (MOI 20:1) as indicated. 120 min after infection, gentamycin was added as well as SYTOX® Green. Fluorescence was measured multiple times for up to 24 h. Cells treated with Triton-X were used as a maximum cell death value and untreated cells were used as background cell death value. Bars for WAP and ΔP infection represent mean values ± SEM of n = 3 experiments. (*** $p < 0.001$, unpaired t-test)

3.3 Examining *Y. enterocolitica*-mediated cell death in different murine knockout cell lines

To study the effects of several potentially relevant molecules in *Yersinia*-mediated death of mouse macrophages, three different knockout cell lines were generated using the genome editing system Alt-R® CRISPR-Cas9 (IDT) on an immortalized macrophage line. The knockout cell lines were validated using immunoblotting. i*Bid*$^{-/-}$ and i*Gsdmd*$^{-/-}$ were generated separately, while i*Bid*$^{-/-}$ *Gsdmd*$^{-/-}$ were created by introducing a *Gsdmd* knockout in previously generated i*Bid*$^{-/-}$ cells. These macrophages were furthermore compared to previously generated BID deficient macrophages that stably expressed Cas9. iWT

cells were used as a basis for all knockouts and compared to deficient cell lines by immunoblotting (Figure 13).

GSDMD is a pore-forming molecule, that can be cleaved into its active fragment by various caspases. It is the executioner of pyroptosis in macrophages and plays an important role during *Yersinia*-mediated cell death, where it is activated by caspase-8 (Sarhan et al., 2018). BID is a pro-apoptotic protein that belongs to the Bcl-2 family. During intrinsic apoptosis, it is cleaved into its active, truncated form and then able to subsequently activate the effector proteins BAX and BAK. BAX and BAK then cause MOMP, which results in release of pro-apoptotic molecules and results finally in the activation of caspases-3 and -7, the executioners of apoptosis (Czabotar et al., 2014, Snyder and Oberst, 2021). Additionally, BID can be cleaved and activated by caspase-8 during extrinsic apoptosis (Li et al., 1998). More recently, two studies found that in the absence of GSDMD, BID can also be activated by caspases-1, which then triggers MOMP and subsequently rapid activation of caspase-3, causing secondary necrosis (Tsuchiya et al., 2019, Heilig et al., 2020). In murine macrophages, infection with *Y. enterocolitica* leads to a processing of BID and consequently MOMP in a YopP-dependent manner (Denecker et al., 2001).

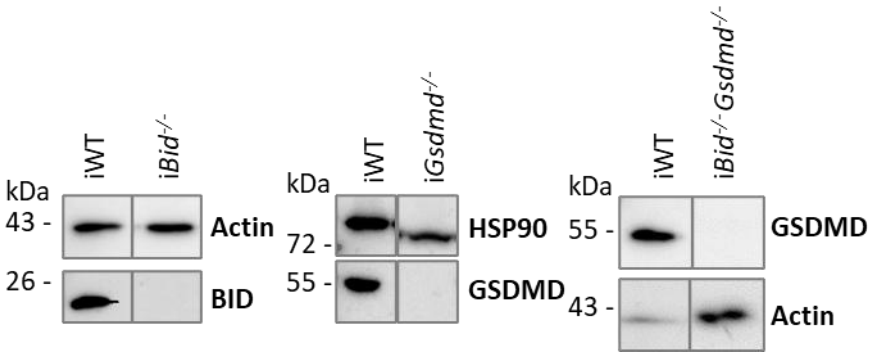

Figure 13: Validation of murine knockout cell lines. i*Bid*$^{-/-}$, i*Gsdmd*$^{-/-}$ and *iBid*$^{-/-}$ *Gsdmd*$^{-/-}$ macrophages were generated using CRISPR / Cas9. iWT cells (control) and individual clones were lysed and lysates were analysed via SDS-PAGE and western blotting with antibodies against BID or GSDMD and Actin or HSP90 as loading controls.

3.3.1 Investigation of *Yersinia* induced cell death rates in murine knockout macrophages

It has already been established, that absence of GSDMD leads to delayed *Yersinia*-mediated cell death in murine macrophages (Sarhan et al., 2018, Chen et al., 2021). However, as cell death is not completely abolished, other mechanisms must function as backup systems in case GSDMD-dependent pyroptosis is supressed. One study showed that during AIM2-inflammasome activation, deletion of both BID and GSDMD results in drastically reduced cell death of murine macrophages (Heilig et al., 2020).

To further our understanding of the involvement of BID, on its own and in combination with GSDMD, several experiments with murine macrophages deficient for either BID or BID and GSDMD were

conducted. First, SYTOX® Green assays were used to determine how lack of BID, GSDMD or both influences the cell death rates upon infection with *Y. enterocolitica*. All four cell lines were infected with either WAP or ΔP. Untreated cells served as a control and cells treated with TritonX as a reference for 100 % cell death. SYTOX® Green was added and fluorescence was measured after 3 and 5 h of infection (Figure 14). BID deficiency did not lead to reduced cell death, while absence of GSDMD resulted in a significant decrease after 3 h, as described in previous studies. Cells lacking both molecules were also significantly protected from *Y. enterocolitica* induced cell death with even lower rates of cell death compared to i*Gsdmd*$^{-/-}$, suggesting a role for BID in the absence of GSDMD. 5 h after infection, the cell death rates were overall higher, but absence of GSDMD or GSDMD and BID still resulted in significant cell death protection. Infection with ΔP only mediate low rates of cell death at both time points, confirming that the observed death of macrophages is YopP-dependent.

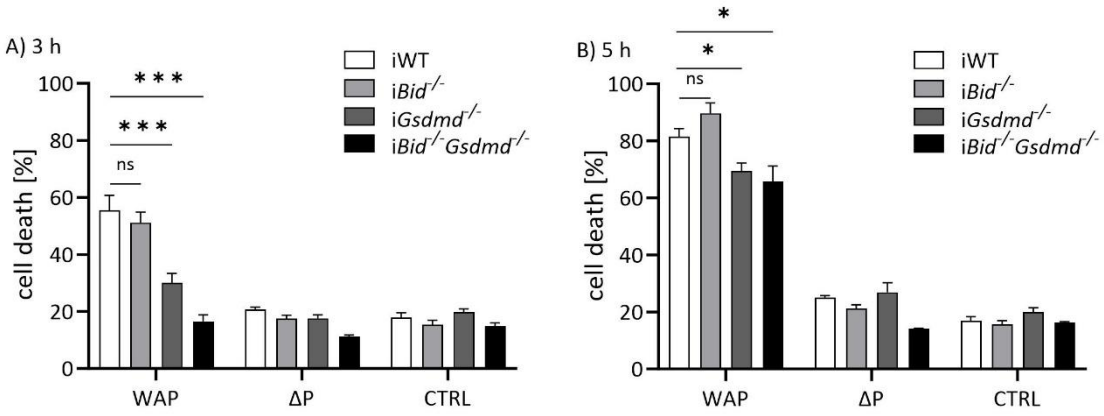

Figure 14: Relative cell death rates of different murine knockout cell lines upon *Y. enterocolitica* infection. iWT, i*Bid*$^{-/-}$, i*Gsdmd*$^{-/-}$ and i*Bid*$^{-/-}$ *Gsdmd*$^{-/-}$ macrophages were infected with WAP or ΔP (MOI 30:1). 90 min after infection, gentamycin was added as well as SYTOX® Green. Fluorescence was measured after A) 3 hours or B) 5 h of infection. Cells treated with Triton-X were used as a maximum cell death value and untreated cells were used as background cell death value. Bars for CTRL, WAP and ΔP infection represent mean values ± SEM of n = 3 experiments. Statistics were applied on values in which CTRL background values were subtracted, as described in 2.2.3.8 (n.s. = not significant, * $p < 0.05$ ***, $p < 0.001$, unpaired t-test).

3.3.2 Influence of BID deficiency on activation of different caspases

The impact of BID deficiency on death of murine macrophages upon *Yersinia* infection was investigated further. First, activation and processing of different caspases involved in cell death signalling was examined.

Caspase-8 has been found to be essential for *Yersinia*-mediated cell death in macrophages (Orning et al., 2018). Formation of a complex with RIP1 and FADD leads to auto-activation and formation of the active p18 fragment. Caspase-8 has a variety of downstream substrates, including caspase-3 and

GSDMD. It can also generate the active tBID fragment and thus trigger MOMP during apoptosis. (Orning et al., 2018, Li et al., 1998, Sarhan et al., 2018).

iWT and i*Bid*$^{-/-}$ macrophages were infected with either WAP or ΔP for up to 4 h before lysates were generated and analysed via SDS-PAGE and immunoblotting. Using antibodies against processes caspase-8, the active fragment (p18) was detectable in both cell lines infected with WAP, with the strongest signal after 3 h (Figure 15). Though the overall signal seemed stronger in iWT cells, there was remarkable caspase-8 activation also observed in BID deficient cells. This was to be expected as caspase-8 acts upstream of BID. Presence of the active fragment, however, indicates that BID-cleavage through caspase-8 is possible during *Yersinia* infection. Infection with ΔP did not trigger cleavage of caspase-8 into the active fragment in either cell line.

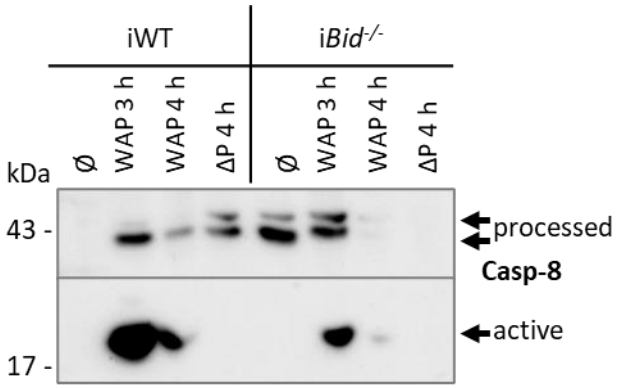

Figure 15: Caspase-8 processing in iWT and i*Bid*$^{-/-}$ cells. iWT and i*Bid*$^{-/-}$ macrophages remained either untreated or were infected with either WAP or ΔP for 3 or 4 h (MOI 30:1). Gentamycin was added after 90 min. Lysates were analysed via SDS-PAGE (12 %) and immunodetection with antibodies against cleaved caspase-8.

Next, processing of caspase-9 was investigated. During intrinsic apoptosis, BID-mediated MOMP leads to cytochrome c released from mitochondria. This, in turn, triggers APAF-1 mediated cleavage of pro-caspase-9 (47 kDa) into its active fragment p35. Alternatively, cleavage into a p37 fragment can be mediated by caspase-3 as a feedback mechanism (Iordanov et al., 2005). Active caspase-9 is able to cleave the effector caspases-3 and -7 to promote apoptosis (Snyder and Oberst, 2021). Murine macrophages deficient for caspase-9 show mildly delayed cell death in response to TAK1 inhibition in combination with LPS stimulation, and the active p35 fragment could be detected under these conditions (Sarhan et al., 2018).

Here, iWT macrophages as well as i*Bid*$^{-/-}$ and i*Bid*$^{-/-}$ *Gsdmd*$^{-/-}$ were infected with WAP or ΔP for 1 to 3 hours. Alternatively, wild type and BID-deficient cells were treated with the TAK1 inhibitor NG25 and stimulated with LPS to mimic *Y. enterocolitica* infection. Cells treated only with LPS served as an additional control. SDS-PAGE and immunoblotting were used to analyse samples with antibodies

recognising full-length and both cleaved fragments of caspase-9 (Figure 16). When using LPS and NG25, both processed fragments were detectable in iWT lysates. In lysates from i*Bid*$^{-/-}$ cells, the signal of the p37 fragment seemed stronger compared to the p35 fragments signal, with the strongest signal detected after 2 h of stimulation. Upon infection with bacteria, only the p37 fragment was detectable in cells lacking BID, while both processed forms seemed to be present in iWT cell lysates. Additionally, in cells infected with *Y. enterocolitica* lacking YopP, only procaspase-9, but no cleaved caspase-9 fragments, were detectable. Overall, the p37 fragment, corresponding to caspase-3-dependent cleavage, seems to be primarily produced in BID-deficient macrophages. This might be because this way of cleavage does not depend on BID-mediated MOMP and subsequent cytochrome c release. In wild type cells, where MOMP should be unaffected, both processed fragments can be detected.

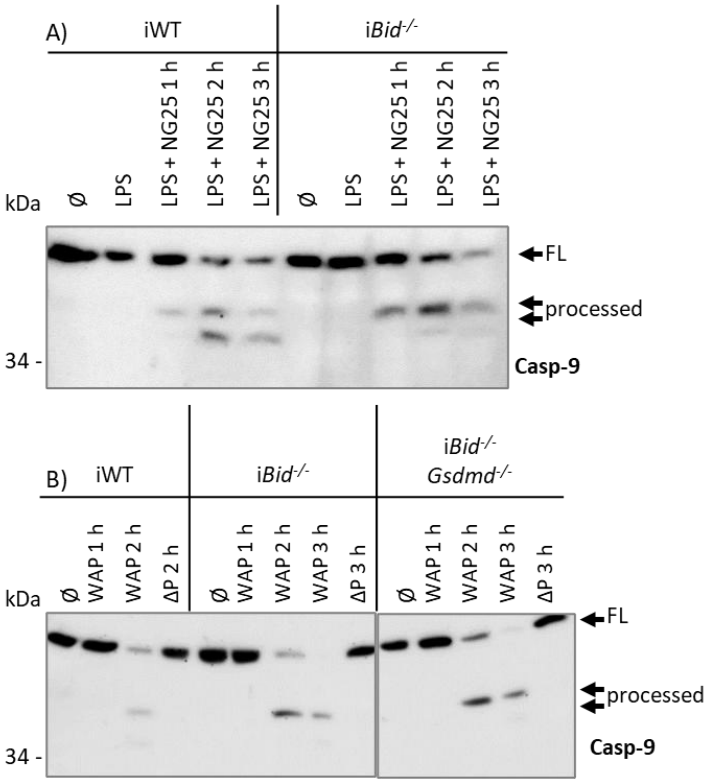

Figure 16: Caspase-9 processing in iWT, i*Bid*$^{-/-}$ and i*Bid*$^{-/-}$ *Gsdmd*$^{-/-}$ macrophages. A) Indicated cell lines were treated with the TAK1 inhibitor NG25 (15 µM) 1 h prior to stimulation with LPS (1 µg/ml). Control samples remained untreated or were only stimulated with LPS. After the indicated time spans, cells were lysed. B) Indicated cell lines were infected with either WAP or ΔP for 1 – 3 h (MOI 30:1). Gentamycin was added after 90 min. Uninfected cells served as a control. All Lysates (A & B) were analysed via SDS-PAGE (10 %) and immunodetection with antibodies recognising full-length and processed caspase-9.

Furthermore, activation of caspase-3 was examined. Caspase-3 is an executioner caspase and plays a vital role in apoptosis. It can be activated through cleavage by either caspase-8 or caspase-9 into its active p17 fragment (Han et al., 1997). It has been shown that infection with *Yersinia* or LPS stimulation with TAK1 inhibition results in generation of the active caspase-3 fragment (Sarhan et al., 2018,

Bergsbaken and Cookson, 2007). Caspase-3 can activate GSDME and inhibit GSDMD through cleavage (Taabazuing et al., 2017).

iWT and i*Bid*$^{-/-}$ were again treated with the TAK1 inhibitor NG25 and stimulated with LPS for up to 3 h. Additionally, wild type and BID deficient cells expressing Cas9 and generated separately, were infected with WAP or ΔP for up to 4 hours. Processing of caspase-3 was analysed using SDS-PAGE and western blotting with antibodies against both the full-length molecule and the active p17 fragment (Figure 17). When using LPS and NG25 treatment, active caspase-3 was detectable at every time point in both cell lines with notably stronger signals in iWT cell lysates. Upon *Yersinia* infection, p17 could also be detected. In wildtype cells, active caspase-3 was detectable from 2 h onward with the strongest signal after 3 h of WAP infection. In the absence of BID, the p17 fragment was detectable from 1 h onward with the strongest signals after 3 and 4 hours. Infection with ΔP did not lead to detection of the active fragments in the used cell lines. Caspase-3 activation can either occur independently of BID-induced MOMP through caspase-8-mediated cleavage or through caspase-9 cleavage after cytochrome c release from mitochondria. It therefore remains to be examined, if the pathways leading to activation are the same here. Additionally, downstream effects of caspase-3 activation remain to be investigated.

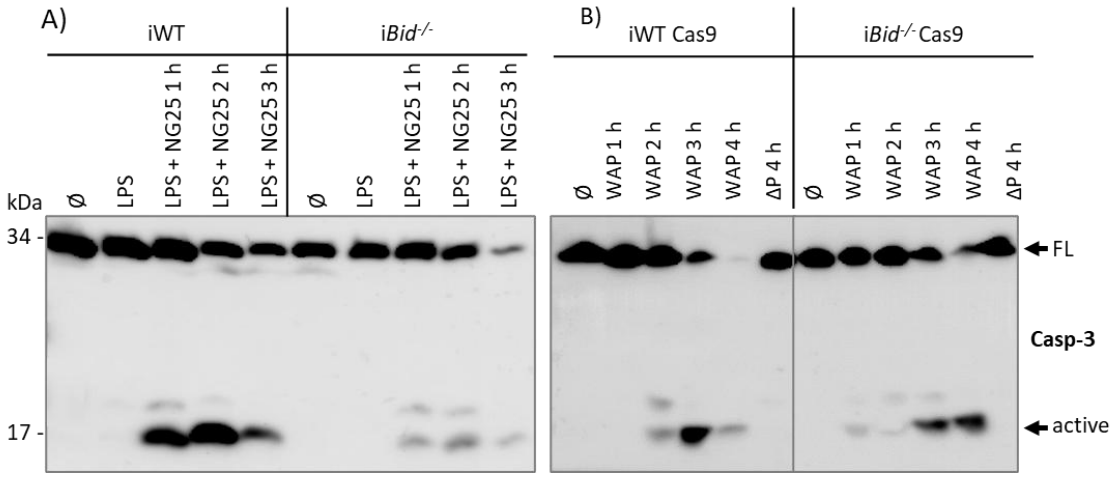

Figure 17: Caspase-3 processing in two different BID deficient cell lines. A) iWT and i*Bid*$^{-/-}$ were treated with TAK1 inhibitor NG25 (15 µM) 1 h prior to stimulation using LPS (1 µg/ml). Control samples remained untreated or were only stimulated with LPS. Cells were incubated for up to 3 h before generating cell lysates. B) iWT Cas9 and i*Bid*$^{-/-}$Cas9 macrophages remained either untreated or were infected with either WAP or ΔP for 1 – 4 h (MOI 30:1). Gentamycin was added after 90 min and lysates were generated at indicated time points. All Lysates (A & B) were analysed via SDS-PAGE (12 %) and immunodetection with antibodies recognising full-length as well as processed caspase-3.

3.3.3 Activation of GSDMD in BID-deficient macrophages

Finally, BID deficient macrophages were examined and compared to wildtype cells regarding processing and activation of GSDMD. Infection with *Yersinia* in mouse macrophages leads to GSDMD cleavage mediated by caspase-8. The active p30 fragment of GSDMD forms pores in the cell membrane and thus induces pyroptosis and release of cytokines. Loss of GSDMD leads to delays in cell death after infection and to a decrease in released IL-1β (Chen et al., 2021, Sarhan et al., 2018). Downstream of inflammasome activation, GSDMD can be activated by caspase-1. Loss of GSDMD upon inflammasome activation results in caspase-1-mediated BID truncation and subsequent caspase-3 cleavage (Heilig et al., 2020). While caspase-8 mediated activation through cleavage of GSDMD, cleavage through caspase-3 produces an inactive p43 fragment (Taabazuing et al., 2017). Caspase-3-mediated cleavage of the already active p30 fragment produces an inactive p21 fragment (Chen et al., 2019). As GSDMD plays an important role in *Yersinia*-mediated cell death, the influence of BID-deficiency on its activation was investigated here.

LPS stimulation paired with TAK1 inhibition was used to mimic infection in iWT and i*Bid*$^{-/-}$ cells, while iWT Cas9 and i*Bid*$^{-/-}$ Cas9 were again infected with either WAP or ΔP for indicated time periods. Lysates from all samples were analysed using SDS-PAGE and immunoblotting with antibodies binding to full-length GSDMD and its processed fragments (Figure 18). In iWT cells treated with LPS and NG25, the processed inactive fragments p43 and p21 were easily detectable but the active fragment p30 was only hardly seen. In i*Bid*$^{-/-}$ on the other hand, signals corresponding to the pore-forming p30 fragment of GSDMD could predominantly be detected in treated cells. Similarly, when using bacterial infection, wild type lysates showed dominant signals for the p43 inactive fragment while BID deficient cells seemed to preferentially process GSDMD into its active p30 form after 3 and 4 h of infection. No processing was detectable upon infection with ΔP. These results might indicate that BID-deficiency influences GSDMD activation downstream. However, it remains unclear why here the active GSDMD fragment was not detect after WAP infection, as its generation has been described by other studies.

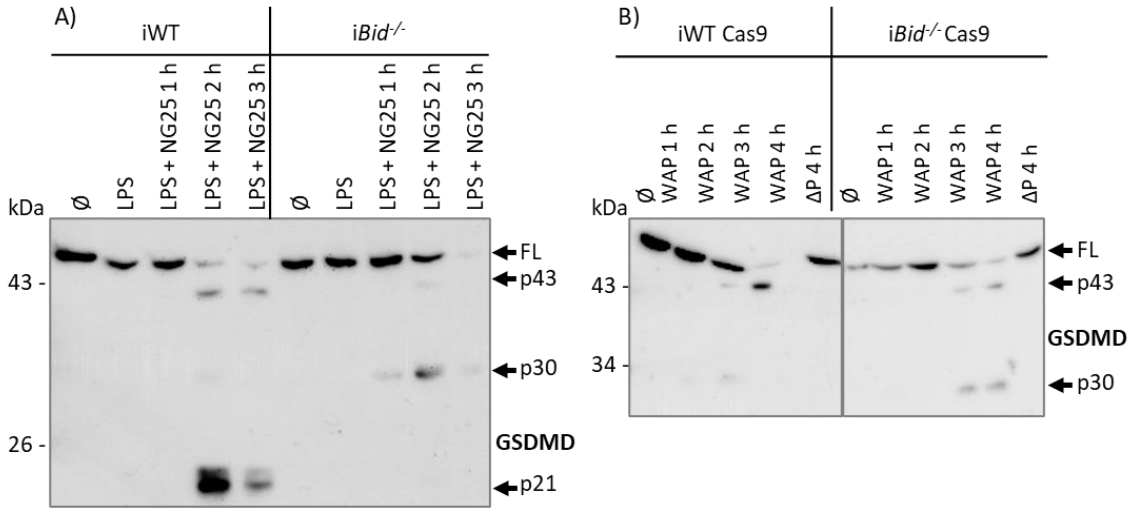

Figure 18: Cleavage of GSDMD in two different BID deficient cell lines. A) iWT and i*Bid*-/- were treated with the TAK1 inhibitor NG25 (15 µM) 1 h prior to stimulation with LPS (1 µg/ml). Control samples remained untreated or were only stimulated with LPS. Cells were incubated for up to 3 h before generating cell lysates. B) iWT Cas9 and i*Bid*-/-Cas9 macrophages remained either untreated or were infected with either WAP or ΔP for 1 – 4 h (MOI 30:1). Gentamycin was added after 90 min and lysates were generated at indicated time points. All Lysates (A & B) were analysed via SDS-PAGE (10 %) and immunoblotting with antibodies recognising full-length as well as processed GSDMD.

4 Discussion

When macrophages are infected with *Yersinia*, several bacterial proteins are injected into the host cell via the TTSS. One of them, YopP/J, is essential for mediating macrophage cell death upon infection (Mills et al., 1997). LPS, which is part of the bacterial outer membrane, is recognised by TLR4 which triggers TAK1-mediated activation of MAPK and NF-κB signalling to promote cell survival (Haase et al., 2003). However, YopP can inhibit phosphorylation and thus activity of TAK1, IKKβ and MAPKK by acetylation (Haase et al., 2005, Paquette et al., 2012) . This leads to blockage of MAPK and NF-κB signalling pathways and thus to a decrease of cytokine release and cell death (Ruckdeschel et al., 2008). *Yersinia*-mediated cell death has been shown to rely on a number of key molecules, including RIP1, FADD and caspase-8. These three form a so-called death-inducing complex (IIa) and mediate downstream signalling. While dying upon *Yersinia* infection was originally mainly connected to apoptosis via caspase-8 mediated activation of the effector caspases-3 and -7, recent studies have shown that pyroptosis might also play an important role here (Mills et al., 1997, Sarhan et al., 2018). Caspase-8 is able to cleave full-length GSDMD into its pore-forming fragment which then can mediate pyroptotic cell death and release of inflammatory cytokines. The closely related molecule GSDME, however, does not influence either of these processes although it is also cleaved into its active fragment upon *Yersinia* infection (Sarhan et al., 2018, Chen et al., 2021). This illustrated that *Yersinia* mediated cell death in macrophages is a complex process reliant on more than one form of programmed cell death as it combines features of apoptosis and pyroptosis. This work set out to further the understanding of cell death signalling upon *Y. enterocolitica* infection by studying infection in human macrophages and by focusing on the role of the MOMP-inducing molecule BID in mouse macrophages.

4.1 Cell death induction by *Y. enterocolitica* infection in primary human macrophages

Multiple studies have demonstrated that murine macrophages die after infection with *Yersinia*. Cell death, either assessed through PI influx or LDH release, could be detected from around 4 h post infection and only in the presence of YopP/J (Mills et al., 1997, Sarhan et al., 2018). One work also investigated cell death in infected human PBMC derived macrophages but did not detect any YopP/J dependent cell death in the first 12 h after infection (Sarhan et al., 2018). Comparably, when cell death of primary human macrophages was assessed in the present study using SYTOX® Green, only low levels of dying cells were recorded 5 h post infection with either wild type bacteria (WAP) or a *Y. enterocolitica* strain lacking YopP (ΔP). However, after longer timespans of 23 to 24 h, cells infected with WAP exhibited significantly higher rates of cell death compared to cells infected with the YopP-deficient strain. This suggests that *Yersinia* infection triggers YopP dependent cell death in human macrophages but on

a different time scale compared to their murine counterparts. This, however, does not provide any insight into how the cells finally die. Thus, this work set out to analyse the underlying mechanisms driving *Yersinia* induced cell death in primary human macrophages.

A key regulator of *Yersinia* induced cell death is TAK1. Its activation can be triggered by different stimuli, including downstream signalling of TLR4. TAK1 associates with its binding proteins TAB1 and TAB2 which leads to auto-phosphorylation of Thr-184 and Thr-187 in its activation loop (Sakurai et al., 2000, Mihaly et al., 2014). Activated TAK1 then promotes NF-κB and MAPK signalling via phosphorylation of different substrates including IκB-kinase (Mihaly et al., 2014). Upon *Yersinia* infection, YopP mediated acetylation blocks auto-phosphorylation and thus activation of TAK1 (Paquette et al., 2012). Inhibition of TAK1 in combination with LPS stimulation triggers release of IL-1β and cell death in macrophages (Orning et al., 2018). This is mediated by promoting RIP1 and caspase-8 activation upon TAK1 inhibition (Guo et al., 2016). Specific antibodies against TAK1 phosphorylated at Thr-184 and Thr-187 can be employed to monitor YopP-mediated TAK1 blockage. We demonstrated here that infection with WAP blocks phosphorylation of TAK1 in primary human macrophages 3 h post infection and thus most likely inhibits downstream MAPK and NF-κB signalling. In the absence of YopP, TAK1 auto-phosphorylation can be detected. 6 h post infection no phosphorylation is detectable, potentially indicating that TAK1 phosphorylation and activation occurs only in early stages of infection. Overall, this points out that human TAK1 is a target of YopP as is its murine counterpart and that inhibition of TAK1 through YopP is essential for cell death as shown above.

Another important regulatory molecule of *Yersinia*-induced cell death is RIP1. Depending on its post-translational modifications, it promotes either cell survival or cell death via association with caspase-8 and FADD or RIP3. The kinase activity of RIP1 has been shown to be essential for *Yersinia*-mediated cell death (Peterson et al., 2017). The underlying mechanisms here remained poorly understood until Laurien et al. demonstrated that auto-phosphorylation of RIP1 at Ser-166 is essential for kinase-activation and thus also crucial for the ability of RIP1 to promote cell death in *Yersinia*-infected macrophages. However, phosphorylation of Ser-166 alone does neither trigger cell death nor promote conformational changes of RIP1 (Laurien et al., 2020). Different studies identified molecules that prevent RIP1 kinase activation via phosphorylation of RIP1 to promote cell survival. MK2, for example, has been shown to phosphorylate RIP1 at Ser-321 which leads to blockage of the essential auto-phosphorylation (Menon et al., 2017). Additionally, TAK1 and IKKβ, upon stimulation by TNF-α, also phosphorylate RIP1 at Ser-321 and Ser-25 respectively, and thus inhibit complex formation with caspase-8 and FADD.

However, this does not impact the role of RIP1 in activating NF-κB signalling which illustrates that RIP1 also has kinase-independent functions (Dannappel et al., 2014, Geng et al., 2017, Dondelinger et al., 2019).

In this study, auto-phosphorylation of RIP1 at Ser-166 could be detected after 6 h of infection with WAP. This phosphorylation was not detectable in uninfected primary human macrophages or in the absence of YopP. Necrostatin-1s was used as a control as this inhibitor has been shown to block the kinase activity of RIP1 (Degterev et al., 2008). This suggests that, like in mouse macrophages, RIP1 kinase-dependent functions might be activated in human macrophages upon infection with *Y. enterocolitica*. To further analyse this, molecules induced downstream of active RIP1 need to be studied in relation to the RIP1 kinase activity. Unphosphorylated RIP1 could be detected under all conditions 3 h and 6 h post-infection, but not after 18 h of infection with WAP. This might be linked to our observation that most cells infected with wild type *Y. enterocolitica* are already dead at that time point and cellular molecules might already be degraded.

Interestingly, inhibition of the RIP1 kinase-activity through Nec1s did not confer protection against *Yersinia*-mediated cell death in primary human macrophages. Cell death rates 23 to 24 h post infection did not differ significantly between WAP-infected macrophages with or without Nec1s. This suggests that cell death at this time point might occur independent of RIP1 activity. Experiments in murine macrophages have previously shown that Nec1s addition during *Yersinia* infection significantly lowers cell death rates compared to infection without inhibition of RIP1 (Menon et al., 2017, Peterson et al., 2017). This might suggest that *Yersinia*-mediated cell death differs in this aspect between murine and human macrophages.

One study found that *Yersinia* infection in the absence of RIP1 leads to an increase in ZBP-1-dependent necroptosis in macrophages. This was assessed by measuring phosphorylation of MLKL, the pore-forming effector protein of necroptosis (Malireddi et al., 2020b). Thus, it would be of interest to study MLKL phosphorylation upon *Yersinia* infection in human macrophages to analyse if necroptosis is triggered independently of RIP1 kinase activity. Alternatively, future studies might focus on measuring cell death upon Nec1s treatment continuously over time to determine if slight delays in cell death can be detected. Overall, the exact involvement of RIP1 kinase activity in cell death of human macrophages upon *Yersinia* infection remains to be studied further, although our data suggests that RIP1-dependent cell death regulation might differ compared to murine macrophages.

As RIP1 kinase activity has been proven essential for *Yersinia*-mediated cell death in murine macrophages, one study set out to further investigate downstream effects of RIP1 deletion in knockout cell lines. This study did not only find the increase in phosphorylation of MLKL mentioned above, but also detected a decrease in activation of caspases-1, -3, -7 and -8, as well as lower levels of active GSDMD

compared to wild type cells. Reduced activity of these molecules can be connected to the blockage of pyroptosis and apoptosis observed in the absence of RIP1 (Malireddi et al., 2020b). Consequently, it might be of interest to study activity of these caspases and GSDMD in human macrophages with and without addition of Nec1s to further determine which role RIP1 plays here.

Caspases play a crucial role in PCD with caspase-8 being one of the key regulators of the cell fate and essential for *Yersinia*-mediated cell death. When extrinsic apoptosis is triggered via death receptors, pro-caspase-8 is recruited by different signalling molecules, including FADD, to form the DISC. As part of this complex, pro-caspase-8 is activated via homodimerization and auto-cleavage into two subunits (p43/41 and p12). The larger subunit is then cleaved once more, producing the active enzyme (p18) (Lavrik et al., 2003). Active caspase-8 has a variety of functions. In the course of apoptosis, caspase-8 cleaves the caspases-3 and -7 into their active forms which then subsequently execute cell death. Moreover, caspase-8 can cleave BID and thus trigger MOMP via activation of BAK and BAX. This leads to an amplification of apoptotic cell death (Kaufmann et al., 2012, Stennicke et al., 1998).
Additionally, caspase-8 is responsible for inhibiting necroptosis by cleavage of RIP1. Consequently, RIP1 cannot form the necrosome with RIP3, and MLKL cannot be phosphorylated to trigger cell death (Newton et al., 2019). Lastly, caspase-8 can cleave the pore-forming molecule GSDMD into its active form. Studies showed that *Yersinia* infection of murine macrophages leads to caspase-8-dependent GSDMD activation resulting in pore formation and pyroptotic cell death (Sarhan et al., 2018).
Here, the active fragment of caspase-8 (p18) was clearly detectable in primary human macrophages infected with *Y. enterocolitica* 6 h and 18 h after infection, with the strongest signal after 6 h as cells already undergo cell death and degradation 18 h post-infection. Active caspase-8 could only be detected in the presence of YopP, indicating that complex IIa formation is dependent on TAK1 inhibition. However, infection with YopP-deficient *Yersinia* still led to a certain degree of cleavage of caspase-8 into the not fully active fragments p41/43. Activation of caspase-8 upon *Yersinia* infection has been shown to be essential for *Yersinia*-mediated cell death in mouse macrophages. Either treating human macrophages with caspase-8-inhibitors or studying specific knockout cell lines in the context of infection with *Y. enterocolitica* remain necessary to determine how much influence caspase-8 activity has on cell death in that case. However, the strong activation of the molecule detected here suggests that caspase-8 is involved in regulating *Yersinia*-mediated cell death in human macrophages, similar to their murine counterparts.

Caspase-3 is one of the executioners of apoptosis alongside caspase-7. It can get activated either by caspase-9 during intrinsic apoptosis or by caspase-8 during extrinsic apoptosis (Kesavardhana et al.,

2020). First, it is processed into a p20 and a p12 fragment, next the p20 fragment gets cleaved further into the fragment p17, which is the active form of caspase-3 (Han et al., 1997). However, caspase-3 is not only involved in apoptosis but can also play a role in pyroptotic cell death as it cleaves the pore-forming molecules GSDMD and GSDME. Unlike caspase-8, which activates GSDMD, caspase-3 cleaves at a different site and produces an inactive form of the molecule, which is unable to form pores. GSDME is cleaved by caspase-3 into its active, pore-forming p31 fragment (Taabazuing et al., 2017, Wang et al., 2017). Studies showed that TAK1 inhibition in combination with LPS stimulation, simulating *Yersinia* infection, leads to activation of caspase-3 in mouse macrophages. However, deletion of caspases-3 and -7 only mildly delays cell death under these conditions, indicating that caspase-3 does not play an indispensable role in *Yersinia*-mediated cell death as several molecules might have overlapping functions (Sarhan et al., 2018).

In this study, we observed that infection of human macrophages with WAP for more than 6 h led to production of the active p17 caspase-3 fragment, with the strongest signal detected 18 h post-infection. This process required YopP and was mediated by inhibition of TAK1 as infection with ΔP did not produce a detectable active fragment. As caspase-8 activity could also be detected following WAP infection, it is likely that caspase-3 is activated by caspase-8 here, following the pathway of extrinsic apoptosis. These results are in accordance with one study that demonstrated activation of caspases-8 and -3 after TAK1 inhibition and LPS stimulation (Sarhan et al., 2018).

Studies showed that absence of caspase-8 in murine macrophages drastically reduced activation of caspase-3 (Sarhan et al., 2018). Nevertheless, caspase-3 can have different downstream substrates, as can caspase-8. Consequently, activity of these caspases does not allow concrete definition by which downstream events cell death of human macrophages is finally executed upon infection with *Yersinia.*

GSDMD and GSDME have been identified as the executioners of pyroptosis. They both belong to the gasdermin family and possess an auto-inhibitory C-terminal domain and an N-terminal domain that can, once released, form pores in the cell membrane and trigger pyroptosis and release of cytokines (Kayagaki et al., 2015, Lieberman et al., 2019). GSDMD can be activated via cleavage by different caspases. During canonical inflammasome formation, caspase-1 cleaves GSDMD to produce the active fragment p30. The non-canonical pathway leads to GSDMD-activation mediated by caspases-4 and -5 in humans or by murine caspase-11 (Kayagaki et al., 2015, Snyder and Oberst, 2021). More recently, several studies found that GSDMD pore formation plays an important role in *Yersinia*-mediated cell death. Inhibition of TAK1 through YopP/J triggers activation of caspase-8, which then cleaves GSDMD into its pore-forming fragment (Orning et al., 2018, Sarhan et al., 2018). This process is considered relevant as absence of GSDMD in murine macrophages leads to a delay in cell death upon infection with *Yersinia*,

measured by PI uptake and LDH release. Additionally, GSDMD pores are necessary for the release of IL-1β during *Yersinia* infection (Sarhan et al., 2018, Chen et al., 2021).

Here, we investigated processing of GSDMD in human macrophages infected with *Y. enterocolitica*. Interestingly, the active p30 fragment was not detectable when infecting with wild type bacteria. 3, 6 and 18 h post-infection, only the full-length protein and the inactive p43 fragment, generated by caspase-3, but not the active p30 fragment, could be detected. The *Y. enterocolitica* strain lacking YopP and YopQ has been shown to trigger pyroptosis by activating caspase-1, which results in GSDMD cleavage (Brodsky et al., 2010). Infection with this strain produced the active p30 fragment of GSDMD in human macrophages at all three time points. This underlines that WAP is apparently unable to induce GSDMD activation.

If GSDMD is not activated in human macrophages, the question arises, what might drive *Yersinia*-mediated final cell death steps instead. To study this, we next examined processing of the closely related GSDME. GSDME can be cleaved into its active fragment p31 by caspase-3 (Wang et al., 2017, Rogers et al., 2017). Studies in murine macrophages reported, that *Yersinia* infection results in cleavage of GSDME, alongside GSDMD. However, so far, no role for processed GSDME could be uncovered in macrophages. Neither *Yersinia*-mediated cell death, nor release of IL-1β were compromised in mouse macrophages lacking GSDME (Chen et al., 2021, Sarhan et al., 2018). When infecting primary human macrophages with *Y. enterocolitica* the processed p31 GSDME fragment was clearly detectable 6 h and 18 h post-infection. Infection with the strains lacking either YopP, or YopP and YopQ did not trigger cleavage. This suggests that the activating cleavage is a direct result of WAP infection and TAK1 inhibition.

Interestingly, the results of this work are similar to results from Sarhan et al. (2018). They found that treatment with a TAK1 inhibitor followed by LPS challenge led to GSDME cleavage in human PMBC-derived macrophages 4 h post-stimulation. Additionally, they were not able to detect the active p30 fragment of GSDMD. However, as has been shown for mouse macrophages, processing of GSDME does not necessarily mean that GSDME mediates pore formation that could play a role in *Yersinia*-mediated cell death and interleukin release. Instead, downstream effects and consequences of a deletion of GSDMD or GSDME need to be further investigated to determine the functions of these molecules.

To further study differences and similarities between murine and human macrophages upon *Yersinia* infection, the release of the cytokines TNF-α and IL-1β was examined in the course of this work.

It has been long established that TNF-α plays an important role in a variety of infections and it is considered an important regulator of inflammation (Bradley, 2008). In mice infected with *Y. enterocolitica* TNF-α is crucial for restricting infection (Autenrieth and Heesemann, 1992). Multiple studies showed that *Yersinia* infection inhibits MAPK and NF-κB signalling and consequently TNF-α production. This

suppression is mediated by and requires YopP (Palmer et al., 1998, Boland and Cornelis, 1998, Ruckdeschel et al., 1998). Infection of mouse macrophages with YopP deficient bacteria results in an increase in TNF-α release compared to release upon wild type infection, which suggests a YopP-dependent blockage of production (Boland and Cornelis, 1998). The results presented here already showed that YopP mediates TAK1 inhibition in primary human macrophages. When investigating release of TNF-α, we could demonstrate that infection with YopP-deficient bacteria led to significantly higher levels of released cytokine compared to infection with WAP. Wild type infection still resulted in an elevated TNF-α release compared to uninfected cells, so production was not blocked completely. However, the approximately 4-fold increase observed in absence of YopP suggests that YopP is responsible for suppressing the TNF-α production in human macrophages. Additional YopQ-deficiency did not alter the cytokine levels.

In contrast to TNF-α, multiple studies described that infection with *Yersinia* induces release of IL-1β, another important inflammatory cytokine. Infection with *Yersinia* triggers caspase-1 auto-activation in a RIP1- and caspase-8-dependend manner (Weng et al., 2014). Caspase-1 then cleaves pro-IL-1β into its active form. This process is dependent on TAK1-inhibition through YopP/J as absence of YopP/J during infection does not trigger IL-1β release and neither does LPS stimulation in combination with TAK1 inhibition (Orning et al., 2018). GSDMD was identified as being responsible for IL-1β release from *Yersinia*-infected murine macrophages. GSDMD deficiency leads to significant reduction in IL-1β release (Orning et al., 2018, Chen et al., 2021, Demarco et al., 2020). Furthermore, GSDMD has also been shown to influence caspase-1 activation. Pore-formation through GSDMD leads to efflux of potassium ions which then triggers formation of the NLRP3 inflammasome and consequently caspase-1 cleavage (Rühl and Broz, 2015, Orning et al., 2018). GSDME on the other hand is not involved in mediating IL-1β release from murine macrophages, even though it is processed into its active fragment upon *Yersinia* infection. However, it is required for IL-1β release from neutrophils infected with *Yersinia* (Chen et al., 2021). In accordance with what was shown for murine macrophages, human macrophages infected with *Y. enterocolitica* in our study released significantly higher amounts of IL-1β compared to uninfected cells. As it was shown that GSDMD is not processed into its active form under these conditions, the release should be GSDMD-independent. It is possible that GSDME is instead required for IL-1β release, since this work showed that GSDME is processed into its active p31 fragment during *Yersinia* infection. To further elucidate the mechanisms behind the cytokine release, human macrophages deficient for either GSDMD or GSDME or both molecules should be studied. Interestingly, we found here that infection with YopP-deficient *Yersinia* led to substantial amounts of released IL-1β compared to WAP-infection. This stands in contrast to other studies, that reported reduced levels of IL-1β release in the absence of YopP/J. As neither GSDMD nor GSDME were active upon ΔP-infection, the release must

be dependent on a different mechanism. Further research is necessary to investigate this phenomenon. Infection with *Yersinia* deficient for both YopP and YopQ led to the highest amount of released IL-1β. As YopQ has been shown to block caspase-1-activation and hence inhibits IL-1β-maturation, it could be expected that absence of YopQ positively regulates the cytokine release (Brodsky et al., 2010).

Overall, our studies on primary human macrophages revealed that the underlying mechanisms of TAK1 inhibition, RIP1 phosphorylation and caspase-activation upon *Yersinia* infection might be comparable to the processes described for murine macrophages. However, the RIP1 kinase activity seems to be dispensable for *Yersinia*-mediated cell death in human macrophages. Furthermore, there was a marked difference in activation of GSDMD and GSDME. These points require further research to understand the exact roles of these molecules in cell death execution during infection of human macrophages with *Y. enterocolitica.*

4.2 *Y. enterocolitica*-mediated cell death in THP-1 macrophages

Studying cells deficient for key molecules is an essential tool to elucidate pathways and mechanisms related to these molecules in cell biology. One aim of this study was, to generate a stable *Gsdme* knock-out cell line, using THP-1 cells, to learn more about the function of GSDME. THP-1 cells are a human monocyte cell line cultured in suspension. When treating the cells with PMA, they become adherent and differentiate into adherent macrophages. This makes them a practical tool and an appropriate substitute for studying primary human macrophages. Reportedly, a wide range of PMA concentrations (10 to 400 ng/ml) and differentiation incubation periods can be used to generate macrophages from THP-1 cells (Park et al., 2007). Previous studies in our group found that differentiation with 20 ng/ml for 24 h, followed by 24 h of PMA-free interval produced viable macrophages with cell type-typical morphology (Appelt, 2021).

To establish that THP-1 macrophages behave similar to primary human macrophages when infected with *Y. enterocolitica,* several key molecules of cell death were examined. *Yersinia* infection led to YopP-dependent inhibition of TAK1 phosphorylation. Phosphorylation could only be detected when infecting THP-1 macrophages with YopP-deficient bacteria. This is comparable with what could be shown for primary human macrophages in this study. Next, caspase-3 cleavage was investigated. Here again, the results were similar to those of primary macrophages. The active p17 fragment was detectable 17 h post-infection and much more prominent in cells infected with WAP compared to those infected with ΔP. As processing of GSDME but not GSDMD was surprisingly observed in *Yersinia*-infected primary macrophages, cleavage of GSDME was also investigated in THP-1 macrophages. Infection with WAP for

6 or 18 h led to the generation of the active p31 fragment of GSDME, supposedly through caspase-3-mediated cleavage. This is also in line with what was found for primary human macrophages infected with *Yersinia.*

Having thus established that *Yersinia* infection of PMA-differentiated THP-1 macrophages triggers similar pathways to those observed in human macrophages, a GSDME-deficient cell line was generated. The aim was to study the effect that lack of GSDME has on *Yersinia*-mediated cell death in human macrophages. In previous experiments, infection led to activation of GSDME while GSDMD was only cleaved into its inactive p43 fragment. Hence, it is unlikely that GSDMD mediates cell death and IL-1β release like it does in murine macrophages (Sarhan et al., 2018, Chen et al., 2021). While another study confirmed activation of GSDME during *Yersinia* infection, the connection to cell death upon infection was so far not studied in human macrophages (Sarhan et al., 2018). GSDME plays a role in mediating interleukin release and cell death in murine neutrophils, which illustrates that this molecule can fulfil its expected functions depending on the cell type (Chen et al., 2021). When investigating cell death rates upon *Yersinia* infection in THP-1 cells, we found that GSDME-deficiency indeed plays a role in these cells. THP-1 macrophages lacking GSDME died significantly less compared to wild type cells after 18 to 20 h of infection. In contrast, infection with ΔP did not trigger high levels of cell death, which underlines that *Yersinia*-mediated cell death in human macrophages is dependent on YopP, like in murine macrophages (Mills et al., 1997). Overall, this result gives further indication, that there are indeed differences between human and murine macrophages in cell death execution upon *Y. enterocolitica* infection. The experiments conducted in this study suggest that involvement of GSDMD and GSDME might be a key difference. However, further research is necessary to elucidate the exact role of GSDME in *Yersinia*-infected human macrophages. Accordingly, release of IL-1β should be studied in GSDME-deficient macrophages, as interleukin release is dependent on GSDMD in murine macrophages (Chen et al., 2021). Additionally, analysing human macrophages deficient for GSDMD could provide further information on the role of GSDMD in these cells. It would also be of interest to study activation of GSDMD in the absence of GSDME, to see if GSDMD could potentially serve as a backup death molecule for GSDME. A further issue would be to check oligomerisation of GSDME in *Yersinia*-infected human macrophages, to ensure that cleavage into the active p31 fragment actually results in pore-formation (Zhou and Abbott, 2021).

4.3 The role of BID in *Y. enterocolitica*-mediated cell death of murine macrophages

Many different molecules are involved in mediating cell death of macrophages in *Yersinia* infection. While some of them have already been extensively studied, the exact role and involvement of others still remain somewhat unclear. Cell death triggered by *Y. enterocolitica* does not rely on one defined pathway, but engages signalling connected to both apoptosis and pyroptosis. The role of the pore-forming protein GSDMD has been the focus of many recent studies in this regard, as it was shown that *Yersinia* infection leads to caspase-8-dependent cleavage and activation of GSDMD. The active GSDMD fragment then triggers pyroptosis-like cell death (Sarhan et al., 2018). However, the role of the pro-apoptotic protein BID during *Yersinia* infection is less well understood so far. One study showed that during *Y. enterocolitica* infection BID gets processed into its active, truncated form tBID (Denecker et al., 2001). tBID can cause MOMP via activation of the molecules BAX and BAK which is a central step of intrinsic apoptosis (Snyder and Oberst, 2021). Recently, BID was identified as playing a role in cell death mediation in the absence of GSDMD. In GSDMD-deficient macrophages, caspase-1 can cleave BID to trigger MOMP, downstream activation of caspase-3 and secondary necrosis (Tsuchiya et al., 2019, Heilig et al., 2020).

Based on these studies, one aim of this study was to further investigate the role of BID in murine macrophages during *Y. enterocolitica* infection. For this, three different knockout cell lines were generated, all derived from immortalised bone-marrow macrophages (iWT), which were kindly provided by the group of Prof. Dr. Petr Broz. Generated knockout macrophages were either deficient for GSDMD or BID or both of these molecules. In a first step, cell death rates were assessed. It is already known that GSDMD-deficiency leads to a delay in cell death in *Yersinia*-infected macrophages (Chen et al., 2021). Additionally, absence of both BID and GSDMD has been shown to decrease macrophage cell death during AIM2-inflammasome activation (Heilig et al., 2020). Here, both cell lines lacking GSDMD exhibited significantly lower cell death rates compared to wild type macrophages 3 h post-infection. Absence of BID alone did not seem to have a protective effect and thus might not play an essential role in *Yersinia*-mediated cell death. However, deficiency of both GSDMD and BID resulted in even lower cell death rates than absence of GSDMD only. After 5 h of infection, cell death rates were higher in all cell lines. Nevertheless, cell death rates of GSDMD-deficient macrophages were still lower compared to wild type macrophages. However, the difference decreased in dependence of time. This indicates that loss of the pore-forming protein does not fully protect macrophages from cell death, it merely results in a delay, as has been described previously (Chen et al., 2021, Sarhan et al., 2018). The slight difference after 3 h of infection between i*Gsdmd*$^{-/-}$ and i*Bid*$^{-/-}$ *Gsdmd*$^{-/-}$ might suggest, that loss of BID further delays cell death in the absence of GSDMD. As expected, cell death observed here was dependent on the presence of YopP, as ΔP-infection did not trigger heightened levels of cell death.

The next aim was to investigate the activities of different caspases in the absence of BID. Caspase-8 operates upstream of BID. During *Yersinia* infection it undergoes auto-cleavage into its active p18 fragment. Alongside FADD and RIP1, caspase-8 is required for mediating cell death during *Yersinia* infection (Orning et al., 2018). During apoptosis, caspase-8 can cleave and active BID to trigger MOMP. This is considered an overlap between the intrinsic and the extrinsic apoptotic pathway (Snyder and Oberst, 2021, Li et al., 1998). Infection of wild type and BID-deficient murine macrophages with WAP led to generation of the active caspase-8 fragment 3 h and 4 h post-infection with the strongest signal after 3 h. Activation was dependent on YopP. Detection of the p18 fragment was expected as activation of caspase-8 during *Yersinia* infection has been described in previous studies (Sarhan et al., 2018, Orning et al., 2018). As BID operates downstream of caspase-8, absence of BID was not thought to influence caspase-8 cleavage. This was confirmed by these experiments.

Caspase-9 is tightly connected to intrinsic apoptosis. BID-mediated MOMP leads to release of cytochrome c into the cytosol. Cytochrome c then interacts with APAF-1 and triggers recruitment of caspase-9 via their respective CARD domains (Jiang and Wang, 2000). Auto-cleavage of caspase-9 generates the active p35 fragment, which in turn is able to cleave caspases-3 and -7, the executioners of apoptosis (Snyder and Oberst, 2021). Studies showed that infection of macrophages with *Y. enterocolitica* leads to cleavage of BID, cytochrome c release and apoptosome-mediated caspase-9 cleavage into the active fragments p35 and p37 (Denecker et al., 2001). Caspases-3 and -7 are subsequently activated as well. Loss of caspase-9 during *Yersinia* infection only leads to minor delays in cell death (Sarhan et al., 2018). As BID operates upstream of caspase-9 activation, we wanted to investigate, how loss of BID influences cleavage of caspase-9. LPS stimulation and TAK1 inhibition of wild type macrophages generated both the p35 and the p37 fragment 2 and 3 h after stimulation. *Yersinia* infection resulted in a weak signal for both fragments after 2 h of infection. Arguably, cleavage of caspase-9 should be investigated at later time points again, to check if signals get stronger as cell death proceeds. Interestingly, in BID-deficient cells, the p37 fragment produced a much stronger signal than the p35 fragment, which was barely detectable, when using LPS stimulation and TAK1 inhibition. During WAP infection only the p37 fragment could be detected in the absence of either BID or both BID and GSDMD. As expected, cleavage of caspase-9 was dependent on YopP-mediated TAK1 inhibition.

Studies suggest that the different fragments of caspase-9, p35 and p37, are generated in distinct ways. The p35 fragment is produced through auto-cleavage at Asp-315. This cleavage is mediated by the apoptosome and thus occurs downstream of cytochrome c release from the mitochondrion. As MOMP during apoptosis is mediated by BID, which in turn activates BAK and BAX, the p35 fragment is expected not to be produced extensively in macrophages deficient for BID, which is confirmed by our results.

Meanwhile, studies showed that the p37 fragment is generated by caspase-3 through a feedback mechanism to enhance apoptotic signalling. In this case, the cleavage occurs at Asp-330 (Iordanov et al., 2005). However, the size is supposedly not the only difference between the p35 and the p37 fragment. One study reported that predominantly the auto-processed p35 fragment is catalytically active. In contrast, caspase-3-mediated cleavage generates a fragment that lacks a binding motif for XIAP (Denault et al., 2007). This pro-survival molecule is able to inhibit caspase-9 activity in order to block apoptosis. It can itself be suppressed by SMAC, which is released into the cytosol through MOMP to propagate cell death (Jost et al., 2009). Hence, caspase-3 cleavage generates a caspase-9 fragment that cannot be blocked which then amplifies apoptosis and downstream processing (Denault et al., 2007). Here, mainly the p37 fragment was detected in BID-deficient macrophages, which suggests that cleavage occurred through caspase-3, independently from cytochrome c release. On the contrary, the p35 fragment, which is produced downstream of MOMP, was detectable in wild type macrophages. To further investigate this difference in caspase-9 cleavage, it should be confirmed that loss of BID results in reduced cytochrome c release from the mitochondrium and that the apoptosome does not form under these conditions. Additionally, inhibition or deletion of caspase-3 could clarify if the observed caspase-9 cleavage in the absence of BID is meditated that way. Furthermore, activity of caspase-9 could be assessed in macrophages with or without BID by using caspase-9-specific substrates. This would support the theory that caspase-9 is not cleaved into the fully active p35 fragment when cells do not express BID, as can be suggested based on the data obtained here.

Caspase-3 can have a variety of functions during programmed cell death. Upon activation through cleavage by caspase-9 or caspase-8, it can either trigger apoptosis or cleave GSDME to induce pyroptosis or secondary necrosis (Kesavardhana et al., 2020, Taabazuing et al., 2017). During infection with *Y. enterocolitica,* cleavage of BID leads to caspase-9 activation and subsequent caspase-3 cleavage in a YopP-dependent manner (Denecker et al., 2001). LPS stimulation and TAK1 inhibition in murine macrophages also results in generation of the active p17 fragment of caspase-3. However, loss of caspase-3 does not drastically reduce cell death after infection or LPS stimulation and TAK1 inhibition (Sarhan et al., 2018). As BID acts upstream of caspse-3, it was of interest to analyse if loss of BID leads to changes in activation of caspase-3 compared to activation in wild type macrophages. The results show, that TAK1 inhibition with LPS stimulation for 1 to 3 h led to generation of the active p17 fragment in both wild type and BID-deficient macrophages. Interestingly, the signal for the active fragment was much stronger in wild type cells. When using *Y. enterocolitica* infection, the p17 fragment was detected in wild type macrophages expressing Cas9 2 to 4 h post-infection with the strongest signal after 3 h. Loss of BID in these cells also resulted in activation of caspase-3. The p17 fragment was, however, detectable

1 to 4 h post-infection, with the strongest signal after 3 and 4 h. Thus, while caspase-3 seems to get activated in the absence of BID, caspase-3 activation appears decreased and decelerated when cells are BID-deficient. In wild type macrophages, caspase-3 can get activated by caspase-8 during *Yersinia* infection. We have demonstrated here that caspase-8 is indeed active in murine macrophages. Loss of BID does not influence its cleavage as it operates upstream of BID. Therefore, caspase-3 activation is likely to be mediated by caspase-8 in macrophages with or without BID. However, caspase-3 can also be activated by caspase-9. Our results show that caspase-9 is auto-processed into its active p35 fragment in wild type macrophages, which suggests that caspase-3 might be activated by caspase-9 additionally. The p37 fragment of caspase-9 that was mainly detected in BID-deficient cells has been shown to mediate cleavage of caspase-3 less efficiently as it is not fully activated (Denault et al., 2007). Consequently, the weaker signal for active caspase-3 detected in BID-deficient macrophages might be predominantly mediated by caspase-8. In contrast, in wild type macrophages caspase-8 and caspase-9 might both be responsible for activation of caspase-3 which could lead to an increase in the active fragment. Additionally, one study found that BID influences caspase-3 cleavage into the active p17 fragment via SMAC release (Heilig et al., 2020). Truncated BID triggers MOMP and hence release of cytochrome c and SMAC. While cytochrome c is necessary for caspase-9 activation, SMAC blocks XIAP and IAP. These pro-survival molecules are otherwise able to inhibit activation of apoptotic caspases-3/7 and -9 (Jost et al., 2009). Thus, lack of SMAC release might be another explanation for lower levels or delayed activation of active caspase-3 that we have found here in BID-deficient macrophages.
Nevertheless, further experiments are necessary to specifically determine how caspase-3 activation is influenced by loss of BID. One possible way would be to quantify caspase-3 activity through assays with DEVD-amc. This tetrapeptide (DEVD) is a caspase-3 specific substrate bound to the fluorogenic group amc (amino-4-methylcoumarin), which is not fluorescent while bound to DEVD. Active caspase-3 mediates the release of amc. Once released, fluorescence of amc can be measured and used to detect and quantify caspase-3 activity (Grootjans et al., 2016). Additionally, work with caspase-3 inhibition or deletion or specific inhibition of the upstream caspases-8 and -9 might provide further inside into regulation of *Yersinia*-mediated cell death in the absence of BID. Additionally, downstream targets of caspase-3, like GSDMD and GSDME, are interesting to be investigated.

Thus, GSDMD activation was examined next. It has been shown multiple times, that GSDMD plays a role in *Yersinia*-mediated cell death in murine macrophages. Cleavage by caspase-8 leads to generation of the active p30 fragment, that is able to form pores in the cell membrane (Sarhan et al., 2018, Chen et al., 2021). This triggers pyroptosis-like cell death. GSDMD pores are responsible for IL-1β release during *Yersinia* infection, and loss of GSDMD leads to a delay in cell death, which was confirmed by our

results (Chen et al., 2021). Caspase-3, on the other hand, negatively regulates GSDMD activity. It can cleave either the full-length molecule or the active p30 fragment, generating inactive p43 and p21 fragments respectively (Chen et al., 2019). So far, the influence that BID might have on GSDMD cleavage has not been studied. Here we found that in wild type macrophages undergoing LPS stimulation and TAK1 inhibition mostly the full-length protein and the inactive fragments p43 and p21 where detectable 2 and 3 h post-stimulation. The active p30 fragment could not be clearly detected. In contrast, signals for the active p30 fragment were detectable in BID-deficient macrophages 1 to 3 h after LPS stimulation and TAK1 inhibition. Using *Y. enterocolitica* to infect macrophages led to similar results. After 4 h of infection a clear band for the inactive p43 fragment could be seen in wild type macrophages, whereas only a very faint band was detected for the active p30 fragment. *Yersinia* infection in the absence of BID, however, led to generation of the active p30 fragment, although the inactive p43 fragment was also detected 3 and 4 h after infection. It is surprising that the active p30 GSDMD fragment was not clearly detectable in wild type macrophages, as GSDMD activity has been reported during *Yersinia* infection in multiple studies (Chen et al., 2021, Sarhan et al., 2018, Orning et al., 2018). However, the generation of the inactive p43 and p21 GSDMD fragments fits our result which showed a strong caspase-3 activation in wild type macrophages. LPS stimulation and TAK1 inhibition led to visibly less cleavage of caspase-3 in BID deficient cells, which might explain why the caspase-3-generated inactive fragments are not detectable here. Instead, as caspase-8 is active in absence of BID, caspase-8 likely produces the active GSDMD fragment to mediate GSDMD activation. Overall, the results obtained here suggest that absence of BID has an enhancing effect on GSDMD activation, possibly mediated by the decreased and delayed activity of caspase-3. However, more intense research is necessary to specify this. For example, the influence of specific inhibition of caspase-3 and caspase-8 in wild type macrophages and BID-deficient cells on GSDMD cleavage should be examined. Additionally, release of interleukins could be studied, as it has been shown that absence of GSDMD leads to a decrease in IL-1β release in murine macrophages (Chen et al., 2021). Next, activation of GSDME should be investigated. Unlike its inhibiting effect on GSDMD, caspase-3 is responsible for activation of GSDME (Taabazuing et al., 2017). Therefore, it would be interesting to see, if the potential BID-mediated changes in caspase-3 activity also influence cleavage of GSDME.

So far, our studies with murine macrophages indicate that loss of BID during *Yersinia* infection has an influence on downstream molecules. There are apparently differences in cleavage of caspase-9 and caspase-3 which need to be further studied and verified by additional methods. Furthermore, activation of GSDMD seems to be enhanced by BID-deficiency. To further investigate the role of BID, several next steps could be undertaken. Cytochrome c and SMAC release from mitochondria should be

investigated to verify that loss of BID actually confers protection against MOMP. Also, the activation of BAX and BAK, the executioners of MOMP, could be investigated here. Additionally, it would be of interest to study cell death morphologically to get further information about how macrophages die during *Yersinia* infection in the absence of BID. We propose that BID is a central control element in the decision of the cell to die preferentially with apoptotic than with pyroptotic features.

5 Literature

ABBY, S. S. & ROCHA, E. P. 2012. The non-flagellar type III secretion system evolved from the bacterial flagellum and diversified into host-cell adapted systems.

ACEHAN, D., JIANG, X., MORGAN, D. G., HEUSER, J. E., WANG, X. & AKEY, C. W. 2002. Three-Dimensional Structure of the Apoptosome: Implications for Assembly, Procaspase-9 Binding, and Activation. *Molecular Cell,* 9**,** 423-432.

ACHTMAN, M., ZURTH, K., MORELLI, G., TORREA, G., GUIYOULE, A. & CARNIEL, E. 1999. *Yersinia pestis*, the cause of plague, is a recently emerged clone of *Yersinia pseudotuberculosis*. *Proceedings of the National Academy of Sciences,* 96**,** 14043-14048.

AEPFELBACHER, M. 2004. Modulation of Rho GTPases by type III secretion system translocated effectors of *Yersinia*. *Reviews of physiology, biochemistry and pharmacology***,** 65-77.

AEPFELBACHER, M. & HEESEMANN, J. 2001. Modulation of Rho GTPases and the actin cytoskeleton by *Yersinia* outer proteins (Yops). *International Journal of Medical Microbiology,* 291**,** 269-276.

AGLIETTI, R. A., ESTEVEZ, A., GUPTA, A., RAMIREZ, M. G., LIU, P. S., KAYAGAKI, N., CIFERRI, C., DIXIT, V. M. & DUEBER, E. C. 2016. GsdmD p30 elicited by caspase-11 during pyroptosis forms pores in membranes. *Proceedings of the National Academy of Sciences,* 113**,** 7858-7863.

ALEKSIĆ, S. & BOCKEMÜHL, J. 1984. Proposed revision of the Wauters et al. antigenic scheme for serotyping of *Yersinia enterocolitica*. *Journal of Clinical Microbiology,* 20**,** 99-102.

ALONSO, A., BOTTINI, N., BRUCKNER, S., RAHMOUNI, S., WILLIAMS, S., SCHOENBERGER, S. P. & MUSTELIN, T. 2004. Lck Dephosphorylation at Tyr-394 and Inhibition of T Cell Antigen Receptor Signaling by *Yersinia* Phosphatase YopH *Journal of Biological Chemistry,* 279**,** 4922-4928.

ANDERSSON, K., CARBALLEIRA, N., MAGNUSSON, K.-E., PERSSON, C., STENDAHL, O., WOLF-WATZ, H. & FÄLLMAN, M. 1996. YopH of *Yersinia pseudotuberculosis* interrupts early phosphotyrosine signalling associated with phagocytosis. *Molecular Microbiology,* 20**,** 1057-1069.

ANDOR, A., TRÜLZSCH, K., ESSLER, M., ROGGENKAMP, A., WIEDEMANN, A., HEESEMANN, J. & AEPFELBACHER, M. 2001. YopE of *Yersinia*, a GAP for Rho GTPases, selectively modulates Rac-dependent actin structures in endothelial cells. *Cellular microbiology,* 3**,** 301-310.

APPELT, L.-S. 2021. *Yersinien-induzierter Zelltod von humanen Makrophagen: Analyse der zellulären Mechanismen.* BSc, Hochschule für Angewandte Wissenschaften Hamburg.

ATKINSON, S. & WILLIAMS, P. 2016. *Yersinia* virulence factors - a sophisticated arsenal for combating host defences. *F1000Res,* 5.

AUTENRIETH, I. B. & FIRSCHING, R. 1996. Penetration of M cells and destruction of Peyer's patches by *Yersinia enterocolitica*: an ultrastructural and histological study. *Journal of Medical Microbiology,* 44**,** 285-294.

AUTENRIETH, I. B. & HEESEMANN, J. 1992. In vivo neutralization of tumor necrosis factor-alpha and interferon-gamma abrogates resistance to *Yersinia enterocolitica* infection in mice. *Medical Microbiology and Immunology,* 181**,** 333-338.

BARBIERI, J. T., RIESE, M. J. & AKTORIES, K. 2002. Bacterial toxins that modify the actin cytoskeleton. *Annual review of cell and developmental biology,* 18**,** 315-344.

BENABDILLAH, R., JAIME MOTA, L. S., LÜTZELSCHWAB, S., DEMOINET, E. & CORNELIS, G. R. 2004. Identification of a nuclear targeting signal in YopM from *Yersinia* spp. *Microbial Pathogenesis,* 36**,** 247-261.

BENGOECHEA, J. A., NAJDENSKI, H. & SKURNIK, M. 2004. Lipopolysaccharide O antigen status of Yersinia enterocolitica O:8 is essential for virulence and absence of O antigen affects the expression of other *Yersinia* virulence factors. *Molecular Microbiology,* 52**,** 451-469.

BERGSBAKEN, T. & COOKSON, B. T. 2007. Macrophage Activation Redirects Yersinia-Infected Host Cell Death from Apoptosis to Caspase-1-Dependent Pyroptosis. *PLOS Pathogens,* 3**,** e161.

BERGSBAKEN, T., FINK, S. L. & COOKSON, B. T. 2009. Pyroptosis: host cell death and inflammation. *Nature Reviews Microbiology,* 7**,** 99-109.

BERNEKING, L., SCHNAPP, M., RUMM, A., TRASAK, C., RUCKDESCHEL, K., ALAWI, M., GRUNDHOFF, A., KIKHNEY, A. G., KOCH-NOLTE, F., BUCK, F., PERBANDT, M., BETZEL, C., SVERGUN, D. I., HENTSCHKE, M. & AEPFELBACHER, M. 2016. Immunosuppressive *Yersinia* Effector YopM Binds DEAD Box Helicase DDX3 to Control Ribosomal S6 Kinase in the Nucleus of Host Cells. *PLOS Pathogens,* 12**,** e1005660.

BERTHERAT, E. 2016. Plague around the world, 2010-2015/La peste a travers le monde: 2010-2015. *Weekly Epidemiological Record,* 91**,** 89+.

BIAŁAS, N., KASPERKIEWICZ, K., RADZIEJEWSKA-LEBRECHT, J. & SKURNIK, M. 2012. Bacterial Cell Surface Structures in *Yersinia enterocolitica*. *Archivum Immunologiae et Therapiae Experimentalis,* 60**,** 199-209.

BIEDZKA-SAREK, M., VENHO, R. & SKURNIK, M. 2005. Role of YadA, Ail, and Lipopolysaccharide in Serum Resistance of *Yersinia enterocolitica* Serotype O:3. *Infection and Immunity,* 73**,** 2232-2244.

BLISKA, J. B. & BLACK, D. S. 1995. Inhibition of the Fc receptor-mediated oxidative burst in macrophages by the *Yersinia pseudotuberculosis* tyrosine phosphatase. *Infection and Immunity,* 63**,** 681-685.

BLISKA, J. B. & FALKOW, S. 1992. Bacterial resistance to complement killing mediated by the Ail protein of *Yersinia enterocolitica*. *Proceedings of the National Academy of Sciences,* 89**,** 3561-3565.

BOLAND, A. & CORNELIS, G. R. 1998. Role of YopP in Suppression of Tumor Necrosis Factor Alpha Release by Macrophages during *Yersinia* Infection. *Infection and Immunity,* 66**,** 1878-1884.

BOTTONE, E. J. 1999. *Yersinia enterocolitica*: overview and epidemiologic correlates. *Microbes and infection,* 1**,** 323-333.

BRADLEY, J. 2008. TNF-mediated inflammatory disease. *The Journal of Pathology,* 214**,** 149-160.

BRENNAN, M. A. & COOKSON, B. T. 2000. Salmonella induces macrophage death by caspase-1-dependent necrosis. *Molecular Microbiology,* 38**,** 31-40.

BRODSKY, I. E., PALM, N. W., SADANAND, S., RYNDAK, M. B., SUTTERWALA, F. S., FLAVELL, R. A., BLISKA, J. B. & MEDZHITOV, R. 2010. A *Yersinia* effector protein promotes virulence by preventing inflammasome recognition of the type III secretion system. *Cell Host Microbe,* 7**,** 376-87.

BRÖKER, B., SCHÜTT, C., FLEISCHER, B. & VISUV. 2019. *Grundwissen Immunologie*, Springer.

BROZ, P., PELEGRÍN, P. & SHAO, F. 2020. The gasdermins, a protein family executing cell death and inflammation. *Nature Reviews Immunology,* 20**,** 143-157.

CAIN, K., BRATTON, S. B. & COHEN, G. M. 2002. The Apaf-1 apoptosome: a large caspase-activating complex. *Biochimie,* 84**,** 203-214.

CARNIEL, E. 1999. The *Yersinia* high-pathogenicity island. *International Microbiology,* 2**,** 161-167.

CARNIEL, E., GUILVOUT, I. & PRENTICE, M. 1996. Characterization of a large chromosomal "high-pathogenicity island" in biotype 1B *Yersinia enterocolitica*. *Journal of Bacteriology,* 178**,** 6743-6751.

CARTER, P. 1975. Animal model of human disease. Yersinia enteritis. Animal model: oral *Yersinia enterocolitica* infection of mice. *The American journal of pathology,* 81**,** 703.

CHEN, K. W., DEMARCO, B., HEILIG, R., SHKARINA, K., BOETTCHER, A., FARADY, C. J., PELCZAR, P. & BROZ, P. 2019. Extrinsic and intrinsic apoptosis activate pannexin-1 to drive NLRP3 inflammasome assembly. *EMBO J,* 38.

CHEN, K. W., DEMARCO, B., RAMOS, S., HEILIG, R., GORIS, M., GRAYCZYK, J. P., ASSENMACHER, C. A., RADAELLI, E., JOANNAS, L. D., HENAO-MEJIA, J., TACCHINI-COTTIER, F., BRODSKY, I. E. & BROZ, P. 2021. RIPK1 activates distinct gasdermins in macrophages and neutrophils upon pathogen blockade of innate immune signaling. *PNAS,* 118.

CHINA, B., SORY, M. P., N'GUYEN, B. T., BRUYERE, M. D. & CORNELIS, G. R. 1993. Role of the YadA protein in prevention of opsonization of *Yersinia enterocolitica* by C3b molecules. *Infection and Immunity,* 61**,** 3129-3136.

CHINNAIYAN, A. M., O'ROURKE, K., TEWARI, M. & DIXIT, V. M. 1995. FADD, a novel death domain-containing protein, interacts with the death domain of Fas and initiates apoptosis. *Cell,* 81**,** 505-512.

CHUNG, L. K., PARK, Y. H., ZHENG, Y., BRODSKY, I. E., HEARING, P., KASTNER, D. L., CHAE, J. J. & BLISKA, J. B. 2016. The *Yersinia* virulence factor YopM hijacks host kinases to inhibit type III effector-triggered activation of the pyrin inflammasome. *Cell host & microbe,* 20**,** 296-306.

CLARK, M. A., HIRST, B. H. & JEPSON, M. A. 1998. M-Cell Surface beta1 Integrin Expression and Invasin-Mediated Targeting of *Yersinia pseudotuberculosis* to Mouse Peyer's Patch M Cells. *Infection and Immunity,* 66**,** 1237-1243.

CORNELIS, G. R. 1998. The *Yersinia* Deadly Kiss. *Journal of Bacteriology,* 180**,** 5495-5504.

CORNELIS, G. R. 2002. The *Yersinia* Ysc-Yop 'type III' weaponry. *Nature Reviews Molecular Cell Biology,* 3**,** 742-52.

CORNELIS, G. R. 2006. The type III secretion injectisome. *Nat Rev Microbiol,* 4**,** 811-25.

CORNELIS, G. R., BOLAND, A., BOYD, A. P., GEUIJEN, C., IRIARTE, M., NEYT, C., SORY, M.-P. & STAINIER, I. 1998. The Virulence Plasmid of *Yersinia*, an Antihost Genome. *Microbiology and Molecular Biology Reviews,* 62**,** 1315-1352.

CULLEN, S. P., KEARNEY, C. J., CLANCY, D. M. & MARTIN, S. J. 2015. Diverse activators of the NLRP3 inflammasome promote IL-1β secretion by triggering necrosis. *Cell reports,* 11**,** 1535-1548.

CZABOTAR, P. E., LESSENE, G., STRASSER, A. & ADAMS, J. M. 2014. Control of apoptosis by the BCL-2 protein family: implications for physiology and therapy. *Nature Reviews Molecular Cell Biology,* 15**,** 49-63.

DANNAPPEL, M., VLANTIS, K., KUMARI, S., POLYKRATIS, A., KIM, C., WACHSMUTH, L., EFTYCHI, C., LIN, J., CORONA, T., HERMANCE, N., ZELIC, M., KIRSCH, P., BASIC, M., BLEICH, A., KELLIHER, M. & PASPARAKIS, M. 2014. RIPK1 maintains epithelial homeostasis by inhibiting apoptosis and necroptosis. *Nature,* 513**,** 90-94.

DE MIGUEL, D., LEMKE, J., ANEL, A., WALCZAK, H. & MARTINEZ-LOSTAO, L. 2016. Onto better TRAILs for cancer treatment. *Cell Death & Differentiation,* 23**,** 733-747.

DEGTEREV, A., HITOMI, J., GERMSCHEID, M., CH'EN, I. L., KORKINA, O., TENG, X., ABBOTT, D., CUNY, G. D., YUAN, C., WAGNER, G., HEDRICK, S. M., GERBER, S. A., LUGOVSKOY, A. & YUAN, J. 2008. Identification of RIP1 kinase as a specific cellular target of necrostatins. *Nature Chemical Biology,* 4**,** 313-321.

DEGTEREV, A., HUANG, Z., BOYCE, M., LI, Y., JAGTAP, P., MIZUSHIMA, N., CUNY, G. D., MITCHISON, T. J., MOSKOWITZ, M. A. & YUAN, J. 2005. Chemical inhibitor of nonapoptotic cell death with therapeutic potential for ischemic brain injury. *Nature Chemical Biology,* 1**,** 112-119.

DELOR, I. & CORNELIS, G. R. 1992. Role of *Yersinia enterocolitica* Yst toxin in experimental infection of young rabbits. *Infection and Immunity,* 60**,** 4269-4277.

DEMARCO, B., GRAYCZYK, J. P., BJANES, E., LE ROY, D., TONNUS, W., ASSENMACHER, C.-A., RADAELLI, E., FETTRELET, T., MACK, V., LINKERMANN, A., ROGER, T., BRODSKY, I. E., CHEN, K. W. & BROZ, P. 2020. Caspase-8–dependent gasdermin D cleavage promotes antimicrobial defense but confers susceptibility to TNF-induced lethality. *Science Advances,* 6**,** eabc3465.

DENAULT, J.-B., ECKELMAN, BRENDAN P., SHIN, H., POP, C. & SALVESEN, GUY S. 2007. Caspase 3 attenuates XIAP (X-linked inhibitor of apoptosis protein)–mediated inhibition of caspase 9. *Biochemical Journal,* 405**,** 11-19.

DENECKER, G., DECLERCQ, W., GEUIJEN, C. A. W., BOLAND, A., BENABDILLAH, R., VAN GURP, M., SORY, M.-P., VANDENABEELE, P. & CORNELIS, G. R. 2001. *Yersinia enterocolitica* YopP-induced Apoptosis of Macrophages Involves the Apoptotic Signaling Cascade Upstream of Bid *Journal of Biological Chemistry,* 276**,** 19706-19714.

DEURETZBACHER, A., CZYMMECK, N., REIMER, R., TRÜLZSCH, K., GAUS, K., HOHENBERG, H., HEESEMANN, J. R., AEPFELBACHER, M. & RUCKDESCHEL, K. 2009. β1 Integrin-Dependent Engulfment of *Yersinia enterocolitica* by Macrophages Is Coupled to the Activation of

Autophagy and Suppressed by Type III Protein Secretion1. *The Journal of Immunology,* 183**,** 5847-5860.

DEWOODY, R., MERRITT, P. & MARKETON, M. 2013. Regulation of the *Yersinia* type III secretion system: traffic control. *Frontiers in Cellular and Infection Microbiology,* 3.

DEWOODY, R., MERRITT, P. M., HOUPPERT, A. S. & MARKETON, M. M. 2011. YopK regulates the *Yersinia pestis* type III secretion system from within host cells. *Molecular Microbiology,* 79**,** 1445-1461.

DIEPOLD, A., AMSTUTZ, M., ABEL, S., SORG, I., JENAL, U. & CORNELIS, G. R. 2010. Deciphering the assembly of the *Yersinia* type III secretion injectisome. *The EMBO Journal,* 29**,** 1928-1940.

DING, J., WANG, K., LIU, W., SHE, Y., SUN, Q., SHI, J., SUN, H., WANG, D.-C. & SHAO, F. 2016. Pore-forming activity and structural autoinhibition of the gasdermin family. *Nature,* 535**,** 111-116.

DONDELINGER, Y., DELANGHE, T., PRIEM, D., WYNOSKY-DOLFI, M. A., SOROBETEA, D., ROJAS-RIVERA, D., GIANSANTI, P., ROELANDT, R., GROPENGIESSER, J., RUCKDESCHEL, K., SAVVIDES, S. N., HECK, A. J. R., VANDENABEELE, P., BRODSKY, I. E. & BERTRAND, M. J. M. 2019. Serine 25 phosphorylation inhibits RIPK1 kinase-dependent cell death in models of infection and inflammation. *Nature Communications,* 10**,** 1729.

DONDELINGER, Y., JOUAN-LANHOUET, S., DIVERT, T., THEATRE, E., BERTIN, J., GOUGH, P. J., GIANSANTI, P., HECK, A. J., DEJARDIN, E. & VANDENABEELE, P. 2015. NF-κB-independent role of IKKα/IKKβ in preventing RIPK1 kinase-dependent apoptotic and necroptotic cell death during TNF signaling. *Molecular cell,* 60**,** 63-76.

DUKUZUMUREMYI, J.-M., ROSQVIST, R., HALLBERG, B., ÅKERSTRÖM, B., WOLF-WATZ, H. & SCHESSER, K. 2000. The *Yersinia* Protein Kinase A Is a Host Factor Inducible RhoA/Rac-binding Virulence Factor *Journal of Biological Chemistry,* 275**,** 35281-35290.

ECDC 2019. Surveillance of antimicrobial resistance in Europe 2018. Annual report of the European Antimicrobial Resistance Surveillance Network (EARS-Net): European Centre for Disease Prevention and Contro.

EFSA, E. F. S. A., PREVENTION, E. C. F. D. & CONTROL 2019. The European Union One Health 2018 Zoonoses Report. *EFSA Journal,* 17**,** e05926.

EL TAHIR, Y. & SKURNIK, M. 2001. YadA, the multifaceted *Yersinia* adhesin. *International Journal of Medical Microbiology,* 291**,** 209-218.

EVDOKIMOV, A. G., ANDERSON, D. E., ROUTZAHN, K. M. & WAUGH, D. S. 2001. Unusual molecular architecture of the *Yersinia pestis* cytotoxin YopM: a leucine-rich repeat protein with the shortest repeating unit. *Journal of Molecular Biology,* 312**,** 807-821.

FÀBREGA, A. & VILA, J. 2012. *Yersinia enterocolitica*: Pathogenesis, virulence and antimicrobial resistance. *Enfermedades Infecciosas y Microbiología Clínica,* 30**,** Pages 24-32.

FÄLLMAN, M., PERSSON, C. & WOLF-WATZ, H. 1997. *Yersinia* proteins that target host cell signaling pathways. *The Journal of clinical investigation,* 99**,** 1153-1157.

FELTHAM, R. & SILKE, J. 2017. The small molecule that packs a punch: ubiquitin-mediated regulation of RIPK1/FADD/caspase-8 complexes. *Cell Death & Differentiation,* 24**,** 1196-1204.

FENG, S., FOX, D. & MAN, S. M. 2018. Mechanisms of Gasdermin Family Members in Inflammasome Signaling and Cell Death. *Journal of Molecular Biology,* 430**,** 3068-3080.

FENG, S., YANG, Y., MEI, Y., MA, L., ZHU, D.-E., HOTI, N., CASTANARES, M. & WU, M. 2007. Cleavage of RIP3 inactivates its caspase-independent apoptosis pathway by removal of kinase domain. *Cellular Signalling,* 19**,** 2056-2067.

FENTON, M. J. & GOLENBOCK, D. T. 1998. LPS-binding proteins and receptors. *Journal of Leukocyte Biology,* 64**,** 25-32.

FINK, S. L. & COOKSON, B. T. 2006. Caspase-1-dependent pore formation during pyroptosis leads to osmotic lysis of infected host macrophages. *Cellular Microbiology,* 8**,** 1812-1825.

FLÜGEL, A., SCHULZE-KOOPS, H., HEESEMANN, J., KÜHN, K., SOROKIN, L., BURKHARDT, H., VON DER MARK, K. & EMMRICH, F. 1994. Interaction of enteropathogenic *Yersinia enterocolitica* with complex basement membranes and the extracellular matrix proteins collagen type IV, laminin-1 and-2, and nidogen/entactin. *Journal of Biological Chemistry,* 269**,** 29732-29738.

FREDERIKSEN, W. 1964. A study of some *Yersinia pseudotuberculosis*-like bacteria ("*Bacterium enterocoliticum*" and "*Pasteurella X*"). *Scand. Congr. Pathol. Microbiol,* 14**,** 103-104.

FREDRIKSSON-AHOMAA, M., STOLLE, A. & STEPHAN, R. 2007. Prevalence of pathogenic *Yersinia enterocolitica* in pigs slaughtered at a Swiss abattoir. *Int J Food Microbiol,* 119**,** 207-12.

FRITSCH, M., GÜNTHER, S. D., SCHWARZER, R., ALBERT, M.-C., SCHORN, F., WERTHENBACH, J. P., SCHIFFMANN, L. M., STAIR, N., STOCKS, H., SEEGER, J. M., LAMKANFI, M., KRÖNKE, M., PASPARAKIS, M. & KASHKAR, H. 2019. Caspase-8 is the molecular switch for apoptosis, necroptosis and pyroptosis. *Nature,* 575**,** 683-687.

FUELLER, F. & SCHMIDT, G. 2008. The polybasic region of Rho GTPases defines the cleavage by *Yersinia enterocolitica* outer protein T (YopT). *Protein Science,* 17**,** 1456-1462.

GALYOV, E. E., HÅKANSSON, S., FORSBERG, Å. & WOLF-WATZ, H. 1993. A secreted protein kinase of *Yersinia pseudotuberculosis* is an indispensable virulence determinant. *Nature,* 361**,** 730-732.

GENG, J., ITO, Y., SHI, L., AMIN, P., CHU, J., OUCHIDA, A. T., MOOKHTIAR, A. K., ZHAO, H., XU, D., SHAN, B., NAJAFOV, A., GAO, G., AKIRA, S. & YUAN, J. 2017. Regulation of RIPK1 activation by TAK1-mediated phosphorylation dictates apoptosis and necroptosis. *Nature Communications,* 8**,** 359.

GRABOWSKI, B., SCHMIDT, M. A. & RÜTER, C. 2017. Immunomodulatory *Yersinia* outer proteins (Yops)– useful tools for bacteria and humans alike. *Virulence,* 8**,** 1124-1147.

GRASSL, G. A., BOHN, E., MÜLLER, Y., BÜHLER, O. T. & AUTENRIETH, I. B. 2003. Interaction of *Yersinia enterocolitica* with epithelial cells: invasin beyond invasion. *International Journal of Medical Microbiology,* 293**,** 41-54.

GREEN, D. R. & KROEMER, G. 2004. The Pathophysiology of Mitochondrial Cell Death. *Science,* 305**,** 626-629.

GROOTJANS, S., HASSANNIA, B., DELRUE, I., GOOSSENS, V., WIERNICKI, B., DONDELINGER, Y., BERTRAND, M. J., KRYSKO, D. V., VUYLSTEKE, M. & VANDENABEELE, P. 2016. A real-time fluorometric method for the simultaneous detection of cell death type and rate. *Nature protocols,* 11**,** 1444-1454.

GROVES, E., RITTINGER, K., AMSTUTZ, M., BERRY, S., HOLDEN, D. W., CORNELIS, G. R. & CARON, E. 2010. Sequestering of Rac by the *Yersinia* Effector YopO Blocks Fcgamma Receptor-mediated Phagocytosis. *Journal of Biological Chemistry,* 285**,** 4087-4098.

GRÜTZKAU, A., HANSKI, C., HAHN, H. & RIECKEN, E. O. 1990. Involvement of M cells in the bacterial invasion of Peyer's patches: a common mechanism shared by *Yersinia enterocolitica* and other enteroinvasive bacteria. *Gut,* 31**,** 1011-1015.

GUAN, K. & DIXON, J. E. 1990. Protein Tyrosine Phosphatase Activity of an Essential Virulence Determinant in *Yersinia*. *Science,* 249**,** 553-556.

GUO, X., YIN, H., CHEN, Y., LI, L., LI, J. & LIU, Q. 2016. TAK1 regulates caspase 8 activation and necroptotic signaling via multiple cell death checkpoints. *Cell Death & Disease,* 7**,** e2381-e2381.

GURUNG, P., ANAND, P. K., MALIREDDI, R., VANDE WALLE, L., VAN OPDENBOSCH, N., DILLON, C. P., WEINLICH, R., GREEN, D. R., LAMKANFI, M. & KANNEGANTI, T.-D. 2014. FADD and caspase-8 mediate priming and activation of the canonical and noncanonical Nlrp3 inflammasomes. *The Journal of Immunology,* 192**,** 1835-1846.

GUTIERREZ, K. D., DAVIS, M. A., DANIELS, B. P., OLSEN, T. M., RALLI-JAIN, P., TAIT, S. W. G., GALE, M., JR. & OBERST, A. 2017. MLKL Activation Triggers NLRP3-Mediated Processing and Release of IL-1β Independently of Gasdermin-D. *The Journal of Immunology,* 198**,** 2156-2164.

HAASE, R., KIRSCHNING, C. J., SING, A., SCHRÖTTNER, P., FUKASE, K., KUSUMOTO, S., WAGNER, H., HEESEMANN, J. R. & RUCKDESCHEL, K. 2003. A Dominant Role of Toll-Like Receptor 4 in the Signaling of Apoptosis in Bacteria-Faced Macrophages 1. *The Journal of Immunology,* 171**,** 4294-4303.

HAASE, R., RICHTER, K., PFAFFINGER, G., COURTOIS, G. & RUCKDESCHEL, K. 2005. Yersinia Outer Protein P Suppresses TGF-β-Activated Kinase-1 Activity to Impair Innate Immune Signaling in *Yersinia enterocolitica*-Infected Cells1. *The Journal of Immunology,* 175**,** 8209-8217.

HAGAR, J. A., POWELL, D. A., AACHOUI, Y., ERNST, R. K. & MIAO, E. A. 2013. Cytoplasmic LPS Activates Caspase-11: Implications in TLR4-Independent Endotoxic Shock. *Science,* 341**,** 1250-1253.

HÅKANSSON, S., BERGMAN, T., VANOOTEGHEM, J. C., CORNELIS, G. & WOLF-WATZ, H. 1993. YopB and YopD constitute a novel class of *Yersinia* Yop proteins. *Infection and Immunity,* 61**,** 71-80.

HAN, Z., HENDRICKSON, E. A., BREMNER, T. A. & WYCHE, J. H. 1997. A Sequential Two-Step Mechanism for the Production of the Mature p17:p12 Form of Caspase-3 *in Vitro*. *Journal of Biological Chemistry,* 272**,** 13432-13436.

HANDLEY, S. A., NEWBERRY, R. D. & MILLER, V. L. 2005. *Yersinia enterocolitica* Invasin-Dependent and Invasin-Independent Mechanisms of Systemic Dissemination. *Infection and Immunity,* 73**,** 8453-8455.

HANSKI, C., NAUMANN, M., HAHN, H. & RIECKEN, E. O. 1989. Determinants of invasion and survival of *Yersinia enterocolitica* in intestinal tissue. *Medical Microbiology and Immunology,* 178**,** 289-296.

HEESEMANN, J. & LAUFS, R. 1983. Construction of a mobilizable *Yersinia enterocolitica* virulence plasmid. *Journal of bacteriology,* 155**,** 761-767.

HEILIG, R., DILUCCA, M., BOUCHER, D., CHEN, K. W., HANCZ, D., DEMARCO, B., SHKARINA, K. & BROZ, P. 2020. Caspase-1 cleaves Bid to release mitochondrial SMAC and drive secondary necrosis in the absence of GSDMD. *Life Sci Alliance,* 3.

HENTSCHKE, M., BERNEKING, L., BELMAR CAMPOS, C., BUCK, F., RUCKDESCHEL, K. & AEPFELBACHER, M. 2010. *Yersinia virulence* factor YopM induces sustained RSK activation by interfering with dephosphorylation. *PLoS One,* 5.

HOICZYK, E. & BLOBEL, G. 2001. Polymerization of a single protein of the pathogen *Yersinia enterocolitica* into needles punctures eukaryotic cells. *Proceedings of the National Academy of Sciences,* 98**,** 4669-4674.

HOICZYK, E., ROGGENKAMP, A., REICHENBECHER, M., LUPAS, A. & HEESEMANN, J. 2000. Structure and sequence analysis of *Yersinia* YadA and Moraxella UspAs reveal a novel class of adhesins. *The EMBO Journal,* 19**,** 5989-5999.

HOLLER, N., ZARU, R., MICHEAU, O., THOME, M., ATTINGER, A., VALITUTTI, S., BODMER, J.-L., SCHNEIDER, P., SEED, B. & TSCHOPP, J. 2000. Fas triggers an alternative, caspase-8–independent cell death pathway using the kinase RIP as effector molecule. *Nature Immunology,* 1**,** 489-495.

HOLMSTRÖM, A., PETTERSSON, J., ROSQVIST, R., HÅKANSSON, S., TAFAZOLI, F., FÄLLMAN, M., MAGNUSSON, K.-E., WOLF-WATZ, H. & FORSBERG, Å. 1997. YopK of *Yersinia pseudotuberculosis* controls translocation of Yop effectors across the eukaryotic cell membrane. *Molecular Microbiology,* 24**,** 73-91.

HOLMSTRÖM, A., ROSQVIST, R., WOLF-WATZ, H. & FORSBERG, A. 1995. Virulence plasmid-encoded YopK is essential for *Yersinia pseudotuberculosis* to cause systemic infection in mice. *Infection and Immunity,* 63**,** 2269-2276.

HORNUNG, V., ABLASSER, A., CHARREL-DENNIS, M., BAUERNFEIND, F., HORVATH, G., CAFFREY, D. R., LATZ, E. & FITZGERALD, K. A. 2009. AIM2 recognizes cytosolic dsDNA and forms a caspase-1-activating inflammasome with ASC. *Nature,* 458**,** 514-518.

HSU, H., XIONG, J. & GOEDDEL, D. V. 1995. The TNF receptor 1-associated protein TRADD signals cell death and NF-κB activation. *Cell,* 81**,** 495-504.

HUANG, D., ZHENG, X., WANG, Z.-A., CHEN, X., HE, W.-T., ZHANG, Y., XU, J.-G., ZHAO, H., SHI, W., WANG, X., ZHU, Y. & HAN, J. 2017. The MLKL Channel in Necroptosis Is an Octamer Formed by Tetramers in a Dyadic Process. *Molecular and Cellular Biology,* 37**,** e00497-16.

INOHARA, N. & NUÑEZ, G. 2003. NODs: intracellular proteins involved in inflammation and apoptosis. *Nature Reviews Immunology,* 3**,** 371-382.

IORDANOV, M. S., RYABININA, O. P., SCHNEIDER, P. & MAGUN, B. E. 2005. Two mechanisms of caspase 9 processing in double-stranded RNA- and virus-triggered apoptosis. *Apoptosis,* 10**,** 153-166.

IRIARTE, M. & CORNELIS, G. R. 1998. YopT, a new *Yersinia* Yop effector protein, affects the cytoskeleton of host cells. *Molecular Microbiology,* 29**,** 915-929.

IVANOV, M. I., STUCKEY, J. A., SCHUBERT, H. L., SAPER, M. A. & BLISKA, J. B. 2005. Two substrate-targeting sites in the *Yersinia* protein tyrosine phosphatase co-operate to promote bacterial virulence. *Molecular Microbiology,* 55**,** 1346-1356.

JALAVA, K., HAKKINEN, M., VALKONEN, M., NAKARI, U.-M., PALO, T., HALLANVUO, S., OLLGREN, J., SIITONEN, A. & NUORTI, J. P. 2006. An Outbreak of Gastrointestinal Illness and Erythema Nodosum from Grated Carrots Contaminated with *Yersinia pseudotuberculosis*. *The Journal of Infectious Diseases,* 194**,** 1209-1216.

JIANG, X. & WANG, X. 2000. Cytochrome c Promotes Caspase-9 Activation by Inducing Nucleotide Binding to Apaf-1 *Journal of Biological Chemistry,* 275**,** 31199-31203.

JORGENSEN, I. & MIAO, E. A. 2015. Pyroptotic cell death defends against intracellular pathogens. *Immunological Reviews,* 265**,** 130-142.

JORGENSEN, I., RAYAMAJHI, M. & MIAO, E. A. 2017. Programmed cell death as a defence against infection. *Nature Reviews Immunology,* 17**,** 151-164.

JOST, P. J., GRABOW, S., GRAY, D., MCKENZIE, M. D., NACHBUR, U., HUANG, D. C. S., BOUILLET, P., THOMAS, H. E., BORNER, C., SILKE, J., STRASSER, A. & KAUFMANN, T. 2009. XIAP discriminates between type I and type II FAS-induced apoptosis. *Nature,* 460**,** 1035-1039.

JOURNET, L., AGRAIN, C., BROZ, P. & CORNELIS, G. R. 2003. The needle length of bacterial injectisomes is determined by a molecular ruler. *Science,* 302**,** 1757-60.

JURIS, S. J., RUDOLPH, A. E., HUDDLER, D., ORTH, K. & DIXON, J. E. 2000. A distinctive role for the *Yersinia* protein kinase: Actin binding, kinase activation, and cytoskeleton disruption. *Proceedings of the National Academy of Sciences,* 97**,** 9431-9436.

JURIS, S. J., SHAO, F. & DIXON, J. E. 2002. *Yersinia* effectors target mammalian signalling pathways. *Cellular Microbiology,* 4**,** 201-211.

KACZMAREK, A., VANDENABEELE, P. & KRYSKO, D. V. 2013. Necroptosis: the release of damage-associated molecular patterns and its physiological relevance. *Immunity,* 38**,** 209-223.

KAISER, W. J. & OFFERMANN, M. K. 2005. Apoptosis Induced by the Toll-Like Receptor Adaptor TRIF Is Dependent on Its Receptor Interacting Protein Homotypic Interaction Motif1. *The Journal of Immunology,* 174**,** 4942-4952.

KAISER, W. J., UPTON, J. W., LONG, A. B., LIVINGSTON-ROSANOFF, D., DALEY-BAUER, L. P., HAKEM, R., CASPARY, T. & MOCARSKI, E. S. 2011. RIP3 mediates the embryonic lethality of caspase-8-deficient mice. *Nature,* 471**,** 368-372.

KAISHO, T. & AKIRA, S. 2006. Toll-like receptor function and signaling. *Journal of Allergy and Clinical Immunology,* 117**,** 979-987.

KALKAVAN, H. & GREEN, D. R. 2018. MOMP, cell suicide as a BCL-2 family business. *Cell Death & Differentiation,* 25**,** 46-55.

KAMBARA, H., LIU, F., ZHANG, X., LIU, P., BAJRAMI, B., TENG, Y., ZHAO, L., ZHOU, S., YU, H. & ZHOU, W. 2018. Gasdermin D exerts anti-inflammatory effects by promoting neutrophil death. *Cell reports,* 22**,** 2924-2936.

KANG, T.-B., YANG, S.-H., TOTH, B., KOVALENKO, A. & WALLACH, D. 2013. Caspase-8 blocks kinase RIPK3-mediated activation of the NLRP3 inflammasome. *Immunity,* 38**,** 27-40.

KAUFMANN, T., STRASSER, A. & JOST, P. J. 2012. Fas death receptor signalling: roles of Bid and XIAP. *Cell Death & Differentiation,* 19**,** 42-50.

KAWAI, T. & AKIRA, S. 2006. TLR signaling. *Cell Death & Differentiation,* 13**,** 816-825.

KAYAGAKI, N., STOWE, I. B., LEE, B. L., O'ROURKE, K., ANDERSON, K., WARMING, S., CUELLAR, T., HALEY, B., ROOSE-GIRMA, M., PHUNG, Q. T., LIU, P. S., LILL, J. R., LI, H., WU, J., KUMMERFELD, S., ZHANG, J., LEE, W. P., SNIPAS, S. J., SALVESEN, G. S., MORRIS, L. X., FITZGERALD, L., ZHANG, Y., BERTRAM, E. M., GOODNOW, C. C. & DIXIT, V. M. 2015. Caspase-11 cleaves gasdermin D for non-canonical inflammasome signalling. *Nature,* 526**,** 666-671.

KELLIHER, M. A., GRIMM, S., ISHIDA, Y., KUO, F., STANGER, B. Z. & LEDER, P. 1998. The death domain kinase RIP mediates the TNF-induced NF-κB signal. *Immunity,* 8**,** 297-303.

KERR, J. F. R., WYLLIE, A. H. & CURRIE, A. R. 1972. Apoptosis: A Basic Biological Phenomenon with Wideranging Implications in Tissue Kinetics. *British Journal of Cancer,* 26**,** 239-257.

KESAVARDHANA, S. & KANNEGANTI, T.-D. 2017. Mechanisms governing inflammasome activation, assembly and pyroptosis induction. *International Immunology,* 29**,** 201-210.

KESAVARDHANA, S., MALIREDDI, R. K. S. & KANNEGANTI, T. D. 2020. Caspases in Cell Death, Inflammation, and Pyroptosis. *Annu Rev Immunol,* 38**,** 567-595.

KETELUT-CARNEIRO, N. & FITZGERALD, K. A. 2022. Apoptosis, Pyroptosis, and Necroptosis—Oh My! The Many Ways a Cell Can Die. *Journal of Molecular Biology,* 434**,** 167378.

KIRJAVAINEN, V., JARVA, H., BIEDZKA-SAREK, M., BLOM, A. M., SKURNIK, M. & MERI, S. 2008. *Yersinia enterocolitica* serum resistance proteins YadA and ail bind the complement regulator C4b-binding protein. *PLoS pathogens,* 4**,** e1000140.

KOVACS, S. B. & MIAO, E. A. 2017. Gasdermins: Effectors of Pyroptosis. *Trends Cell Biol,* 27**,** 673-684.

KUANG, S., ZHENG, J., YANG, H., LI, S., DUAN, S., SHEN, Y., JI, C., GAN, J., XU, X.-W. & LI, J. 2017. Structure insight of GSDMD reveals the basis of GSDMD autoinhibition in cell pyroptosis. *Proceedings of the National Academy of Sciences,* 114**,** 10642-10647.

LAER, L. V., HUIZING, E. H., VERSTREKEN, M., ZUIJLEN, D. V., WAUTERS, J. G., BOSSUYT, P. J., VAN DE HEYNING, P., MCGUIRT, W. T., SMITH, R. J. H., WILLEMS, P. J., LEGAN, P. K., RICHARDSON, G. P. & VAN CAMP, G. 1998. Nonsyndromic hearing impairment is associated with a mutation in DFNA5. *Nature Genetics,* 20**,** 194-197.

LAFONT, E., DRABER, P., RIESER, E., REICHERT, M., KUPKA, S., DE MIGUEL, D., DRABEROVA, H., VON MÄSSENHAUSEN, A., BHAMRA, A., HENDERSON, S., WOJDYLA, K., CHALK, A., SURINOVA, S., LINKERMANN, A. & WALCZAK, H. 2018. TBK1 and IKKε prevent TNF-induced cell death by RIPK1 phosphorylation. *Nature Cell Biology,* 20**,** 1389-1399.

LALAOUI, N., BOYDEN, S. E., ODA, H., WOOD, G. M., STONE, D. L., CHAU, D., LIU, L., STOFFELS, M., KRATINA, T., LAWLOR, K. E., ZAAL, K. J. M., HOFFMANN, P. M., ETEMADI, N., SHIELD-ARTIN, K., BIBEN, C., TSAI, W. L., BLAKE, M. D., KUEHN, H. S., YANG, D., ANDERTON, H., SILKE, N., WACHSMUTH, L., ZHENG, L., MOURA, N. S., BECK, D. B., GUTIERREZ-CRUZ, G., OMBRELLO, A. K., PINTO-PATARROYO, G. P., KUEH, A. J., HEROLD, M. J., HALL, C., WANG, H., CHAE, J. J., DMITRIEVA, N. I., MCKENZIE, M., LIGHT, A., BARHAM, B. K., JONES, A., ROMEO, T. M., ZHOU, Q., AKSENTIJEVICH, I., MULLIKIN, J. C., GROSS, A. J., SHUM, A. K., HAWKINS, E. D., MASTERS, S. L., LENARDO, M. J., BOEHM, M., ROSENZWEIG, S. D., PASPARAKIS, M., VOSS, A. K., GADINA, M., KASTNER, D. L. & SILKE, J. 2020. Mutations that prevent caspase cleavage of RIPK1 cause autoinflammatory disease. *Nature,* 577**,** 103-108.

LAMKANFI, M., DECLERCQ, W., KALAI, M., SAELENS, X. & VANDENABEELE, P. 2002. Alice in caspase land. A phylogenetic analysis of caspases from worm to man. *Cell Death & Differentiation,* 9**,** 358-361.

LAMKANFI, M. & DIXIT, VISHVA M. 2014. Mechanisms and Functions of Inflammasomes. *Cell,* 157**,** 1013-1022.

LAMKANFI, M., KANNEGANTI, T.-D., VAN DAMME, P., VANDEN BERGHE, T., VANOVERBERGHE, I., VANDEKERCKHOVE, J., VANDENABEELE, P., GEVAERT, K. & NUÉNÑEZ, G. 2008. Targeted Peptidecentric Proteomics Reveals Caspase-7 as a Substrate of the Caspase-1 Inflammasomes. *Molecular & Cellular Proteomics,* 7**,** 2350-2363.

LARA-TEJERO, M., KATO, J., WAGNER, S., LIU, X. & GALÁN, J. E. 2011. A Sorting Platform Determines the Order of Protein Secretion in Bacterial Type III Systems. *Science,* 331**,** 1188-1191.

LAROCK, C. N. & COOKSON, B. T. 2012. The *Yersinia* virulence effector YopM binds caspase-1 to arrest inflammasome assembly and processing. *Cell host & microbe,* 12**,** 799-805.

LAURIEN, L., NAGATA, M., SCHÜNKE, H., DELANGHE, T., WIEDERSTEIN, J. L., KUMARI, S., SCHWARZER, R., CORONA, T., KRÜGER, M., BERTRAND, M. J. M., KONDYLIS, V. & PASPARAKIS, M. 2020.

Autophosphorylation at serine 166 regulates RIP kinase 1-mediated cell death and inflammation. *Nature Communications,* 11**,** 1747.

LAVRIK, I., KRUEGER, A., SCHMITZ, I., BAUMANN, S., WEYD, H., KRAMMER, P. H. & KIRCHHOFF, S. 2003. The active caspase-8 heterotetramer is formed at the CD95 DISC. *Cell Death & Differentiation,* 10**,** 144-145.

LE GUERN, A.-S., MARTIN, L., SAVIN, C. & CARNIEL, E. 2016. Yersiniosis in France: overview and potential sources of infection. *International Journal of Infectious Diseases,* 46**,** 1-7.

LE GUERN, A. S., SAVIN, C., ANGERMEIER, H., BRÉMONT, S., CLERMONT, D., MÜHLE, E., OROZOVA, P., NAJDENSKI, H. & PIZARRO-CERDÁ, J. 2020. *Yersinia artesiana* sp. nov., *Yersinia proxima* sp. nov., *Yersinia alsatica sp. nov., Yersina vastinensis sp. nov., Yersinia thracica sp. nov. and Yersinia occitanica sp. nov.,* isolated from humans and animals. *Int J Syst Evol Microbiol,* 70**,** 5363-5372.

LEE, W. L., GRIMES, J. M. & ROBINSON, R. C. 2015. *Yersinia* effector YopO uses actin as bait to phosphorylate proteins that regulate actin polymerization. *Nature Structural & Molecular Biology,* 22**,** 248-255.

LEIBIGER, R., NIEDUNG, K., GEGINAT, G., HEESEMANN, J. & TRÜLZSCH, K. 2008. *Yersinia enterocolitica* Yop mutants as oral live carrier vaccines. *Vaccine,* 26**,** 6664-6670.

LEO, J. C. & SKURNIK, M. 2011. Adhesins of Human Pathogens from the Genus *Yersinia*. *In:* LINKE, D. & GOLDMAN, A. (eds.) *Bacterial Adhesion: Chemistry, Biology and Physics.* Dordrecht: Springer Netherlands.

LEONG, J. M., FOURNIER, R. S. & ISBERG, R. R. 1990. Identification of the integrin binding domain of the *Yersinia pseudotuberculosis* invasin protein. *The EMBO Journal,* 9**,** 1979-1989.

LI, H., ZHU, H., XU, C.-J. & YUAN, J. 1998. Cleavage of BID by Caspase 8 Mediates the Mitochondrial Damage in the Fas Pathway of Apoptosis. *Cell,* 94**,** 491-501.

LI, J., MCQUADE, T., SIEMER, ANSGAR B., NAPETSCHNIG, J., MORIWAKI, K., HSIAO, Y.-S., DAMKO, E., MOQUIN, D., WALZ, T., MCDERMOTT, A., CHAN, FRANCIS K.-M. & WU, H. 2012. The RIP1/RIP3 Necrosome Forms a Functional Amyloid Signaling Complex Required for Programmed Necrosis. *Cell,* 150**,** 339-350.

LI, P., NIJHAWAN, D., BUDIHARDJO, I., SRINIVASULA, S. M., AHMAD, M., ALNEMRI, E. S. & WANG, X. 1997. Cytochrome c and dATP-Dependent Formation of Apaf-1/Caspase-9 Complex Initiates an Apoptotic Protease Cascade. *Cell,* 91**,** 479-489.

LI, X., ZHONG, C.-Q., WU, R., XU, X., YANG, Z.-H., CAI, S., WU, X., CHEN, X., YIN, Z., HE, Q., LI, D., XU, F., YAN, Y., QI, H., XIE, C., SHUAI, J. & HAN, J. 2021. RIP1-dependent linear and nonlinear recruitments of caspase-8 and RIP3 respectively to necrosome specify distinct cell death outcomes. *Protein & Cell,* 12**,** 858-876.

LIEBERMAN, J., WU, H. & KAGAN, J. 2019. Gasdermin D activity in inflammation and host defense.

LIN, Y., DEVIN, A., RODRIGUEZ, Y. & LIU, Z.-G. 1999. Cleavage of the death domain kinase RIP by caspase-8 prompts TNF-induced apoptosis. *Genes & development,* 13**,** 2514-2526.

LIU, X., ZHANG, Z., RUAN, J., PAN, Y., MAGUPALLI, V. G., WU, H. & LIEBERMAN, J. 2016. Inflammasome-activated gasdermin D causes pyroptosis by forming membrane pores. *Nature,* 535**,** 153-158.

LIU, Z., WANG, C., YANG, J., ZHOU, B., YANG, R., RAMACHANDRAN, R., ABBOTT, D. W. & XIAO, T. S. 2019. Crystal structures of the full-length murine and human gasdermin D reveal mechanisms of autoinhibition, lipid binding, and oligomerization. *Immunity,* 51**,** 43-49. e4.

LONG, C., JONES, T. F., VUGIA, D. J., SCHEFTEL, J., STROCKBINE, N., RYAN, P., SHIFERAW, B., TAUXE, R. V. & GOULD, L. H. 2010. *Yersinia pseudotuberculosis* and *Y. enterocolitica* infections, FoodNet, 1996-2007. *Emerging Infectious Diseases,* 16**,** 566-7.

MALIK, H. S. & BLISKA, J. B. 2020. The pyrin inflammasome and the *Yersinia* effector interaction. *Immunological Reviews,* 297**,** 96-107.

MALIREDDI, R. K. S., GURUNG, P., KESAVARDHANA, S., SAMIR, P., BURTON, A., MUMMAREDDY, H., VOGEL, P., PELLETIER, S., BURGULA, S. & KANNEGANTI, T. D. 2020a. Innate immune priming in the absence of TAK1 drives RIPK1 kinase activity-independent pyroptosis, apoptosis, necroptosis, and inflammatory disease. *J Exp Med,* 217.

MALIREDDI, R. K. S., GURUNG, P., MAVULURI, J., DASARI, T. K., KLCO, J. M., CHI, H. & KANNEGANTI, T.-D. 2018. TAK1 restricts spontaneous NLRP3 activation and cell death to control myeloid proliferation. *Journal of Experimental Medicine,* 215**,** 1023-1034.

MALIREDDI, R. K. S., KESAVARDHANA, S., KARKI, R., KANCHARANA, B., BURTON, A. R. & KANNEGANTI, T. D. 2020b. RIPK1 Distinctly Regulates Yersinia-Induced Inflammatory Cell Death, PANoptosis. *Immunohorizons,* 4**,** 789-796.

MAN, S. M. & KANNEGANTI, T.-D. 2016. Converging roles of caspases in inflammasome activation, cell death and innate immunity. *Nature Reviews Immunology,* 16**,** 7-21.

MANDAL, P., BERGER, S. B., PILLAY, S., MORIWAKI, K., HUANG, C., GUO, H., LICH, J. D., FINGER, J., KASPARCOVA, V. & VOTTA, B. 2014. RIP3 induces apoptosis independent of pronecrotic kinase activity. *Molecular cell,* 56**,** 481-495.

MASCARENHAS, D. P. A., CERQUEIRA, D. M., PEREIRA, M. S. F., CASTANHEIRA, F. V. S., FERNANDES, T. D., MANIN, G. Z., CUNHA, L. D. & ZAMBONI, D. S. 2017. Inhibition of caspase-1 or gasdermin-D enable caspase-8 activation in the Naip5/NLRC4/ASC inflammasome. *PLOS Pathogens,* 13**,** e1006502.

MCDONALD, C., VACRATSIS, P. O., BLISKA, J. B. & DIXON, J. E. 2003. The *Yersinia* Virulence Factor YopM Forms a Novel Protein Complex with Two Cellular Kinases *Journal of Biological Chemistry,* 278**,** 18514-18523.

MCNALLY, A., THOMSON, N. R., REUTER, S. & WREN, B. W. 2016. 'Add, stir and reduce': *Yersinia* spp. as model bacteria for pathogen evolution. *Nature Reviews Microbiology,* 14**,** 177-90.

MCPHEE, J. B., MENA, P. & BLISKA, J. B. 2010. Delineation of Regions of the *Yersinia* YopM Protein Required for Interaction with the RSK1 and PRK2 Host Kinases and Their Requirement for Interleukin-10 Production and Virulence. *Infection and Immunity,* 78**,** 3529-3539.

MEDZHITOV, R. & JANEWAY, C. 2000. Innate Immunity. *New England Journal of Medicine,* 343**,** 338-344.

MEINZER, U., BARREAU, F., ESMIOL-WELTERLIN, S., JUNG, C., VILLARD, C., LEGER, T., BEN-MKADDEM, S., BERREBI, D., DUSSAILLANT, M. & ALNABHANI, Z. 2012. *Yersinia pseudotuberculosis* effector YopJ subverts the Nod2/RICK/TAK1 pathway and activates caspase-1 to induce intestinal barrier dysfunction. *Cell host & microbe,* 11**,** 337-351.

MENG, Y., DAVIES, K. A., FITZGIBBON, C., YOUNG, S. N., GARNISH, S. E., HORNE, C. R., LUO, C., GARNIER, J.-M., LIANG, L.-Y., COWAN, A. D., SAMSON, A. L., LESSENE, G., SANDOW, J. J., CZABOTAR, P. E. & MURPHY, J. M. 2021. Human RIPK3 maintains MLKL in an inactive conformation prior to cell death by necroptosis. *Nature Communications,* 12**,** 6783.

MENON, M. B., GROPENGIEßER, J., FISCHER, J., NOVIKOVA, L., DEURETZBACHER, A., LAFERA, J., SCHIMMECK, H., CZYMMECK, N., RONKINA, N., KOTLYAROV, A., AEPFELBACHER, M., GAESTEL, M. & RUCKDESCHEL, K. 2017. p38MAPK/MK2-dependent phosphorylation controls cytotoxic RIPK1 signalling in inflammation and infection. *Nature Cell Biology,* 19**,** 1248-1259.

MICHEAU, O. & TSCHOPP, J. 2003. Induction of TNF Receptor I-Mediated Apoptosis via Two Sequential Signaling Complexes. *Cell,* 114**,** 181-190.

MIHALY, S. R., NINOMIYA-TSUJI, J. & MORIOKA, S. 2014. TAK1 control of cell death. *Cell Death & Differentiation,* 21**,** 1667-1676.

MIKULSKIS, A. V., DELOR, I., THI, V. H. & CORNELIS, G. R. 1994. Regulation of the *Yersinia enterocolitica* enterotoxin Yst gene. Influence of growth phase, temperature, osmolarity, pH and bacterial host factors. *Molecular Microbiology,* 14**,** 905-915.

MILLER, V. L., BLISKA, J. B. & FALKOW, S. 1990. Nucleotide sequence of the *Yersinia enterocolitica* ail gene and characterization of the Ail protein product. *Journal of Bacteriology,* 172**,** 1062-1069.

MILLER, V. L. & FALKOW, S. 1988. Evidence for two genetic loci in *Yersinia enterocolitica* that can promote invasion of epithelial cells. *Infection and Immunity,* 56**,** 1242-1248.

MILLS, S. D., BOLAND, A., SORY, M.-P., VAN DER SMISSEN, P., KERBOURCH, C., FINLAY, B. B. & CORNELIS, G. R. 1997. *Yersinia enterocolitica* induces apoptosis in macrophages by a process requiring functional type III secretion and translocation mechanisms and involving YopP, presumably

acting as an effector protein. *Proceedings of the National Academy of Sciences,* 94**,** 12638-12643.

MITTAL, R., PEAK-CHEW, S.-Y. & MCMAHON, H. T. 2006. Acetylation of MEK2 and IκB kinase (IKK) activation loop residues by YopJ inhibits signaling. *Proceedings of the National Academy of Sciences,* 103**,** 18574-18579.

MONACK, D. M., MECSAS, J., GHORI, N. & FALKOW, S. 1997. *Yersinia* signals macrophages to undergo apoptosis and YopJ is necessary for this cell death. *Proceedings of the National Academy of Sciences,* 94**,** 10385-10390.

MUELLER, C. A., BROZ, P., MÜLLER, S. A., RINGLER, P., ERNE-BRAND, F., SORG, I., KUHN, M., ENGEL, A. & CORNELIS, G. R. 2005. The V-antigen of *Yersinia* forms a distinct structure at the tip of injectisome needles. *Science,* 310**,** 674-6.

MÜHLENKAMP, M., OBERHETTINGER, P., LEO, J. C., LINKE, D. & SCHÜTZ, M. S. 2015. *Yersinia* adhesin A (YadA) – Beauty & beast. *International Journal of Medical Microbiology,* 305**,** 252-258.

MUKHERJEE, S., KEITANY, G., LI, Y., WANG, Y., BALL, H. L., GOLDSMITH, E. J. & ORTH, K. 2006. *Yersinia* YopJ Acetylates and Inhibits Kinase Activation by Blocking Phosphorylation. *Science,* 312**,** 1211-1214.

NEJEDLIK, L., PIERFELICE, T. & GEISER, J. R. 2004. Actin distribution is disrupted upon expression of *Yersinia* YopO/YpkA in yeast. *Yeast,* 21**,** 759-768.

NEWTON, K., WICKLIFFE, K. E., DUGGER, D. L., MALTZMAN, A., ROOSE-GIRMA, M., DOHSE, M., KŐMŰVES, L., WEBSTER, J. D. & DIXIT, V. M. 2019. Cleavage of RIPK1 by caspase-8 is crucial for limiting apoptosis and necroptosis. *Nature,* 574**,** 428-431.

NEYT, C. & CORNELIS, G. R. 1999. Insertion of a Yop translocation pore into the macrophage plasma membrane by *Yersinia enterocolitica:* requirement for translocators YopB and YopD, but not LcrG. *Molecular Microbiology,* 33**,** 971-981.

OBERST, A., DILLON, C. P., WEINLICH, R., MCCORMICK, L. L., FITZGERALD, P., POP, C., HAKEM, R., SALVESEN, G. S. & GREEN, D. R. 2011. Catalytic activity of the caspase-8–FLIPL complex inhibits RIPK3-dependent necrosis. *Nature,* 471**,** 363-367.

ORNING, P., WENG, D., STARHEIM, K., RATNER, D., BEST, Z., LEE, B., BROOKS, A., XIA, S., WU, H., KELLIHER, M. A., BERGER, S. B., GOUGH, P. J., BERTIN, J., PROULX, M. M., GOGUEN, J. D., KAYAGAKI, N., FITZGERALD, K. A. & LIEN, E. 2018. Pathogen blockade of TAK1 triggers caspase-8–dependent cleavage of gasdermin D and cell death. *Science,* 362**,** 1064-1069.

PAI, C. H. & MORS, V. 1978. Production of enterotoxin by *Yersinia enterocolitica*. *Infection and Immunity,* 19**,** 908-911.

PALMER, L. E., HOBBIE, S., GALÁN, J. E. & BLISKA, J. B. 1998. YopJ of *Yersinia pseudotuberculosis* is required for the inhibition of macrophage TNF-α production and downregulation of the MAP kinases p38 and JNK. *Molecular Microbiology,* 27**,** 953-965.

PAN, G., O'ROURKE, K., CHINNAIYAN, A. M., GENTZ, R., EBNER, R., NI, J. & DIXIT, V. M. 1997. The Receptor for the Cytotoxic Ligand TRAIL. *Science,* 276**,** 111-113.

PAQUETTE, N., CONLON, J., SWEET, C., RUS, F., WILSON, L., PEREIRA, A., ROSADINI, C. V., GOUTAGNY, N., WEBER, A. N. R., LANE, W. S., SHAFFER, S. A., MANIATIS, S., FITZGERALD, K. A., STUART, L. & SILVERMAN, N. 2012. Serine/threonine acetylation of TGF-β-activated kinase (TAK1) by *Yersinia pestis* YopJ inhibits innate immune signaling. *Proceedings of the National Academy of Sciences,* 109**,** 12710-12715.

PARK, E., JUNG, H., YANG, H., YOO, M., KIM, C. & KIM, K. 2007. Optimized THP-1 differentiation is required for the detection of responses to weak stimuli. *Inflammation research,* 56**,** 45-50.

PAVLIDIS, D. E., FILTER, M., BUSCHULTE, A. & (BFR), B. F. R. 2019. Application of data science in risk assessment and early warning. *EFSA Journal,* 17**,** e170908.

PEARSON, J. S. & MURPHY, J. M. 2017. Down the rabbit hole: Is necroptosis truly an innate response to infection? *Cellular Microbiology,* 19**,** e12750.

PECHOUS, R. D., SIVARAMAN, V., STASULLI, N. M. & GOLDMAN, W. E. 2016. Pneumonic Plague: The Darker Side of *Yersinia pestis*. *Trends Microbiol,* 24**,** 190-197.

PELTZER, N., DARDING, M. & WALCZAK, H. 2016. Holding RIPK1 on the Ubiquitin Leash in TNFR1 Signaling. *Trends in Cell Biology,* 26**,** 445-461.

PEPE, J. C., BADGER, J. L. & MILLER, V. L. 1994. Growth phase and low pH affect the thermal regulation of the *Yersinia enterocolitica* inv gene. *Molecular Microbiology,* 11**,** 123-135.

PEPE, J. C. & MILLER, V. L. 1993. *Yersinia enterocolitica* invasin: a primary role in the initiation of infection. *Proceedings of the National Academy of Sciences,* 90**,** 6473-6477.

PEPE, J. C., WACHTEL, M. R., WAGAR, E. & MILLER, V. L. 1995. Pathogenesis of defined invasion mutants of *Yersinia enterocolitica* in a BALB/c mouse model of infection. *Infection and immunity,* 63**,** 4837-4848.

PERRY, R. D. & FETHERSTON, J. D. 1997. *Yersinia pestis*-etiologic agent of plague. *Clinical Microbiology Reviews,* 10**,** 35-66.

PETERSON, L. W., PHILIP, N. H., DELANEY, A., WYNOSKY-DOLFI, M. A., ASKLOF, K., GRAY, F., CHOA, R., BJANES, E., BUZA, E. L., HU, B., DILLON, C. P., GREEN, D. R., BERGER, S. B., GOUGH, P. J., BERTIN, J. & BRODSKY, I. E. 2017. RIPK1-dependent apoptosis bypasses pathogen blockade of innate signaling to promote immune defense. *Journal of Experimental Medicine,* 214**,** 3171-3182.

PHA, K. & NAVARRO, L. 2016. *Yersinia* type III effectors perturb host innate immune responses. *World Journal of Biological Chemistry,* 7**,** 1-13.

PHILIP, N. H., DILLON, C. P., SNYDER, A. G., FITZGERALD, P., WYNOSKY-DOLFI, M. A., ZWACK, E. E., HU, B., FITZGERALD, L., MAULDIN, E. A., COPENHAVER, A. M., SHIN, S., WEI, L., PARKER, M., ZHANG, J., OBERST, A., GREEN, D. R. & BRODSKY, I. E. 2014. Caspase-8 mediates caspase-1 processing and innate immune defense in response to bacterial blockade of NF-κB and MAPK signaling. *Proceedings of the National Academy of Sciences,* 111**,** 7385-7390.

PIERSON, D. E. & FALKOW, S. 1993. The ail gene of *Yersinia enterocolitica* has a role in the ability of the organism to survive serum killing. *Infection and Immunity,* 61**,** 1846-1852.

PREHNA, G., IVANOV, M. I., BLISKA, J. B. & STEBBINS, C. E. 2006. *Yersinia* Virulence Depends on Mimicry of Host Rho-Family Nucleotide Dissociation Inhibitors. *Cell,* 126**,** 869-880.

PUJOL, C. & BLISKA, J. B. 2005. Turning *Yersinia pathogenesis* outside in: subversion of macrophage function by intracellular yersiniae. *Clinical Immunology,* 114**,** 216-226.

RAMIREZ, M. L. G. & SALVESEN, G. S. 2018. A primer on caspase mechanisms. *Seminars in Cell & Developmental Biology,* 82**,** 79-85.

REBSAMEN, M., HEINZ, L. X., MEYLAN, E., MICHALLET, M.-C., SCHRODER, K., HOFMANN, K., VAZQUEZ, J., BENEDICT, C. A. & TSCHOPP, J. 2009. DAI/ZBP1 recruits RIP1 and RIP3 through RIP homotypic interaction motifs to activate NF-κB. *EMBO reports,* 10**,** 916-922.

REVELL, P. A. & MILLER, V. L. 2001. *Yersinia* virulence: more than a plasmid. *FEMS Microbiology Letters,* 205**,** 159-164.

RINK, L., KRUSE, A. & HAASE, H. 2012. *Immunologie für Einsteiger*, Springer.

ROBERT-KOCH-INSTITUT. 2019. *Yersiniose* [Online]. Epidemiologisches Bulletin 2/2019. Available: https://www.rki.de/DE/Content/Infekt/EpidBull/Merkblaetter/Ratgeber_Yersiniose.html#doc11934216bodyText7 [Accessed 25.10.2023 2023].

ROCHA, J. M., RICHARDSON, C. J., ZHANG, M., DARCH, C. M., CAI, E., DIEPOLD, A. & GAHLMANN, A. 2018. Single-molecule tracking in live *Yersinia enterocolitica* reveals distinct cytosolic complexes of injectisome subunits. *Integrative Biology,* 10**,** 502-515.

ROGERS, C., FERNANDES-ALNEMRI, T., MAYES, L., ALNEMRI, D., CINGOLANI, G. & ALNEMRI, E. S. 2017. Cleavage of DFNA5 by caspase-3 during apoptosis mediates progression to secondary necrotic/pyroptotic cell death. *Nature Communications,* 8**,** 14128.

ROSQVIST, R., FORSBERG, Å., RIMPILÄINEN, M., BERGMAN, T. & WOLF-WATZ, H. 1990. The cytotoxic protein YopE of *Yersinia* obstructs the primary host defence. *Molecular Microbiology,* 4**,** 657-667.

RUCKDESCHEL, K., DEURETZBACHER, A. & HAASE, R. 2008. Crosstalk of signalling processes of innate immunity with *Yersinia* Yop effector functions. *Immunobiology,* 213**,** 261-269.

RUCKDESCHEL, K., HARB, S., ROGGENKAMP, A., HORNEF, M., ZUMBIHL, R., KÖHLER, S., HEESEMANN, J. & ROUOT, B. 1998. *Yersinia enterocolitica* Impairs Activation of Transcription Factor NF-κB: Involvement in the Induction of Programmed Cell Death and in the Suppression of the Macrophage Tumor Necrosis Factor α Production. *Journal of Experimental Medicine,* 187**,** 1069-1079.

RUCKDESCHEL, K., PFAFFINGER, G., HAASE, R., SING, A., WEIGHARDT, H., HÄCKER, G., HOLZMANN, B. & HEESEMANN, J. R. 2004. Signaling of Apoptosis through TLRs Critically Involves Toll/IL-1 Receptor Domain-Containing Adapter Inducing IFN-β, but Not MyD88, in Bacteria-Infected Murine Macrophages. *The Journal of Immunology,* 173**,** 3320-3328.

RÜHL, S. & BROZ, P. 2015. Caspase-11 activates a canonical NLRP3 inflammasome by promoting K+ efflux. *European Journal of Immunology,* 45**,** 2927-2936.

RÜHL, S., SHKARINA, K., DEMARCO, B., HEILIG, R., SANTOS, J. C. & BROZ, P. 2018. ESCRT-dependent membrane repair negatively regulates pyroptosis downstream of GSDMD activation. *Science,* 362**,** 956-960.

SABINA, Y., RAHMAN, A., RAY, R. C. & MONTET, D. 2011. *Yersinia enterocolitica*: Mode of Transmission, Molecular Insights of Virulence, and Pathogenesis of Infection. *Journal of Pathogens,* 2011**,** 429069.

SAKURAI, H., MIYOSHI, H., MIZUKAMI, J. & SUGITA, T. 2000. Phosphorylation-dependent activation of TAK1 mitogen-activated protein kinase kinase kinase by TAB1. *FEBS Letters,* 474**,** 141-145.

SANSONETTI, P. J. 2004. War and peace at mucosal surfaces. *Nature Reviews Immunology,* 4**,** 953-964.

SARHAN, J., LIU, B. C., MUENDLEIN, H. I., LI, P., NILSON, R., TANG, A. Y., RONGVAUX, A., BUNNELL, S. C., SHAO, F., GREEN, D. R. & POLTORAK, A. 2018. Caspase-8 induces cleavage of gasdermin D to elicit pyroptosis during *Yersinia* infection. *PNAS,* 115**,** E10888-E10897.

SAUVONNET, N., LAMBERMONT, I., BRUGGEN, P. V. D. & CORNELIS, G. R. 2002. YopH prevents monocyte chemoattractant protein 1 expression in macrophages and T-cell proliferation through inactivation of the phosphatidylinositol 3-kinase pathway. *Molecular Microbiology,* 45**,** 805-815.

SBORGI, L., RÜHL, S., MULVIHILL, E., PIPERCEVIC, J., HEILIG, R., STAHLBERG, H., FARADY, C. J., MÜLLER, D. J., BROZ, P. & HILLER, S. 2016. GSDMD membrane pore formation constitutes the mechanism of pyroptotic cell death. *The EMBO Journal,* 35**,** 1766-1778.

SCHLEIFSTEIN, J. & COLEMAN, M. 1939. An Unidentified Microorganism Resembling *B. lignieri* and Past, pseudotuberculosis, and Pathogenic for Man. *New York State Journal of Medicine,* 39**,** 1749-53.

SCHOBERLE, T. J., CHUNG, L. K., MCPHEE, J. B., BOGIN, B. & BLISKA, J. B. 2016. Uncovering an Important Role for YopJ in the Inhibition of Caspase-1 in Activated Macrophages and Promoting *Yersinia* pseudotuberculosis Virulence. *Infection and Immunity,* 84**,** 1062-1072.

SCHOTTE, P., DENECKER, G., VAN DEN BROEKE, A., VANDENABEELE, P., CORNELIS, G. R. & BEYAERT, R. 2004. Targeting Rac1 by the *Yersinia* Effector Protein YopE Inhibits Caspase-1-mediated Maturation and Release of Interleukin-1β. *Journal of Biological Chemistry,* 279**,** 25134-25142.

SCHULZE-KOOPS, H., BURKHARDT, H., HEESEMANN, J., KIRSCH, T., SWOBODA, B., BULL, C., GOODMAN, S. & EMMRICH, F. 1993. Outer membrane protein YadA of enteropathogenic *yersiniae* mediates specific binding to cellular but not plasma fibronectin. *Infection and immunity,* 61**,** 2513-2519.

SCHWARZER, R., LAURIEN, L. & PASPARAKIS, M. 2020. New insights into the regulation of apoptosis, necroptosis, and pyroptosis by receptor interacting protein kinase 1 and caspase-8. *Current Opinion in Cell Biology* 63**,** 186-193.

SHAO, F., VACRATSIS, P. O., BAO, Z., BOWERS, K. E., FIERKE, C. A. & DIXON, J. E. 2003. Biochemical characterization of the *Yersinia* YopT protease: Cleavage site and recognition elements in Rho GTPases. *Proceedings of the National Academy of Sciences,* 100**,** 904-909.

SHAYEGANI, M., DEFORGE, I., MCGLYNN, D. M. & ROOT, T. 1981. Characteristics of *Yersinia enterocolitica* and related species isolated from human, animal, and environmental sources. *Journal of Clinical Microbiology,* 14**,** 304-312.

SHEPPE, A. E. F., SANTELICES, J., CZYZ, D. M. & EDELMANN, M. J. 2021. *Yersinia pseudotuberculosis* YopJ Limits Macrophage Response by Downregulating COX-2-Mediated Biosynthesis of PGE2 in a MAPK/ERK-Dependent Manner. *Microbiology Spectrum,* 9**,** 10.1128/spectrum.00496-21.

SHI, J., ZHAO, Y., WANG, K., SHI, X., WANG, Y., HUANG, H., ZHUANG, Y., CAI, T., WANG, F. & SHAO, F. 2015. Cleavage of GSDMD by inflammatory caspases determines pyroptotic cell death. *Nature,* 526**,** 660-665.

SHIOZAKI, E. N., CHAI, J. & SHI, Y. 2002. Oligomerization and activation of caspase-9, induced by Apaf-1 CARD. *Proceedings of the National Academy of Sciences,* 99**,** 4197-4202.

SIMONET, M. & FALKOW, S. 1992. Invasin expression in *Yersinia pseudotuberculosis*. *Infection and Immunity,* 60**,** 4414-4417.

SIMS, J. E. & SMITH, D. E. 2010. The IL-1 family: regulators of immunity. *Nature Reviews Immunology,* 10**,** 89-102.

SKURNIK, M. & TOIVANEN, P. 1993. *Yersinia enterocolitica* lipopolysaccharide: genetics and virulence. *Trends in Microbiology,* 1**,** 148-52.

SKURNIK, M., VENHO, R., BENGOECHEA, J.-A. & MORIYÓN, I. 1999. The lipopolysaccharide outer core of *Yersinia enterocolitica* serotype O:3 is required for virulence and plays a role in outer membrane integrity. *Molecular Microbiology,* 31**,** 1443-1462.

SNYDER, A. G. & OBERST, A. 2021. The Antisocial Network: Cross Talk Between Cell Death Programs in Host Defense. *Annual Review of Immunology,* 39**,** 77-101.

SRINIVASULA, S. M., POYET, J.-L., RAZMARA, M., DATTA, P., ZHANG, Z. & ALNEMRI, E. S. 2002. The PYRIN-CARD Protein ASC Is an Activating Adaptor for Caspase-1 *Journal of Biological Chemistry,* 277**,** 21119-21122.

STENNICKE, H. R., JÜRGENSMEIER, J. M., SHIN, H., DEVERAUX, Q., WOLF, B. B., YANG, X., ZHOU, Q., ELLERBY, H. M., ELLERBY, L. M., BREDESEN, D., GREEN, D. R., REED, J. C., FROELICH, C. J. & SALVESEN, G. S. 1998. Pro-caspase-3 Is a Major Physiologic Target of Caspase-8 *Journal of Biological Chemistry,* 273**,** 27084-27090.

STRALEY, S. C. & PERRY, R. D. 1995. Environmental modulation of gene expression and pathogenesis in *Yersinia*. *Trends in microbiology,* 3**,** 310-317.

SUN, L., WANG, H., WANG, Z., HE, S., CHEN, S., LIAO, D., WANG, L., YAN, J., LIU, W. & LEI, X. 2012. Mixed lineage kinase domain-like protein mediates necrosis signaling downstream of RIP3 kinase. *Cell,* 148**,** 213-227.

TAABAZUING, C. Y., OKONDO, M. C. & BACHOVCHIN, D. A. 2017. Pyroptosis and apoptosis pathways engage in bidirectional crosstalk in monocytes and macrophages. *Cell chemical biology,* 24**,** 507-514. e4.

TAIT, S. W. G. & GREEN, D. R. 2010. Mitochondria and cell death: outer membrane permeabilization and beyond. *Nature Reviews Molecular Cell Biology,* 11**,** 621-632.

TAYLOR, R. C., CULLEN, S. P. & MARTIN, S. J. 2008. Apoptosis: controlled demolition at the cellular level. *Nature Reviews Molecular Cell Biology,* 9**,** 231-241.

TENNANT, S. M., GRANT, T. H. & ROBINS-BROWNE, R. M. 2003. Pathogenicity of *Yersinia enterocolitica* biotype 1A. *FEMS Immunology & Medical Microbiology,* 38**,** 127-137.

TERTTI, R., SKURNIK, M., VARTIO, T. & KUUSELA, P. 1992. Adhesion protein YadA of *Yersinia* species mediates binding of bacteria to fibronectin. *Infection and immunity,* 60**,** 3021-3024.

TERTTI, R., VUENTO, R., MIKKOLA, P., GRANFORS, K., MÄKELÄ, A. L. & TOIVANEN, A. 1989. Clinical manifestations of *Yersinia pseudotuberculosis* infection in children. *Eur J Clin Microbiol Infect Dis,* 8**,** 587-91.

TROISFONTAINES, P. & CORNELIS, G. R. 2005. Type III Secretion: More Systems Than You Think. *Physiology,* 20**,** 326-339.

TRÜLZSCH, K., HEESEMANN, J. & OELLERICH, M. F. 2007. Invasion and Dissemination of *Yersinia enterocolitica* in the Mouse Infection Model. *In:* PERRY, R. D. & FETHERSTON, J. D. (eds.) *The Genus Yersinia: From Genomics to Function.* New York, NY: Springer New York.

TRÜLZSCH, K., SPORLEDER, T., IGWE, E. I., RÜSSMANN, H. & HEESEMANN, J. 2004. Contribution of the Major Secreted Yops of *Yersinia enterocolitica* O:8 to Pathogenicity in the Mouse Infection Model. *Infection and Immunity,* 72**,** 5227-5234.

TSUCHIYA, K., NAKAJIMA, S., HOSOJIMA, S., THI NGUYEN, D., HATTORI, T., MANH LE, T., HORI, O., MAHIB, M. R., YAMAGUCHI, Y., MIURA, M., KINOSHITA, T., KUSHIYAMA, H., SAKURAI, M., SHIROISHI, T. & SUDA, T. 2019. Caspase-1 initiates apoptosis in the absence of gasdermin D. *Nature Communications,* 10**,** 2091.

TUMMERS, B. & GREEN, D. R. 2017. Caspase-8: regulating life and death. *Immunological Reviews,* 277**,** 76-89.

VANCE, R. E. 2015. The NAIP/NLRC4 inflammasomes. *Current Opinion in Immunology,* 32**,** 84-89.

VANDENABEELE, P., GALLUZZI, L., VANDEN BERGHE, T. & KROEMER, G. 2010. Molecular mechanisms of necroptosis: an ordered cellular explosion. *Nature Reviews Molecular Cell Biology,* 11**,** 700-714.

VIBOUD, G. I. & BLISKA, J. B. 2005. *Yersinia* outer proteins: role in modulation of host cell signaling responses and pathogenesis. *Annual Review of Microbiology,* 59**,** 69-89.

WAJANT, H. 2014. Principles and mechanisms of CD95 activation. *Biological Chemistry,* 395**,** 1401-1416.

WALCZAK, H. 2011. TNF and ubiquitin at the crossroads of gene activation, cell death, inflammation, and cancer. *Immunological Reviews,* 244**,** 9-28.

WALCZAK, H. 2013. Death receptor–ligand systems in cancer, cell death, and inflammation. *Cold Spring Harbor perspectives in biology,* 5**,** a008698.

WANG, Y., GAO, W., SHI, X., DING, J., LIU, W., HE, H., WANG, K. & SHAO, F. 2017. Chemotherapy drugs induce pyroptosis through caspase-3 cleavage of a gasdermin. *Nature,* 547**,** 99-103.

WANG, Y. & KANNEGANTI, T.-D. 2021. From pyroptosis, apoptosis and necroptosis to PANoptosis: A mechanistic compendium of programmed cell death pathways. *Computational and Structural Biotechnology Journal,* 19**,** 4641-4657.

WAUTERS, G., KANDOLO, K. & JANSSENS, M. 1987. Revised biogrouping scheme of *Yersinia enterocolitica*. *Contributions to microbiology and immunology,* 9**,** 14-21.

WENG, D., MARTY-ROIX, R., GANESAN, S., PROULX, M. K., VLADIMER, G. I., KAISER, W. J., MOCARSKI, E. S., POULIOT, K., CHAN, F. K.-M., KELLIHER, M. A., HARRIS, P. A., BERTIN, J., GOUGH, P. J., SHAYAKHMETOV, D. M., GOGUEN, J. D., FITZGERALD, K. A., SILVERMAN, N. & LIEN, E. 2014. Caspase-8 and RIP kinases regulate bacteria-induced innate immune responses and cell death. *Proceedings of the National Academy of Sciences,* 111**,** 7391-7396.

WHO. 2022. *Plague* [Online]. World Health Organisation. Available: https://www.who.int/news-room/fact-sheets/detail/plague [Accessed 25.10.2023 2023].

YAO, T., MECSAS, J., HEALY, J. I., FALKOW, S. & CHIEN, Y.-H. 1999. Suppression of T and B lymphocyte activation by a *Yersinia pseudotuberculosis* virulence factor, yopH. *The Journal of experimental medicine,* 190**,** 1343-1350.

YOUNG, V. B., FALKOW, S. & SCHOOLNIK, G. K. 1992. The invasin protein of *Yersinia enterocolitica*: internalization of invasin-bearing bacteria by eukaryotic cells is associated with reorganization of the cytoskeleton. *Journal of Cell Biology,* 116**,** 197-207.

ZHANG, Z. Y., CLEMENS, J. C., SCHUBERT, H. L., STUCKEY, J. A., FISCHER, M. W., HUME, D. M., SAPER, M. A. & DIXON, J. E. 1992. Expression, purification, and physicochemical characterization of a recombinant *Yersinia* protein tyrosine phosphatase. *Journal of Biological Chemistry,* 267**,** 23759-23766.

ZHAO, Y. & SHAO, F. 2015. The NAIP–NLRC4 inflammasome in innate immune detection of bacterial flagellin and type III secretion apparatus. *Immunological Reviews,* 265**,** 85-102.

ZHOU, B. & ABBOTT, D. W. 2021. Gasdermin E permits interleukin-1 beta release in distinct sublytic and pyroptotic phases. *Cell Rep,* 35**,** 108998.

ZUMBIHL, R., AEPFELBACHER, M., ANDOR, A., JACOBI, C. A., RUCKDESCHEL, K., ROUOT, B. & HEESEMANN, J. 1999. The Cytotoxin YopT of *Yersinia enterocolitica* Induces Modification and Cellular Redistribution of the Small GTP-binding Protein RhoA *Journal of Biological Chemistry,* 274**,** 29289-29293.

6 Danksagung

An allererster Stelle natürlich ein herzliches Dankeschön an Professor Klaus Ruckdeschel für die Möglichkeit, meine Promotion in seiner Arbeitsgruppe durchführen zu dürfen. Vielen Dank für die tolle Unterstützung, angefangen bei der freundlichen Aufnahme, über die zahlreichen gemeinsamen Blot-Besprechungen bis hin zur Hilfe bei Fertigstellung der Arbeit in den letzten Monaten.

Zudem möchte ich mich aufrichtig bei Professor Dr. Streit für die freundliche Übernahme der Co-Betreuung, sowie des Zweitgutachtens dieser Dissertation bedanken!

Ein großes Dankeschön auch an Professor Dr. Aepfelbacher, für die Möglichkeit, meine Promotion an diesem Institut durchführen zu dürfen.

Tatkräftig unterstützt bei der Durchführung diverser Versuche wurde ich zudem von der Cytometry und Cell Sorting Core Unit des UKE unter der Leitung von Regine Thiele. Vielen Dank für eure Expertise!

Ein riesiges Dankeschön geht außerdem an alle aktuellen und ehemaligen Mitglieder der AG Ruck und natürlich an den ganzen Rest der MIBI-Familie. Ihr habt meine Promotionszeit auf so viele verschiedene Arten bereichert, sowohl innerhalb als auch außerhalb des Labors. Vielen Dank für die herzliche Aufnahme vor inzwischen fast 5 Jahren, für tolle und kompetente Unterstützung beim Erlernen neuer Methoden, für die 9-Uhr-Kaffeepausen, für das geduldige Beantworten vieler Fragen, für Salat-Dienstage, für gemeinsames Trouble Shooting (vor allem, wenn der Blot mal wieder leer war), für Film-Abende, für 15-Uhr-Kaffeepausen, für die Versorgung mit Hunde-Videos, für Boulder-Nachmittage, für fleißiges Kuchenessen, für quatschige Ablenkung in der Zellkultur und ganz insgesamt für die Schaffung eines tollen Arbeitsumfeldes.

Ganz besonders in Bezug auf diese Arbeit ein großes Dankeschön an Lea und Sarah, die mich im Rahmen ihrer jeweiligen Bachelor-Arbeiten tatkräftig im Labor unterstützt haben, und an Nina und Su fürs fleißige und kompetente Korrekturlesen!

Mama und Papa, vielen Dank für so vieles! Ohne euch, und die bestimmt 20 kg per Post geschickter Schokolade, wäre diese Promotion um einiges schwieriger geworden. Danke für entspannte Wochenenden in Köln und Hamburg, für viele schlaue Zeitungsartikel und für eure bedingungslose Unterstützung!

Ein großes, großes Dankeschön außerdem an diverse Freund:innen in Köln, Münster, Hamburg und im FF-Discord! Danke für eure Unterstützung, bereits im Bachelor- und Masterstudium und nun durch die ganze Promotion hindurch. Danke fürs geduldige Zuhören, fürs stete Ermutigen und fürs dringend nötige Ablenken und Aufmuntern zwischendurch – sei es durch gemeinsame Wochenenden, am Telefon oder online.

Und natürlich an Hannes - ich müsste mich eigentlich für so vieles bei dir bedanken, aber ich mache es kurz: THANK YOU…most ardently!

7 Eidesstattliche Versicherung

Eidesstattliche Versicherung - Declaration on oath

Hiermit erkläre ich an Eides statt, dass ich die vorliegende Dissertationsschrift selbst verfasst und keine anderen als die angegebenen Quellen und Hilfsmittel benutzt habe.
I hereby declare, on oath, that I have written the present dissertation by my own and have not used other than the acknowledged resources and aids.

Hamburg, den

Unterschrift _____

Marie Kriwet